

March 2022



Student Report No. 55

Understanding interactions between *Ramularia collo-cygni* and barley leaf physiology to target improvements in host resistance and disease control strategy

Clarinda Molly Rose Burrell

SRUC, West Mains Road, Edinburgh EH9 3JG

Supervisors: Ian Bingham and Neil Havis

This is the final report of a PhD project (21120035) that started in October 2016. The work was partly funded by a contract for £54,000 from AHDB Cereals & Oilseeds. Additional funding was provided by SRUC.

While the Agriculture and Horticulture Development Board seeks to ensure that the information contained within this document is accurate at the time of printing, no warranty is given in respect thereof and, to the maximum extent permitted by law, the Agriculture and Horticulture Development Board accepts no liability for loss, damage or injury howsoever caused (including that caused by negligence) or suffered directly or indirectly in relation to information and opinions contained in or omitted from this document.

Reference herein to trade names and proprietary products without stating that they are protected does not imply that they may be regarded as unprotected and thus free for general use. No endorsement of named products is intended, nor is any criticism implied of other alternative, but unnamed, products.

AHDB Cereals & Oilseeds is a part of the Agriculture and Horticulture Development Board (AHDB).

CONTENTS

1.	ABSTRACT	1
2.	INTRODUCTION	2
	2.1.1 Barley pests and diseases	2
	2.1.2 Physiological responses of plants to fungal pathogens	3
	2.1.3 Ramularia collo-cygni (Rcc)	5
	2.1.4 Project objectives	9
3.	MATERIALS AND METHODS	11
	3.1. Impact of ramularia on photosynthesis	11
	3.1.1. Plant material and growth conditions	11
	3.1.2. Inoculation of plants with Rcc	12
	3.1.3. Experimental design	12
	3.1.4. Chlorophyll fluorescence imaging	13
	3.1.5. Visual assessment of disease progress	14
	3.1.6. DNA extraction and quantification.....	14
	3.1.7. Infra-red gas analysis	14
	3.1.8. Experimental set 2.....	15
	3.2. Relative impact of Rcc life phases on barley yield	15
	3.2.1. Effects of fungal pathogens on crop growth and yield – site and experimental design.....	15
	3.2.2. Measurements.....	16
	3.2.3. Calculations and statistical analysis.....	19
	3.3. Effects of varying rates of leaf senescence on RLS disease development....	21
	3.3.1 Experimental design	21
	3.3.1. Preparation and foliar application of pH 6.5 cytokinin (6-Benzylaminopurine) solution	21
	3.3.2. Measurement of relative leaf-chlorophyll content	22
	3.3.3. Data and statistical analysis.....	22
4.	RESULTS	24
	4.1. Impact of ramularia on photosynthesis	24
	4.1.1. Experimental series 1	24

4.1.2.	Experimental series 2	37
4.2.	Impact of Rcc life phases on barley yield.....	69
4.2.1.	Disease severity and % green area	69
4.2.2.	Fungal growth in planta	73
4.2.3.	Crop biomass	74
4.2.4.	Chlorophyll fluorescence	74
4.2.5.	Healthy area light interception	75
4.2.6.	Crop yield	76
4.3.	Effects of varying rates of leaf senescence on RLS disease development....	79
4.3.1.	Senescence and visible symptom progression	79
4.3.2.	Fungal growth in planta	82
4.3.3.	Rcc DNA levels in leaves at the end of the experiment.....	83
5.	DISCUSSION	84
5.1.	Effect of Rcc infection on photosynthesis	84
5.2.	Impact of Rcc infection on barley yield	87
5.3.	Effect of varying rates of leaf senescence on RLS development.....	90
5.4.	General discussion	91
6.	REFERENCES	94

1. Abstract

Ramularia leaf spot (RLS) is an increasingly problematic disease of barley. As the causal fungus, *Ramularia collo-cygni* (Rcc), has developed resistance to several major fungicide groups, control options are limited. The fungus can grow systemically from infected seed, with visible symptoms often only appearing after flowering. As the relative contribution of the latent and symptomatic stages of the fungal life cycle to reduced barley yields is not known with any certainty, it was the focus of this research. Two possibilities are that the effect of asymptomatic infection on pre-flowering photosynthetic activity, and the development of grain sink capacity, plays an important role; or that reduction in photosynthetic activity during grain filling, resulting from lesion development and loss of green leaf area, is the predominant factor.

In controlled environment (CE) experiments, leaf photosynthetic activity was measured – using infra-red gas analysis (IRGA), chlorophyll fluorescence analysis and imaging – in inoculated seedlings before and after visible symptom development. No reduction in photosynthesis was observed in infected leaves, compared to non-infected leaves, during the latent phase of infection. After visible symptoms appeared, photosynthesis within lesions reduced as they developed. However, this did not reduce photosynthetic activity across the whole leaf area. This result suggests that for whole leaf photosynthetic activity to be affected, visible symptoms must develop into mature lesions and coalesce to cover larger areas of the leaf surface.

In field experiments, plots were either untreated, treated with a full fungicide regime, or inoculated with *R. collo-cygni* and treated with fungicide to which *R. collo-cygni* is resistant. RLS was the only disease of significance that developed in untreated or inoculated plots, with symptoms appearing after flowering (around growth stage 72). Fungicide-treated plots remained free of disease. Plants showed no effect of infection on the maximum quantum efficiency of Photosystem II (Fv/Fm) before visible symptoms, consistent with results from CE experiments. Grain yield was predicted from radiation use efficiency (RUE) and utilisation of soluble sugar reserves, and post-flowering healthy (green) leaf area light interception. Grain yields predicted from the difference in post-flowering light interception between treated and untreated or inoculated plants displaying symptoms of RLS were comparable with the measured yield response to fungicide. This suggests that yield loss to RLS is primarily associated with a reduction in light capture during grain filling, resulting from lesion development and loss of green leaf area.

Results suggested that symptom expression was associated with leaf senescence. CE experiments tested this relationship by using treatments to vary the onset and rate of leaf senescence. Seedlings that were treated with cytokinin to delay senescence after inoculation developed fewer lesions than control plants. Fungal growth was also restricted in the treated plants. Collectively, these results suggest that prevention of visible symptom development, rather than prevention of asymptomatic growth, is the most important target for management of this disease. Control methods targeted at delaying senescence could be a useful avenue for further investigation.

2. Introduction

Barley (*Hordeum vulgare*) is an ancient crop with a wide geographic range and a reputation for resilience. It has been part of human diets since its domestication in the Middle East and central Asia more than 10,000 years ago and is now grown around the world (Von Bothmer and Komatsuda, 2011). The total worldwide harvested area of barley has fallen from around 80 million hectares in the late 1970s and early 1980s to just under 50 million hectares today. Global annual production currently stands at around 145 million tonnes (FAOSTAT, 2020). Barley is still grown as a basic food crop, particularly in areas where resources are limited or the climate less suitable for other cereal crops, as barley yield is generally less variable than that of other major cereals and it can be grown successfully across an extensive range of altitudes and climates (Newton *et al.*, 2011). In richer countries with milder climates, despite experiencing a small renaissance as a health food (Hecker *et al.*, 1998), barley is now grown mainly for use in animal feed or alcohol production.

In Scotland, where whisky is one of the nation's most valuable export commodities, 53% of the 2019 barley harvest was sold to the malting industry (The Scottish Government, 2020). Barley is the most widely grown crop in Scotland, accounting for 65% of total crop production in 2020; with spring barley alone accounting for 55% (The Scottish Government, 2020).

2.1.1 Barley pests and diseases

Barley can be affected by a range of biotic stresses. Free-living nematodes, bacterial pathogens such as *Pseudomonas syringae*, birds such as crows (particularly during crop establishment) and viral pathogens such as barley yellow dwarf virus (vectored by aphids) are all causes for concern for growers. However, fungal pathogens are responsible for some of the most economically important diseases of barley.

Rhynchosporium commune, the causal agent of barley leaf blotch (or scald), is the most significant foliar disease of barley in northern Europe. Net blotch and brown rust, two more damaging foliar diseases of barley, are caused by the fungal pathogens *Pyrenophora teres* and *Puccinia hordei*, respectively. Fusarium species, including *Fusarium graminearum*, contribute to seedling wilt and Fusarium head blight (Bottalico and Perrone, 2002).

Powdery mildew (*Blumeria graminis* f. sp. *hordei*) has historically been a problematic disease for barley growers. However, resistant spring barley varieties are now widely grown. Loss of function mutations at the *Mildew resistance locus O (MLO)* were found to confer resistance to powdery mildew (Piffanelli *et al.*, 2002), leading breeders to develop *mlo*-mediated resistant spring barley cultivars.

Widespread adoption of spring barley varieties with *mlo*-mediated resistance to powdery mildew has been suggested as a contributing factor in the emergence of *Ramularia* leaf spot (RLS), an increasingly problematic disease of barley caused by the fungus *Ramularia collo-cygni*. Spring barley varieties carrying the mutant *mlo* allele have been found to be more susceptible to RLS (Pinnschmidt *et al.*, 2006; Pinnschmidt and Sindberg, 2009; McGrann *et al.*, 2014), although the strength of this observed affect appears to vary across different locations, environments and genetic backgrounds (Hofer *et al.*, 2014; Havis *et al.*, 2015).

2.1.2 Physiological responses of plants to fungal pathogens

Fungal pathogens of plants utilise varied strategies to obtain sufficient nutrition for growth and development from host plants. The way in which they obtain their nutrition has commonly been used to categorise them as biotrophs, necrotrophs or hemibiotrophs. Biotrophs gain nourishment from living plant tissue, necrotrophs kill plant cells and gain nourishment from dead plant tissue, and hemibiotrophs have an initial biotrophic stage, followed by a switch to necrotrophy.

Some crop pathogens, including *Zymoseptoria tritici* (Septoria leaf blotch of wheat), *Rhynchosporium commune* (Barley leaf blotch/scald), *Cladosporium fulvum* (Tomato leaf mould) and *Ramularia collo-cygni* (Ramularia leaf spot of barley), exhibit lifestyles characterised by a period of asymptomatic growth within the host plant, followed by a switch to causing necrotic lesions. These fungi grow intercellularly during the asymptomatic period of growth, and do not produce specialised feeding structures, thus the first phase of their lifecycle, prior to the necrotrophic phase, does not fit so neatly into the classification of biotrophy. *R. collo-cygni* has sometimes been described as growing endophytically in barley prior to the appearance of visible foliar disease symptoms, and Salamati and Reitan (2006) hypothesised that it may have been an endophyte that subsequently evolved to be capable of pathogenicity. Although *R. collo-cygni* presumably obtains nourishment from barley plants in the apoplast where fungal hyphae grow for extended periods, the precise form of this and mechanisms of uptake are not yet certain.

Negative effects on host plants of being used as a source of nourishment by pests can arise from direct physical damage or from indirect impacts on plant functions. Localised responses, for example at individual leaf level, can add up to impact the yield or quality of a crop if circumstances are conducive. Boote *et al.* (1983), in a paper coupling plant pests and their effects on plants to carbon flow processes in crop growth simulators, suggested classifying pests into seven groups according to the nature of their impact on plants: tissue consumers, leaf senescence accelerators, stand reducers, light stealers, photosynthetic rate reducers, assimilate sappers, and turgor reducers. Johnson (1987) suggested a further, broader classification into pests mainly affecting solar radiation interception (RI) and those mainly affecting radiation use efficiency (RUE). Effects of fungal pathogens on plants such as the development of necrotic lesions, accelerated leaf

senescence, or defoliation can, therefore, be thought of as impacting RI, and effects such as a reduction in photosynthetic rate, or changes caused by the redirection of host soluble assimilates for fungal nutrition, can be thought of as impacting RUE. Clearly, single pathogens can have effects on both RI and RUE, particularly those that change between different trophic states during their lifecycle.

Biotrophic growth of fungal pathogens in plants can lead to an extensive reprogramming of host primary metabolism. Source-sink balance is often affected, creating sinks for assimilate at infection sites, resulting in an increase in import of photosynthetic products to infected areas and/or a decrease in export away from them (Biemelt and Sonnewald, 2006). The nutrition obtained by biotrophic fungi from living plant tissue is thought to be mainly in the form of hexoses and amino acids. Studies using the biotrophic rust, *Uromyces fabae* identified hexose and amino acid transporters expressed specifically in haustoria (Hahn *et al.*, 1997; Voegelé *et al.*, 2001) and another amino acid transporter expressed in both haustoria and intercellular hyphae (Struck *et al.*, 2002). Increased expression of host and/or fungal cell-wall invertases, necessary to cleave apoplastic sucrose into hexoses, has been shown to occur in response to infection by several biotrophic or hemibiotrophic fungal pathogens (Heisterüber *et al.*, 1994; Chou *et al.*, 2000; Fotopoulos *et al.*, 2003; Behr *et al.*, 2010). Increased invertase activity, and accumulation of hexoses, has been linked to the down-regulation of photosynthesis which is also frequently observed in association with infection by biotrophic and hemibiotrophic plant pathogens. Scholes *et al.* (1994) proposed that accumulation of hexoses functions together with changes to carbohydrate translocation patterns to downregulate photosynthetic gene expression via a transduction pathway or pathways, leading to a reduction in photosynthetic rate. Increased cell-wall invertase activity and accumulation of hexoses in the apoplast may benefit fungi by providing nutrition, however, hexose accumulation can also serve as a signal for triggering plant defence responses (Koch, 1996; Ehness *et al.*, 1997; Chou *et al.*, 2000; Bilgin *et al.*, 2010).

While photosynthesis is often reduced in plants infected with biotrophic or hemibiotrophic fungal pathogens, respiration is frequently increased, including in incompatible interactions. A comparison of the respiratory reactions of barley to inoculation with virulent and avirulent strains of powdery mildew (Smedegaard-Petersen and Stolen, 1981) found that respiration in resistant plants increased rapidly in the first 16 hours after inoculation, before declining again after a few days, whereas respiration in susceptible plants only began to increase after 72 hours and then remained high until the onset of senescence. Although resistant plants remained free of symptoms, grain yield and quality were reduced, suggesting that mobilisation of the defence response may have come at a cost to other processes via a reduction in available energy, reducing power or precursor molecules for biosynthesis.

Biotrophic pathogens can cause significant reductions in growth and yield despite the fact that they do not directly kill plant cells. Effects on carbohydrate partitioning may play an important role in this. Using $^{14}\text{CO}_2$ feeding, Livne and Daly (1966) found that infection of mature French bean leaves with the rust fungus, *Uromyces appendiculatus* led to a substantial increase in both retention and import of assimilate in these leaves, with consequent reductions in translocations of assimilate to roots and younger, developing leaves. Similar work in barley leaves infected with brown-rust showed increased retention of assimilate in infected leaves (Owera *et al.*, 1983). Increased cell-wall invertase activity has been linked to the sink-capacity of infected leaves through downregulation of photosynthesis, as discussed above, and is also thought to catalyse phloem unloading of sucrose due to the creation of a sucrose gradient (Roitsch *et al.*, 2003).

In contrast to biotrophic pathogens, necrotrophs directly kill plant cells. Agricultural yield losses may occur due to direct damage to the parts of the plant used as produce, for example direct damage to fruit or grain, or due to damage to other parts of a plant which are severe enough to interfere with plant functions, for example, foliar necrotic lesions reducing solar radiation interception sufficiently to limit the availability of assimilates for yield-forming processes. Disease severity, timing, duration, and location within the plant can all affect the outcome of pathogen infection on crop yield (Gaunt, 1995). The timing of pathogen infection in relation to crop growth stage is an important factor in both the degree of yield loss, and the yield components which are primarily affected. For example, early-season infection of barley with powdery mildew (up to stem elongation) has been found to reduce the number of fertile tillers produced (Scott and Griffiths, 1980), therefore, early infection can have a compounding effect on the reduction in grain size normally associated with infection later in the season. Some fungal diseases of barley still have the potential to cause significant yield loss when infection occurs late in the season, particularly if they attack the ear or the flag and upper leaves (Jordan *et al.*, 1985; Jebbouj and El Yousfi, 2009). *R. collo-cygni* infection of barley typically leads to the appearance of late-season, post-anthesis foliar disease symptoms, therefore, yield loss to this disease may be due to a reduction in assimilates from post-anthesis photosynthesis during grain filling. However, *R. collo-cygni* can grow within barley plants for an extended period prior to the appearance of visible symptoms (Frei *et al.*, 2007; Havis *et al.*, 2014). Whether this asymptomatic growth period can affect yield formation processes, and, if so, the relative impact on yield of asymptomatic and symptomatic growth periods, is not yet known

2.1.3 *Ramularia collo-cygni* (Rcc)

Fungal structures associated with the foliar symptoms in barley now known as *Ramularia* leaf spot (RLS) were first identified in Italy in the 1890s. The fungus was originally named *Ophiocladium hordei* (Cavara, 1893), then subsequently renamed *Ramularia collo-cygni* (Sutton and Waller, 1988). The name refers to a perceived resemblance of the tortuose conidiophores to a swan's

neck (Figure 1). More recent molecular studies have confirmed that *R. collo-cygni* belongs to the class of Dothidiomycetes, in the Mycosphaerellaceae family, and the genus *Ramularia* (Crous *et al.*, 2000; Crous *et al.*, 2001; Crous *et al.*, 2009). The development of molecular diagnostic techniques has enabled rapid and accurate detection of *R. collo-cygni* even at low levels and early stages of infection (Havis *et al.*, 2006; Frei *et al.*, 2007; Taylor *et al.*, 2010), and sequencing of the first *R. collo-cygni* genome in 2016 allowed further clarification by phylogenetic analysis of the relationships between *R. collo-cygni* and other plant pathogens (McGrann *et al.*, 2016). *R. collo-cygni* was found to be closely related to *Zymoseptoria tritici*, the causal agent of the most damaging wheat disease in Europe, Septoria tritici blotch (STB). Other close relatives included the tomato pathogen *Cladosporium fulvum*, the banana pathogen *Pseudocercospora fijiensis*, and the pine pathogen *Dothistroma septosporum*.

Typical symptoms of RLS found on plants in the field (Figure 1) are dark, reddish-brown, rectangular lesions on leaves, surrounded by a 'halo' of chlorotic tissue, restricted by leaf veins. Symptoms are not usually observed until after flowering has occurred (Walters *et al.*, 2008). The development of necrotic symptoms of RLS on barley leaves is thought to be associated with the production of secondary metabolites by the fungus. Heiser *et al.* (2003) identified one of a number of coloured metabolites produced by *R. collo-cygni* as the anthraquinoid phytotoxin rubellin D, which produces light- and concentration-dependent necrosis when applied to barley leaves. The authors used a model system to demonstrate photodynamic activity of rubellin D, triggering the light-dependent production of reactive oxygen species (ROS) and peroxidation of α -linolenic acid. *R. collo-cygni* can also produce different isomers of rubellin that exhibit similar photodynamic activity (Miethbauer *et al.*, 2003; Heiser *et al.*, 2004; Miethbauer *et al.*, 2006). Heiser *et al.*, (2004) proposed that rubellins produced by *R. collo-cygni* could act as pathogenicity factors, causing or exacerbating oxidative stress in barley and leading to the formation of necrotic symptoms. A similar mechanism of pathogenicity to that hypothesised for *R. collo-cygni* by Heiser *et al.*, (2004) has been shown for *Cercospora* species, plant pathogenic fungi which produce the light-activated phytotoxin cercosporin (Daub and Ehrenshaft, 2000). However, Dussart *et al.*, (2018), in experiments infiltrating barley leaves with rubellin D, found that RLS susceptibility did not correspond with rubellin D sensitivity. The *R. collo-cygni* genome contains several clusters of genes associated with secondary metabolism, indicating that the fungus may be capable of producing a wide range of secondary metabolites (Dussart *et al.*, 2018b), and co-expression of secondary metabolism core genes and their predicted transcriptional regulators has been demonstrated in the early stages of RLS symptom development in barley seedlings (Dussart *et al.*, 2018a).

Abiotic stress factors such as high light levels can cause physiological leaf spotting on barley leaves that is similar in appearance to early RLS symptoms (Wu and Von Tiedemann, 2002).

However, RLS lesions are distinguishable as they 'go right through' the leaf i.e. a developed lesion will be clearly visible on both the adaxial and abaxial leaf surface. RLS symptoms are also relatively easily confused with those of some other fungal pathogens of barley, particularly *Pyrenophora teres* (net blotch) in its spot form (*P. teres f. maculata*).

Recorded yield losses to RLS are typically around 5 – 10%, although losses as high as 70% have been reported in South America, and grain quality can also be affected (Havis *et al.*, 2015). A higher proportion of small grains (screenings), often observed in grain from barley affected by RLS, can reduce the value of a crop as it may then not meet criteria for the malting market, such as an even germination of seed.

Over the last two decades, RLS has become more prevalent globally. Multiple factors may have contributed to this, including increased global trade, climatic changes, agricultural practices, or genetic changes in *R. collo-cygni* or barley.

Susceptibility of barley lines with *mlo*-mediated resistance to powdery mildew, the possibility of historic misidentification of RLS symptoms, and human movement of infected seed have all been suggested as contributors to the global spread of RLS. Population structure analyses of *R. collo-cygni* isolates from two northern European barley populations (Hjortshøj *et al.*, 2012) and from diverse hosts across several European locations (Stam *et al.*, 2019) found high genetic diversity within local sub-populations rather than distinctions between countries (Hjortshøj *et al.*, 2012) and revealed little evidence of global clustering or host specification (Stam *et al.*, 2019). These studies suggest that human movement of infected seed is likely to play an important role in dispersal.

R. collo-cygni is a commercially important pathogen of barley; however, it can also infect a wide range of other hosts, including wheat (*Triticum aestivum*), oat (*Avena sativa*), maize (*Zea mays*) and rye (*Secale cereale*) (Huss, 2004), as well as several wild grasses (Huss, 2004; Frei and Gindro, 2015; Kaczmarek *et al.*, 2017) and the model grass species *Brachypodium distachyon* (Peraldi *et al.*, 2014).

R. collo-cygni in barley (Figure 1) can be seed-borne and grow internally through plants, moving into new leaf layers as they emerge, without displaying any visible symptoms (Frei *et al.*, 2007; Havis *et al.*, 2014). Symptoms are sometimes observed on lower leaves of young plants early in the growing season, particularly when plants have experienced adverse environmental conditions such as waterlogging (McGrann and Havis, 2017). However, typically *R. collo-cygni* has a long period of asymptomatic growth and symptoms only appear after flowering. Spotting and lesions appear on upper leaves, and can spread to other leaves, stems and awns as the disease

develops. Lesions often multiply and coalesce, accompanied by chlorosis and necrosis of leaves (Walters *et al.*, 2008).

The role of spores in *R. collo-cygni* epidemics is less clear, but infection from spores overwintering on straw and stubble, from senescing lower leaves during the growing season, or from alternative hosts may be significant in some years and locations (Mäe *et al.*, 2018), although further research is needed on the role of alternative hosts to establish evidence for spore movement. Spore germination occurs on the barley leaf surface in moist conditions. Fungal hyphae enter leaves through stomata and grow intercellularly in the mesophyll. After symptom appearance, fungal sporulation can occur in necrotic tissue, with conidiophores emerging through stomata (Sutton and Waller, 1988; Stabentheiner *et al.*, 2009; Thirugnanasambandam *et al.*, 2011; Kaczmarek *et al.*, 2017) and also directly through the mesophyll (Kaczmarek *et al.*, 2017). There is evidence that *R. collo-cygni* can reproduce sexually (Piotrowska *et al.*, 2016) so spread may also occur through sexual ascospores, but this has yet to be confirmed.

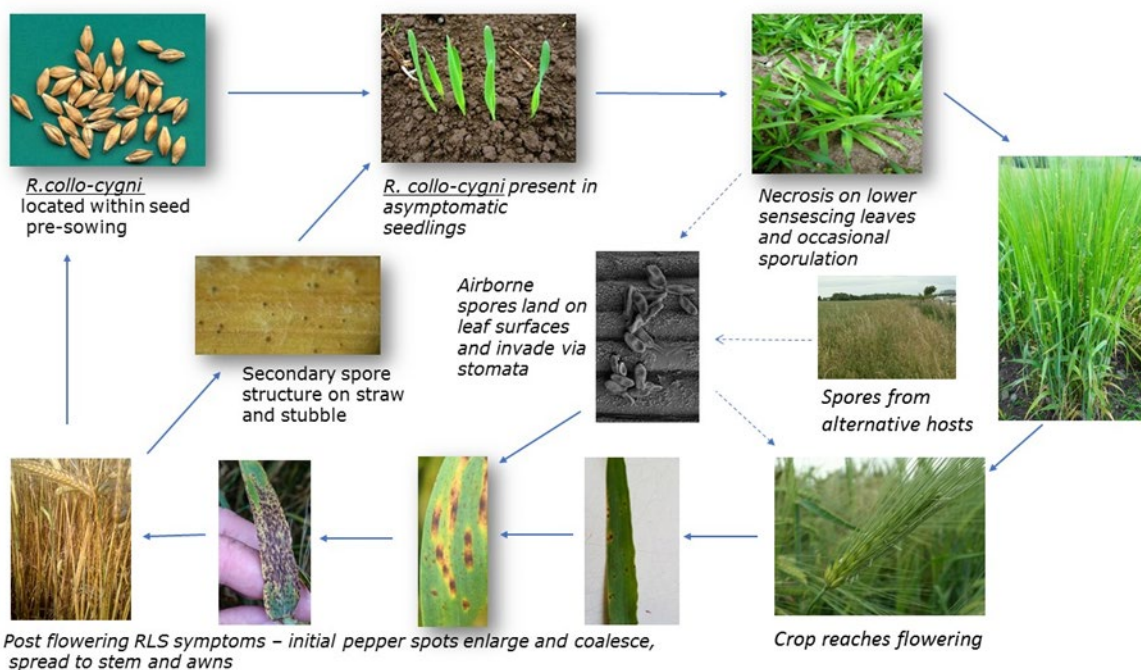


Figure 1. Life cycle of *R. collo-cygni* on barley. Adapted from Havis *et al.* (2015).

RLS is a concern for barley growers as it is now widespread globally and can, in some years, cause severe yield losses. The genetic similarity of *R. collo-cygni* to other damaging pathogens like *Zymoseptoria tritici*, its broad host range, and its suspected ability to reproduce sexually all contribute to concern about possible future developments. *R. collo-cygni* has developed resistance to strobilurin (Quinone outside inhibitor: QOI) fungicides and resistance to succinate dehydrogenase inhibitor (SDHI) fungicides is increasing (Piotrowska *et al.*, 2017). The multisite fungicide chlorothalonil remains an effective control, but EU approval for this product has been withdrawn and it is no longer in use in the EU as of May 2020.

Breeding barley varieties for resistance to RLS is complicated by the effects of environment on disease expression. Prolonged leaf wetness during stem extension has been reported as a key factor in RLS development and symptom severity (Formayer *et al.*, 2004; Huss, 2004; Salamati and Reitan, 2006). However, multi-year analysis of data from an investigation into the potential for a period of leaf wetness for 14 days at GS30/31 to act as a risk predictor for RLS in barley, found that disease levels could not be predicted using this parameter alone, despite some observed within-season correlation between leaf wetness and eventual disease levels (Havis *et al.*, 2018). Light intensity has also been associated with RLS symptom severity. However, reports of this affect vary. Unpublished results from E. Sachs, published in Heiser *et al.*, (2003), suggested that light intensity can influence RLS symptom levels on barley leaves. Subsequently, Makepeace (2006) reported higher levels of RLS symptoms on barley plants exposed to high light intensity prior to inoculation with *R. collo-cygni* than on barley plants grown under low light intensity. Makepeace (2006) also found that plants grown in high light intensity after inoculation with *R. collo-cygni* developed fewer RLS symptoms than plants grown under lower light intensity, suggesting that the timing of exposure to high light intensity is an important factor, possibly negatively affecting pathogenicity later in the life cycle of *R. collo-cygni* in barley. Increased RLS symptoms were reported in barley seedlings exposed to abiotic stress (either waterlogging or high light intensity) prior to inoculation with *R. collo-cygni*, by McGrann and Brown (2018), but this response was found to differ across barley varieties. Formayer *et al.*, (2004) reported that humidity, but not light intensity, affected RLS symptom development in experiments in Austria, and Mařík *et al.*, (2011) found that increased RLS symptom severity in the Czech Republic was associated with a greater number of rainy days during the three weeks post-heading, and lower rainfall and higher temperatures after flowering was associated with reduced symptom severity. More work is still needed to fully understand the effects of individual or combinations of environmental factors on the incidence and severity of RLS in barley, and how these may interact with host or fungal genotype.

2.1.4 Project objectives

R. collo-cygni infection of barley is characterised by a long period of latent growth, i.e. no visible disease symptoms apparent on plants, followed (sometimes, but not always) by a 'lifestyle switch' to necrotrophic growth and visible symptom expression. Understanding the effects of *R. collo-cygni* on barley physiology during asymptomatic growth and the switch to symptomatic growth is, therefore, important to target improvements in host resistance and disease control strategies. Infected seed is an important source of *R. collo-cygni* infection in barley, and the fungus can be present in plants from the earliest stages of their development (Havis *et al.*, 2014). Although *R. collo-cygni* has sometimes been described as leading an endophytic lifestyle in barley prior to visible symptom appearance on leaves late in the growing season (McGrann *et al.*, 2016), gaps in

our knowledge remain about what impact this long latent stage of infection may have on host plants.

It is possible that the latent stage of *R. collo-cygni* infection in barley could be a contributor to eventual yield loss, as in the field asymptomatic infection coincides with processes contributing to the establishment of grain sink capacity, such as the development of tillers, ears, and spikelets. In the UK, and other countries with similar climates, yield formation in non-diseased barley crops is thought to be predominantly sink-limited (Bingham *et al.*, 2007a; Bingham *et al.*, 2019). Therefore, the latent phase of *R. collo-cygni* infection could potentially contribute to reduction in barley yield due to effects on the development of grain sink capacity, for example, due to reduced carbon assimilation from pre-anthesis photosynthesis, or changes to pre-anthesis resource allocation within the plant. Alternatively, reduction in photosynthetic activity during grain filling, due to necrotic lesion development and loss of green leaf area, or post-anthesis effects on resource allocation, could be significant contributing factors to the yield reduction associated with RLS.

The experiments described in this report were designed to investigate whether the visually asymptomatic period of *R. collo-cygni* growth in barley impacts host photosynthesis and, ultimately, grain yield.

The following hypotheses were tested:

- Infection of barley seedlings with *R. collo-cygni* does not impact leaf photosynthesis prior to the appearance of visible RLS symptoms.
- Net leaf photosynthesis is reduced after the appearance of visible RLS symptoms on leaves of barley seedlings infected with *R. collo-cygni*.
- Infection of field grown barley plants with *R. collo-cygni* does not impact leaf photosynthesis prior to the appearance of visible RLS symptoms.
- Yield loss to RLS in barley is due to post-anthesis reduction in PAR interception due to visible RLS symptom expression.

The factors involved in triggering the *R. collo-cygni* switch to necrotrophic growth in barley and the appearance of RLS symptoms are not yet fully understood. It has been linked to adverse environmental conditions, and differences in varietal responses to these, as described above. Transgenic barley plants exhibiting delayed leaf senescence due to overexpression of a Stress-induced NAC1 transcription factor, also linked to drought tolerance, were found to have increased resistance to RLS (McGrann *et al.*, 2015), and there is some evidence to suggest that changes in host reactive oxygen species (ROS) status that can lead to senescence are involved in the transition to necrotrophic growth (McGrann and Brown, 2018; McGrann *et al.*, 2020). It is possible,

therefore, that treatments designed to delay the onset of senescence could interfere with processes affecting the *R. collo-cygni* switch to necrotrophic growth.

The work described in the later parts of this report investigate the effect of delaying foliar senescence of barley seedlings on *R. collo-cygni* growth *in planta* and RLS symptom development.

The following hypotheses were tested:

- Delaying foliar senescence in barley seedlings infected with *R. collo-cygni* reduces visible RLS symptom severity.
- Delaying foliar senescence in barley seedlings infected with *R. collo-cygni* reduces fungal growth in planta.

3. Materials and methods

3.1. Impact of ramularia on photosynthesis

3.1.1. Plant material and growth conditions

Leaf photosynthetic activity and quantity of *R. collo-cygni* DNA in inoculated and control plants were measured throughout the time-course of disease development. Infra-red gas analysis and chlorophyll fluorescence imaging were used as non-invasive ways to probe photosynthetic performance. Quantitative polymerase chain reaction analysis (qPCR) was used to quantify the amount of *R. collo-cygni* DNA present in leaves.

All experiments were conducted on spring barley (*Hordeum vulgare* L.) varieties Concerto or Fairing. Seeds were germinated by placing them in a Petri-dish lined with Whatman filter paper (GE Healthcare Life Sciences, Buckinghamshire, UK) soaked in tap water. The Petri-dishes were wrapped in aluminium foil to exclude light and left at room temperature for two to four days until the seeds had germinated. The germinated seeds were then planted in plastic pots with a volume of 147 cm³ and placed in trays in a controlled environment growth chamber. The growth medium used was Levington M3 high nutrient pot and bedding compost (ICL, Suffolk, UK).

The growth cabinets used were the JUMO IMAGO F3000 model (Snijders Labs, Tilburg, The Netherlands). The cabinet conditions were set to 18°C during the light period and 12°C during the dark period, 90 % Relative Humidity, photoperiod 16 h light and 8 h dark, and Photosynthetically Active Radiation (PAR) was supplied by fluorescent lamps (TLD-90 36W/950 6K, Philips, Amsterdam, Netherlands) giving a photon flux density of 230 $\mu\text{mol m}^{-2} \text{s}^{-1}$ at initial plant height. The compost was kept moist, but not water-logged, by inspecting daily and watering as required. The seedlings were inoculated with *R. collo-cygni* 14 days after sowing at growth stage 12 of the Zadoks decimal code for cereals (Tottman *et al.*, 1979) when plants had two fully emerged leaves.

3.1.2. Inoculation of plants with Rcc

The inoculation protocol was adapted from Makepeace *et al.* (2008). Five 1 cm² blocks of fungal mycelium were cut from a Petri-dish containing *R. collo-cygni* isolate DK05 Rcc 001, isolated from susceptible spring barley cv Braemar in Denmark in 2005, which had been growing on potato dextrose agar (PDA) for two weeks. These blocks were then placed in 250 ml of potato dextrose broth (PDB) and incubated in the dark on a shaker at 125 rpm at 18°C for a further two weeks. The PDA was prepared with 39.0 g l⁻¹ PDA powder (Sigma-Aldrich, Dorset, UK) in sterile distilled water (SDW). This solution was autoclaved, then 0.1 % streptomycin was added to give a concentration of 1 ml l⁻¹. The PDB was prepared with 24.0 g l⁻¹ PDB powder (Sigma-Aldrich, Dorset, UK) in SDW. This solution was autoclaved, then 0.1 % streptomycin was added to give a concentration of 1 ml l⁻¹.

Two controls were made using five 1 cm² blocks of PDA with no fungus in 250 ml of either PDB or SDW, with streptomycin added at the same concentration as above. The controls were also incubated in the dark on a shaker at 125 rpm at 18°C. After two weeks of incubation, the *R. collo-cygni* culture and controls were used to inoculate the plants. The fungal cultures and controls were each blended until smooth in a clean kitchen blender, in three runs of 30 seconds each. Polyoxyethylene-sorbitan monolaurate (Tween 20) (Sigma-Aldrich, Dorset, UK) was added at a concentration of 0.01% (or approximately 1 drop per 50 ml) to all three treatments to break the surface tension of the spray droplets on the leaf surface. The inoculum was then sprayed onto the barley plants using an air brush (Clarke Wiz Air®, Clarke International, Essex, UK) at an application rate of 0.5 ml per plant. The plants were sprayed evenly from different directions to ensure the inoculum was uniformly distributed over them.

The plants were placed in propagators, which were then sealed with microporous tape. Each treatment group was in a separate propagator to avoid cross contamination. The propagators were each placed inside two black plastic bags to exclude light and sealed with microporous tape. After two days, the bags were removed. This process created favourable conditions for fungal growth and infection by facilitating a period of high humidity. After a further three days, the lids of the propagators were removed. The three treatment groups were kept separate until the leaves were completely dry. Once the plants had dried, they were arranged into randomised blocks in the cabinet. Open-ended clear plastic tubes were used to keep the plants upright and avoid damage during sampling

3.1.3. Experimental design

Two series of experiments were conducted. The first series was conducted on cv. Concerto and the second on cv. Fairing. In each series, chlorophyll fluorescence images were captured on leaf 2 of intact plants (the youngest fully emerged leaf at the time of inoculation) using the MAXI-head

version of the IMAGING-PAM M-Series Chlorophyll Fluorescence System (Walz, Effeltrich, Germany), resolution 1392 x 1040 pixels, which utilises ImagingWin software. Depending on the experimental series, other supporting measurements of disease development and photosynthetic activity were made. In series 1, no supplementary mineral nutrients were given. In series 2 additional nutrients were supplied twenty-eight days after sowing (14 d.p.i.). 0.06 ml of Liquid Growmore fertiliser solution (Doff Portland Ltd., Nottingham, UK) was added to 10 ml of water, then this solution was pipetted directly onto the surface of the soil at the base of the plants (10 ml of solution applied to each plant). The undiluted fertiliser solution contained 7 % Nitrogen (N), 7 % Phosphorus Pentoxide (P₂O₅), and 7 % Potassium Oxide (K₂O).

3.1.4. Chlorophyll fluorescence imaging

Chlorophyll fluorescence measurements were taken at six time points: 6, 8, 10, 13, 16, and 25 days post inoculation (d.p.i.) during photosynthetic induction in dark-adapted plants. The general induction process and calculation of fluorescence parameters were as described by Baker (2008). Leaves (leaf 2) from a single replicate of each treatment were placed in the Imaging PAM leaf holder and covered with a black cloth to exclude light. The instrument was also located in a dark room with green safe light to guard against light straying around the edges of the cloth. This arrangement of leaves allowed measurements on all treatments to be made simultaneously. The position of a given treatment within the holder was randomised for each measurement occasion and replicate.

Leaves were left to dark adapt for 30 min after which they were exposed to a weak measuring beam for 8 seconds to capture minimal, or dark, fluorescence (F_o), then a saturating pulse was applied to capture maximal fluorescence (F_m). Variable fluorescence (F_v) was estimated as (F_m – F_o). These values were used to calculate maximal efficiency of PSII (F_v/F_m). Forty seconds after the measurement of minimal and maximal fluorescence (referred to here as the F_oF_m measurement), the actinic light was switched on at 230 μmol m⁻² s⁻¹. This light was provided by blue LED-lamps (450 nm). Over the next 15 minutes (940 s), as the plants adapted to the new light conditions, a saturating pulse was applied every 20 seconds to differentiate between non-photochemical quenching (NPQ) and photochemical quenching, or operating efficiency of PSII (ΦPSII). Electron transport rate (ETR) was given as 0.5 x ΦPSII x PAR x Leaf Absorptivity μequivalents m⁻² s⁻¹. The Absorptivity measurement was used as the common assumption of a PAR-Absorptivity of 0.84, i.e. that 84% of the incident photons of photosynthetically active radiation will be absorbed by a leaf, can be inaccurate in cases of diseased or senescing leaves. Red (660 nm) and near-infrared (780 nm) LED-lamps were used to measure absorptivity. Leaves were illuminated with red, then near-infrared light. Absorptivity was then calculated pixel by pixel from the red and near-infrared light remission images captured by the camera, using this formula: Absorptivity of photosynthetically active light = 1 – R/NIR

Where:

R = Red light remission: an inverse measure of the absorption of photosynthetically active radiation, and;

NIR = Near-infrared light remission: a measure of the remission of light that is not absorbed by photosynthetically active pigments

3.1.5. Visual assessment of disease progress

After completion of chlorophyll fluorescence imaging, a digital photograph of the leaves in the leaf holder was taken using a SONY® Cyber-shot DSC-HX9V camera. The visible disease severity (% area of leaf surface occupied by *Ramularia* leaf spot symptoms) was assessed visually for the section of leaf that had been used for chlorophyll fluorescence measurements. This was > 80% of the total leaf surface. The percentage of remaining green leaf area was also visually assessed

3.1.6. DNA extraction and quantification

The leaf was then excised from the plant, snap-frozen in liquid nitrogen directly, and stored at -20°C to await analysis. Total DNA (leaf and pathogen) was extracted from leaf tissue using the Illustra Nucleon Phytopure Genomic DNA Extraction Kit (GE Healthcare Europe GmbH, Freiburg, Germany). Leaves were ground to a powder using liquid nitrogen in a mortar and pestle. After DNA extraction, the quantity of DNA in each sample was measured using a Nanodrop. Samples were then diluted to 20 ng/μl. 5 μl of each diluted sample was used in a total reaction volume of 25 μl for Quantitative real-time PCR of *R. collo-cygni*, carried out using the method described in Taylor *et al.* (2010).

3.1.7. Infra-red gas analysis

The same leaves were used on different measurement occasions for simultaneous measurement of leaf gas exchange (infra-red gas analysis) and light-adapted chlorophyll fluorescence (an area-averaged measure), using the LI-6400XT Portable Fluorescence System with the 6400-40 Leaf Chamber Fluorometer (LI-COR Biosciences, Lincoln, USA).

Net CO² uptake was measured using a flow rate of 300 μmol, CO² concentration of 400 ppm and chamber air temperature of 18°C. A central section of leaf two was placed in the chamber and an irradiance of 260 μmol m⁻² s⁻¹ provided at the leaf surface. The value of irradiance was selected because it was close to that used during the growth of plants in the growth cabinet. The leaf was allowed to acclimate for 20 minutes and the rate of CO² uptake to stabilise before readings commenced. Readings were then logged every minute, for a duration of five minutes.

The irradiance was then increased to 1500 $\mu\text{mol m}^{-2}\text{s}^{-1}$ to measure CO_2 uptake at light saturation. Readings were logged after allowing a further 20 minutes for leaves to adjust to the new light regime. The actinic light was then switched off and measurements of dark respiration logged over another five-minute period. The measured chlorophyll fluorescence outputs were ΦPSII and ETR. After gas exchange and fluorescence measurements had been completed the ramularia leaf spot severity and % green leaf area were also assessed visually on the upper surface of the section of leaf that was in the chamber.

3.1.8. Experimental set 2

The experiments outlined above were repeated with the barley variety cv. Fairing.

3.2. Relative impact of Rcc life phases on barley yield

3.2.1. Effects of fungal pathogens on crop growth and yield – site and experimental design

The experiment took place in 2017 at Boghall farm, SRUC, Edinburgh, Midlothian, EH10 7DX (latitude 55° 52' 36.35" N and longitude 003° 12' 12.59" W), in the south-east facing Anchordales field on a gentle slope at an elevation of 200 m. The soil type was sandy loam (Macmerry Series), pH 6.0, and organic matter 6.48 % (loss on ignition). The previous crop was spring barley. Plots (10 x 2 m) of spring barley cv. Concerto were drilled on 29th March at a seed rate of 360 seeds m^{-2} . The experiment was laid out in a randomised block design with three treatments and four replicates. Fertiliser application was consistent with local practice for a malting barley crop (N = 120 kg/ha, and P_2O_5 and K_2O = 60 kg/ha).

The three treatments (Table 1) were:

- Treatment 1: Untreated (no inoculation or fungicide).
- Treatment 2: Full fungicide treatment (bixafen + prothioconazole [Siltra Xpro 0.4 l ha^{-1}] at GS30 followed by prothioconazole [Proline 0.4 l ha^{-1}] plus chlorothalonil [Bravo 1.0 l ha^{-1}] at GS 45).
- Treatment 3: Fungicide treatment (pyraclostrobin [Comet 0.6 l ha^{-1}]) at GS30 followed by inoculation with *R. collo-cygni* mycelial suspension at GS 32/33.

Table 1. Field experiment treatments

Treatment number	Treatment name	T1 (GS 30)	GS 32/33	TS GS 45
1	Untreated	No treatment	No treatment	No treatment
2	Fungicide	0.4 l/ha Siltra XPro	No treatment	Proline (0.4 l/ha) + Bravo (1.0 l/ha)
3	Inoculated	0.6 l/ha Comet	Inoculate with <i>R. collo-cygni</i>	No treatment

The treatments were designed with the aim of achieving plants displaying RLS symptoms only (no other diseases present), and completely disease-free plants. Disease development in untreated crops is quite unpredictable, and there was no guarantee that RLS would develop on the untreated crops, or, if it did, whether it would be the sole disease present. Therefore, one group of plants (treatment 3) were inoculated with *R. collo-cygni* in case natural infection did not occur. This group was also treated with a strobilurin fungicide (to which *R. collo-cygni* isolates are resistant) to control *Rhynchosporium commune* (barley leaf blotch/scald), *Pyrenophora teres* (net blotch) and *Puccinia hordei* (brown rust) in case these diseases took hold in the 2017 growing season. Two further treatments were initially included with the aim of providing non-inoculated controls for the plants inoculated with *R. collo-cygni*. These consisted of fungicide treatment at GS 30 (pyraclostrobin [Comet 0.6 l ha⁻¹]) and then an application of either dilute nutrient broth (to match the medium in which the fungus used for inoculations was grown) or sterile distilled water at GS 32/33. However, these treatments had to be dropped due to limited time and workload capacity.

3.2.2. Measurements

Crop biomass, absolute area, and % green area (GA) were determined 85 days after sowing (GS 55 + 5 days) and then at two further time points at two-week intervals during grain filling. Plants were sampled from a 0.5 m length of rows three and four at diagonally opposite points in each plot as shown in Figure 2. For all field sampling or measurements in this experiment the outer two rows (rows one and two) and areas within 0.5 m of the ends of the plots were avoided to minimise edge effects, the roots were severed from the shoots and discarded, and plants collected in the field were placed 'ears first' into long, clear plastic bags for transport, then stored in a walk-in chiller at -4°C in the dark prior to processing.

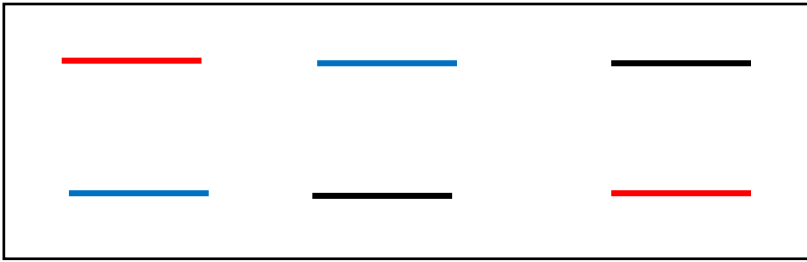


Figure 2. Diagrammatic representation of areas in each plot sampled for measurements of biomass, absolute area and % green area (GA). The three colours represent individual sampling dates. Each line represents a 0.5 m length of plants from rows 3 and 4.

The fresh samples were weighed using a precision balance (Kern PLJ, D-72336, Kern & Sohn Gontbl, Balingen, Germany). Subsamples were taken by 'dealing' shoots from each of these larger samples into ten equal piles, then selecting two of these piles at random to form the subsample. The fresh subsamples were weighed, then dried in individual paper bags in an oven (Ecocell, MMM Medcenter, Munich, Germany) for 48 hours at 80°C, and weighed again.

Ten shoots were selected randomly from the remaining original fresh samples for determination of absolute area and % GA. These were broken down into fractions of individual leaf layers, sections of stem (including leaf sheath) between leaves, peduncle, and ear, as shown in Figure 3.

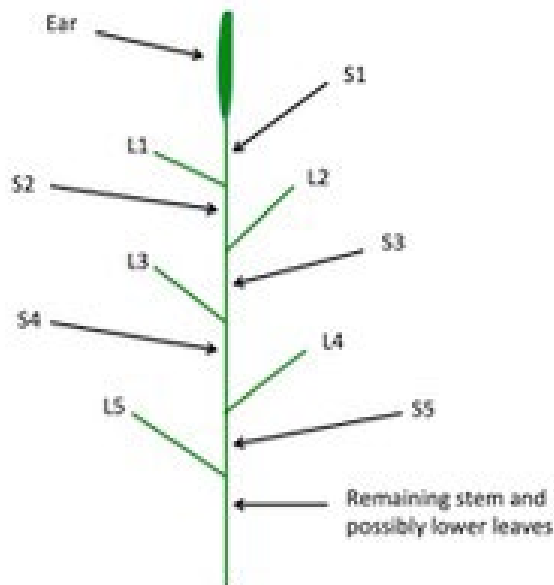


Figure 3. Diagram showing the fractions of barley shoots used for determination of absolute area and % green area (GA).

The % GA was visually estimated for each fraction (upper surfaces of fully emerged leaves, stem sections plus leaf sheaths, peduncle, and ear), then the absolute projected area of each fraction was measured using a leaf area meter (Li-Cor Biosciences, Lincoln, USA). No distinction was made between GA lost specifically to disease lesions or that lost to any associated chlorosis or necrosis for these % GA visual estimates.

PAR interception by the canopy was determined on the same days on which the samples for measurement of crop biomass, absolute area and % GA were collected, using a Sunscan Canopy Analysis System (Delta T Devices Ltd, Cambridge, UK), which records simultaneous measurements of incident PAR above and transmitted PAR below the canopy. Measurements were taken at six different points in each plot. The Sunscan probe was inserted below the canopy at an angle of 45° to the crop rows for the canopy base measurements, to capture representative samples of canopy structure throughout the plot.

Disease severity and fungal growth *in planta* were determined 65 days after sowing (approximately GS 37), then at four further time points at two-week intervals. Ten shoots were selected at random from each plot. Disease severity was visually assessed on the upper surface of each fully emerged leaf. Visual estimates were made of the % area of the leaf covered by spotting and lesions, and of the % area of the leaf that was chlorotic, necrotic, or still green. Leaves were then snap-frozen in liquid nitrogen and stored at -20°C. Due to time constraints, only the leaf below the flag leaf (F-1) was later processed for DNA quantification. The DNA extraction and quantification methodology was as described in Section 2 of this report.

Photosynthetic efficiency was assessed 73 days after sowing (one week before GS 55), then at four further time points at intervals of 8 to 9 days on average. Maximal efficiency of PSII (Fv/Fm) was determined for five randomly selected F-1 leaves per plot using an OS-30p+ Chlorophyll Fluorometer (Opti-Sciences, Hudson, New Hampshire, USA). Leaves were dark-adapted for 30 minutes prior to measurement. Dark-adaptation clips consisted of a light-weight, padded clamp with a sliding shutter to exclude light positioned at the bottom of a hollow tube. The tube was designed to fit the measuring probe of the fluorometer without allowing incident light to reach the area of the leaf which was to be measured. Dark-adaptation clips were placed onto the leaves, and after 30 minutes the fluorometer measuring probe was positioned in the tube, then the shutter was opened for the measurement to be taken. The fluorometer measured minimum fluorescence using a weak, red, modulated light source, then maximal fluorescence using a saturating actinic light (3500 µmol). Measurements were taken in the medial area of the leaf, avoiding the midrib, on green areas initially, until lesions and/or chlorotic/necrotic tissue spread across this area.

The date of canopy senescence was recorded when less than 5% of peduncles remained green. Meteorological data were monitored continuously at the site. Plots were harvested by small plot combine for determination of grain yield. Samples were taken for measurement of mean grain weight (MGW) and grain moisture content was determined gravimetrically after oven drying. Yields and MGW were adjusted and expressed at 15% moisture content.

3.2.3. Calculations and statistical analysis

The fresh and dry weights recorded for crop biomass samples were used to calculate an average dry weight value (kg m^{-2}) for each plot. The total quadrat area from which plants were collected for each sample was, in this case, 0.23 m^{-2} (a total row length of 2 m of plants collected from rows planted with 11.5 cm spacing). Whole sample fresh weight was divided by subsample fresh weight, and the resulting values were then multiplied by subsample dry weight to obtain the dry weight per quadrat. Dry weight m^{-2} was obtained by multiplying the dry weight per quadrat by the quadrat area.

PAR interception by healthy (green) tissue was estimated using methods adapted from Bingham *et al.* (2019) and (Bingham *et al.*, 2021). The measurements of incident and transmitted PAR were used to calculate a canopy area index (*CAI*) representing the total projected area per ground unit area, as shown in Equation 1, using Beer's law analogy and an assumed light extinction coefficient (*k*) of 0.5.

Equation 1

$$CAI = [\ln(I_t/I_o)]/k$$

where I_t is the incident PAR above the canopy and I_o is the transmitted PAR at the canopy base.

The proportional distribution of projected area was calculated using the measurements of absolute area for the sections shown in Figure 3. The projected area was taken as the sum of the absolute areas within five 'layers', then expressed as a fraction of the sum of all the layers. The ear was counted as a separate layer, then leaf layer 1 consisted of the peduncle and the flag leaf lamina, leaf layer 2 consisted of the leaf below the flag leaf and the section of stem plus leaf sheath between that leaf and the flag leaf, and so on down to leaf 5. The stem below leaf 5 was included in leaf layer 5, along with any remaining senesced leaves found there. The fractional distribution of projected area from the measured samples was then used to estimate the *CAI* in each layer as shown in Equation 2.

Equation 2

$$CAI_h = CAI \times fLA_h$$

where CAI_h is the *CAI* of layer h and fLA_h is the projected area of layer h given as a fraction of the total projected area of all layers.

PAR intercepted by each layer was then calculated as shown in Equation 3.

Equation 3

$$I_h = I_{oh} \times [1 - \exp(-k \times CAI_h)]$$

where I_h is the PAR intercepted by layer h , and I_{oh} is the PAR incident on leaf h (calculated as the difference between the daily incident PAR at the top of the canopy and the sum of that daily incident PAR intercepted by all the layers above layer h). k is the assumed light extinction coefficient of 0.5.

PAR intercepted by healthy (green) tissue in each layer was then calculated as shown in Equation 4.

Equation 4

$$HA_{inth} = I_h \times [HAI_h/CAI_h]$$

where HA_{inth} is the healthy area PAR interception by layer h and HAI_h/CAI_h is the healthy (green) fraction of the CAI in layer h (calculated from a weighted average of the measured % GA of the leaf lamina and stem plus leaf sheath for the leaf layers, or from the measured % GA for the ear).

HA_{int} for the canopy as a whole was calculated as the sum of all the individual layers, then expressed as a fraction (F_{PAR}) of the incident PAR for a given day ($I_o \text{ day}$) as shown in Equation 5.

Equation 5

$$F_{PAR} = HA_{int}/I_o \text{ day}$$

To estimate HA_{int} over a selected interval between growth stages, the value of F_{PAR} for each of the bordering growth stages was averaged and multiplied by the sum of the daily incident PAR for the selected interval.

To test whether reductions in light interception resulting from symptom development could account for the yield differences between the fungicide-treated and the inoculated and untreated plots, a predicted yield loss was calculated. The reduction in post anthesis HA_{int} was calculated for each replicate block by subtracting the HA_{int} for inoculated and untreated plots from that of the fungicide-treated plot. This was multiplied by the average post-anthesis RUE for the experiment and the resulting dry matter estimated, adjusted to 15% moisture content. This represents the difference in grain yield at 15% moisture content, assuming that all post-anthesis net dry matter produced is allocated to grain and there are no differences between treatments in the contribution from remobilised stem carbohydrate reserves. Statistical significance of differences between predicted and observed yield losses were tested using a paired t-test for each treatment. All other data were analysed using analysis of variance using GenStat software (19th Edition, VSN International, Hemel Hempstead, UK). Residuals were checked for normality of distribution and homogeneity of variance before analysis.

3.3. Effects of varying rates of leaf senescence on RLS disease development

3.3.1 Experimental design

All seedlings (cv Fairing) were inoculated with *R. collo-cygni* 14 days after sowing, when the third leaf was partially emerged. The inoculation method and plant and fungal growth conditions were as described previously.

Seven days after inoculation with *R. collo-cygni*, a foliar cytokinin spray (0.1 mM 6-Benzylamino/purine (6-BAP) solution) was applied to half of the plants (see methodology for preparation and application below), and a control foliar spray application of sterile distilled water (SDW) was applied to the remaining plants.

After a further seven days (28 days after sowing), half the plants which had previously been treated with cytokinin, and half the plants which had been sprayed with SDW, were given additional nutrients (fertiliser composition and application method were as described in Section 3.2).

Disease progress and leaf senescence were tracked over the course of the experiment by visual assessment, use of a Soil Plant Analysis Development (SPAD) chlorophyll meter, and quantification of *R. collo-cygni* DNA extracted from leaves. The methodology for extraction and quantification of DNA was as described in Section 3.2.

Materials and methods not described in previous sections are detailed below.

3.3.1. Preparation and foliar application of pH 6.5 cytokinin (6-Benzylaminopurine) solution

To make 100 ml of 0.1 mM 6-Benzylaminopurine (6-BAP) solution, 2.5 mg of 6-BAP powder (Sigma-Aldrich, Dorset, UK) was dissolved in 10 ml of 1 M HCl (Sigma-Aldrich, Dorset, UK). This solution was then added to 90 ml of SDW. NaOH tablets (Sigma-Aldrich, Dorset, UK) were added gradually to bring the solution up to pH 6.5.

Polyoxyethylene-sorbitan monolaurate (Tween 20) (Sigma-Aldrich, Dorset, UK) was added at approximately 1 drop per 50 ml to either 6-BAP solution or SDW for the controls to give a final concentration of 0.01% v/v.

Foliar applications were conducted using an air brush (Clarke Wiz Air®, Clarke International, Essex, UK) at an application rate of 0.5 ml per plant. The plants were sprayed evenly from different directions to ensure uniform coverage. Care was taken to carry out the application of 6-BAP and SDW in different rooms, using a large plastic bag around the plants as an additional screen, to

minimise the chance of aerial drift of cytokinin to control plants. Plants that were treated with cytokinin were kept separate from those that were not until the leaves were completely dry.

3.3.2. Measurement of relative leaf-chlorophyll content

Two measurements were made on the adaxial surface of second leaves of intact plants using a SPAD 502 Plus Chlorophyll Meter (Konica Minolta, Warrington, UK). One measurement was made in the distal region of the leaf, approximately mid-way between the tip and centre point of the leaf length. The other was made in the basal section of the leaf, approximately mid-way between the ligule and the centre point of the leaf length. The two measurements from the leaf were averaged.

3.3.3. Data and statistical analysis

264 plants were divided into five randomised blocks of 52 plants each, with 13 replicates in each block. Each replicate consisted of one plant from each of four treatment groups: 1) no cytokinin and no fertiliser; 2) with cytokinin and no fertiliser; 3) no cytokinin and with fertiliser; 4) with cytokinin and with fertiliser. A full description of the treatment regime for these four groups is presented in Table 2.

A subset of plants consisting of five replicates was repeatedly assessed for visual disease development and relative chlorophyll content throughout the experiment; i.e. 1, 2, 3, 4, 5, 8, 11, 15, 18, 20, 22 and 27 days after cytokinin application (d.a.c). These five replicates were destructively sampled for DNA extraction and quantification of *R. collo-cygni* DNA at the end of the experiment (27 d.a.c). Four unique sets of plants (5 replicates on each occasion) were also destructively sampled for DNA extraction and quantification at 1, 5, 11 and 15 days after cytokinin application. Data was analysed using either repeated measures or standard analysis of variance as appropriate using GenStat software (19th Edition, VSN International, Hemel Hempstead, UK). Residuals were checked for normality of distribution and homogeneity of variance before analysis.

Table 2. Senescence experiment treatments

Treatment number	Treatment description	Treatment abbreviation	Treatment colour code
1	Rcc inoculum at 0.5 ml per plant applied 14 days after seeds sown. SDW at 0.5 ml per plant applied 21 days after seeds sown.	no cyt no fert	
2	Rcc inoculum at 0.5 ml per plant applied 14 days after seeds sown. 0.1 mM cytokinin at 0.5 ml per plant applied 21 days after seeds sown.	with cyt no fert	
3	Rcc inoculum at 0.5 ml per plant applied 14 days after seeds sown. SDW at 0.5 ml per plant applied 21 days after seeds sown. 0.06 ml Growmore fertiliser in 10 ml water added to each pot 28, 35 and 42 days after seeds sown.	no cyt with fert	
4	Rcc inoculum at 0.5 ml per plant applied 14 days after seeds sown. 0.1 mM cytokinin at 0.5 ml per plant applied 21 days after seeds sown. 0.06 ml Growmore fertiliser in 10 ml water added to each pot 28, 35 and 42 days after seeds sown.	with cyt with fert	

4. Results

4.1. Impact of ramularia on photosynthesis

4.1.1. Experimental series 1

4.1.1.1 Fungal growth in planta

R. collo-cygni DNA was detected in plants inoculated with fungal mycelium throughout the experiment (Figure 4 and Table 3). A two-way ANOVA with time as a factor did not reveal a significant interaction between time and treatment. Fungal biomass in second leaves, as indicated by *R. collo-cygni* DNA, did not increase, or decrease significantly during the experiment.

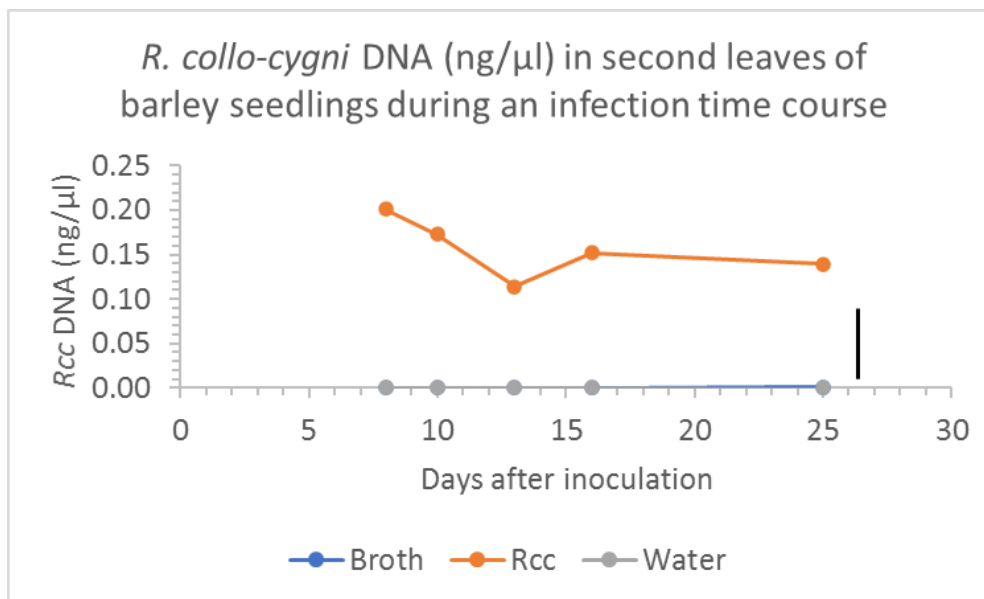


Figure 4. *R. collo-cygni* DNA in second leaves of barley seedlings cv. Concerto during disease development. Rcc = plants inoculated with *R. collo-cygni* mycelial suspension grown in Potato Dextrose Broth (PDB). Broth = plants inoculated with a control treatment of PDB. Water = plants inoculated with a control treatment of sterile distilled water. Black vertical line to the right of the graph represents the least significant difference (l.s.d., $P=0.05$) for Treatment.Days after inoculation from a two-way ANOVA with inoculation treatment and time as factors. Note that symbols for Broth treatment are hidden by those for Water.

Table 3. Mean values for *R. collo-cygni* DNA quantity (ng/μl) in second leaves of barley seedlings during disease development.

	Days after inoculation				
	8	10	13	16	25
Broth	0.00	0.00	0.00	0.00	0.00
Rcc	0.20	0.17	0.11	0.15	0.14
Water	0.00	0.00	0.00	0.00	0.00

Table 4. ANOVA analysis results from a two-way ANOVA with inoculation treatment and time after inoculation as factors for *R. collo-cygni* DNA quantity in second leaves of barley seedlings during disease development.

	P value	I.s.d.
Treatment	<0.001	0.034
Days after inoculation	0.723	0.043
Treatment.Days after inoculation	0.839	0.075

4.1.1.2 Visible symptom development and green leaf area

The first symptoms (lesions) were observed on one infected leaf around 10 days after inoculation (Figure 5 and Table 5). Symptoms had increased marginally on infected leaves by 16 days after inoculation, and by 25 days after inoculation an average of 13 % of the measured leaf area was covered by lesions in infected leaves. At both 13 and 16 days after inoculation, only one infected leaf (out of 5) displayed more advanced symptoms, with around 20 % of the measured leaf area covered by lesions. Other infected leaves at these time points had either no or very mild symptoms, with only 0 – 2 % of the measured leaf area covered by lesions. By 25 days after inoculation symptoms were more advanced in all infected leaves; however, there was still some variation, with the percentage of measured leaf area covered by lesions ranging from 5 – 20 %. Water and broth controls remained free of any lesions throughout the experiment. Control plants maintained 100 % green leaf area (GLA) within the measured area throughout the experiment (Table 5). Infected leaves lost 5 % of GLA on average by 16 days after inoculation, then a further 20 % by 25 days after inoculation. The % GLA observed in infected leaves at 25 days after inoculation ranged from 60 – 95 %. GLA was reduced in infected leaves by a combination of lesions and, in some cases, areas of chlorotic tissue extending beyond the lesions (Figure 6).

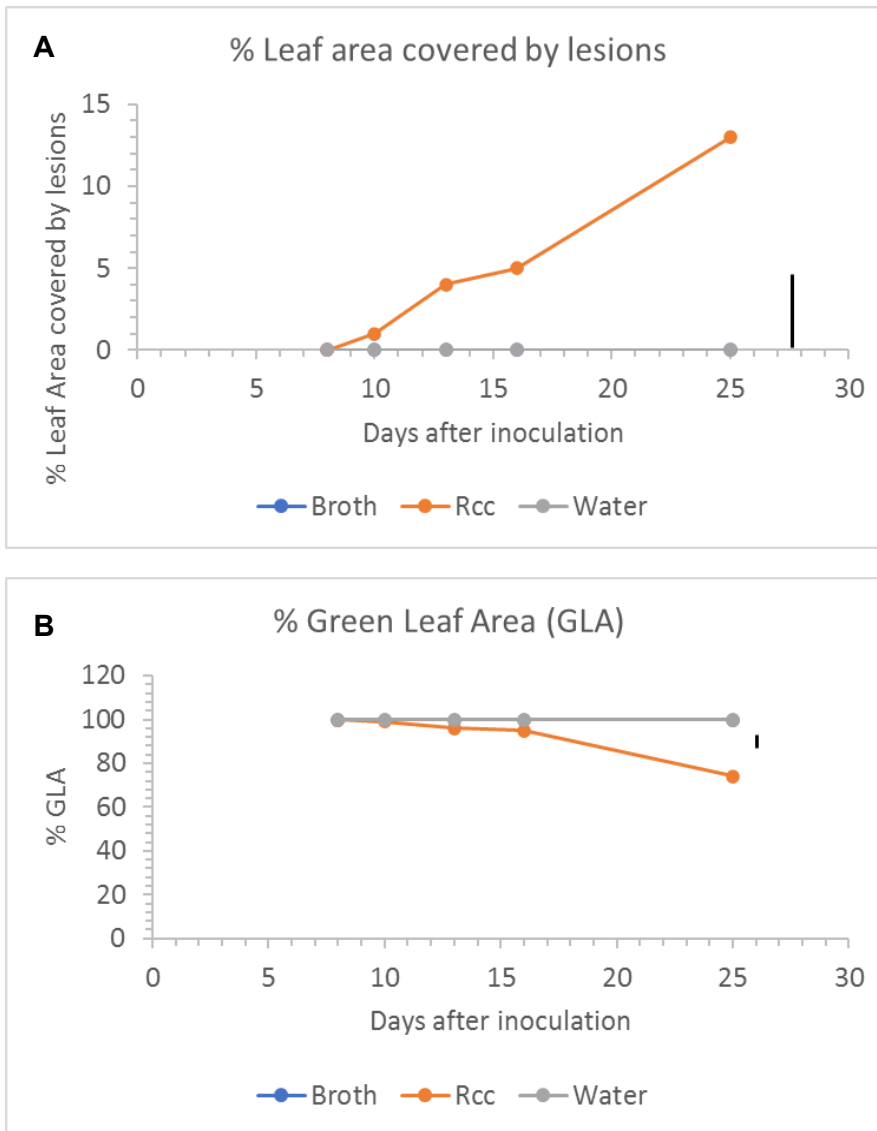


Figure 5. Visual disease progress over time. A) RLS lesion development and B) Green leaf area (both as percentages of total measured leaf area). Second leaves of barley cv. Concerto seedlings inoculated with *R. collo-cygni* (Rcc) and control leaves sprayed with water or potato dextrose broth. Black vertical lines to the right of the graphs represent the least significant difference (l.s.d., $P=0.05$) for Treatment. Days after inoculation from a two-way ANOVA with inoculation and time as factors. Symbols for Broth are hidden by those for Water.

Table 5. Mean % leaf area covered by lesions and mean % green leaf area (GLA) over an infection time course.

Treatment	Days after inoculation				
	8	10	13	16	25
% Lesions					
Broth	0.0	0.0	0.0	0.0	0.0
Rcc	0.0	0.8	4.2	4.8	12.5
Water	0.0	0.0	0.0	0.0	0.0
% GLA					
Broth	100.0	100.0	100.0	100.0	100.0
Rcc	100.0	99.2	95.8	95.2	73.8
Water	100.0	100.0	100.0	100.0	100.0

Table 6 Two-way ANOVA analysis results for % leaf area covered by lesions and % green leaf area (GLA) over an infection time course.

	P value	I.s.d.
% Lesions		
Treatment	<0.001	1.980
Days after inoculation	0.016	2.556
Treatment.Days after inoculation	0.003	4.428
% GLA		
Treatment	<0.001	2.442
Days after inoculation	<0.001	3.153
Treatment.Days after inoculation	<0.001	5.461

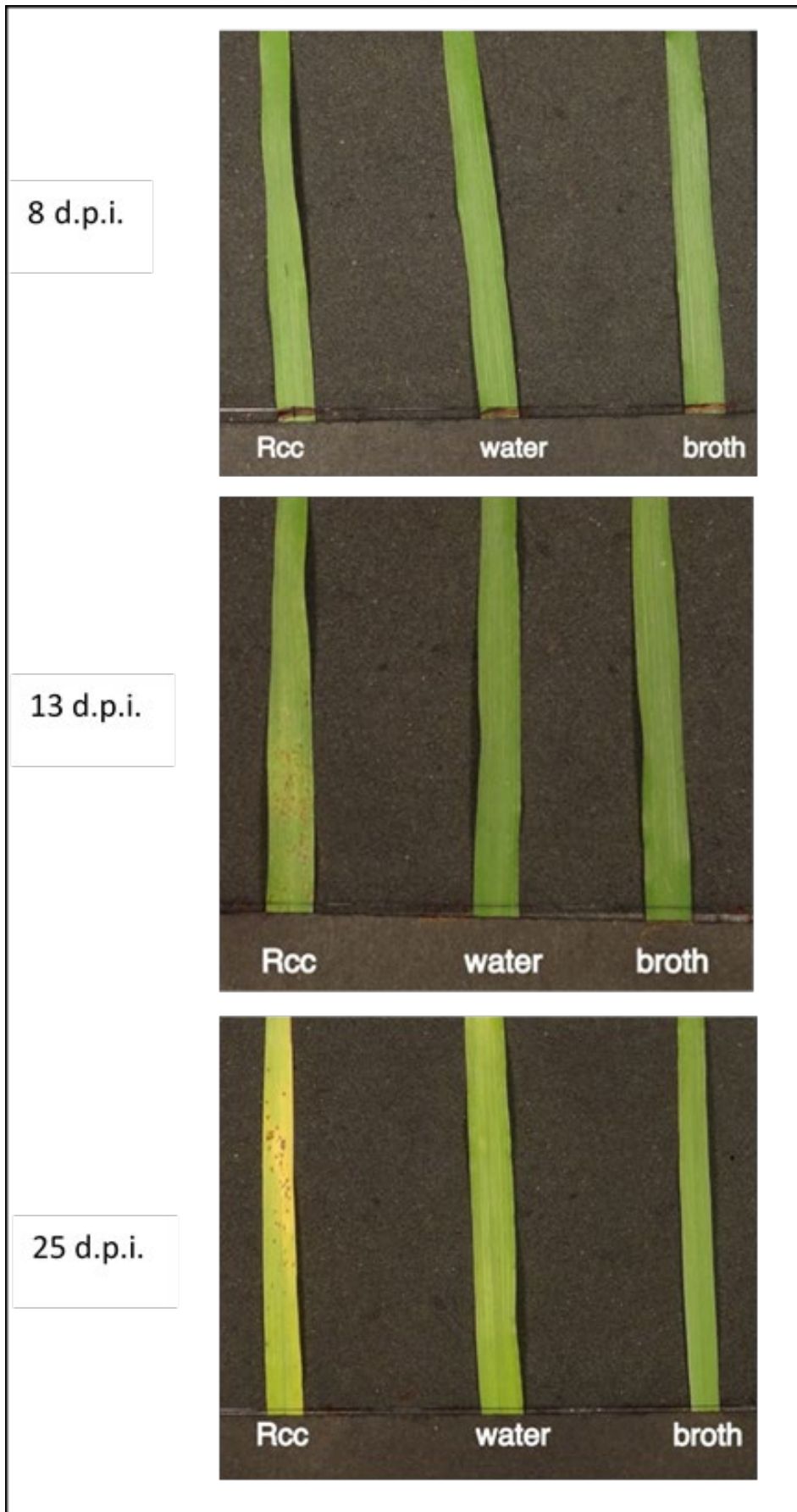


Figure 6. Photographs of second leaves of barley cv. Concerto seedlings inoculated with *R. collo-cygni* (Rcc) and control leaves sprayed with water or potato dextrose broth. Photographs taken at 8, 13 and 25 days post inoculation (d.p.i.).

4.1.1.3 Chlorophyll fluorescence imaging

Chlorophyll fluorescence imaging – steady state photosynthesis

Maximal efficiency of PSII (Fv/Fm) (Figure 7 & Table 7) increased with leaf age for all treatments until 10 days after inoculation. Values peaked by 10 days after inoculation for control plants, and by 13 days after inoculation for plants infected with *R. collo-cygni*. Fv/Fm values dropped between 13 and 16 days after inoculation for all treatments. Between 16 and 25 days after inoculation, values for control plants remained relatively stable, while values for infected plants dropped again, coinciding with increasing symptom severity. A two-way ANOVA found a close to significant ($P = 0.053$) effect of treatment. The interaction between treatment and time had a P value of 0.069 indicating a weak effect.

The effects of inoculation treatments on operating efficiency of PSII (Φ PSII), non-photochemical quenching (NPQ) and Electron Transport Rate (ETR) at the end of the induction period after the leaves had reached steady state are presented in 7 and 7. A two-way ANOVA found no significant effect of treatment on steady state photosynthesis during this experiment, but photosynthetic parameters did change significantly ($P < 0.001$) with time (Table 8). Φ PSII values remained quite stable throughout the infection time course. By 25 days after inoculation, Φ PSII values had dropped in both infected and control plants. Steady state NPQ values rose for control plants between 8 and 13 days after inoculation; however, no increase was observed in infected plants.

There was a reduction in steady state NPQ values for both infected and control plants between 16 and 25 days after inoculation. Steady state ETR values remained quite stable until 16 days after inoculation. There was a reduction in steady state ETR values for both infected and control plants between 16 and 25 days after inoculation.

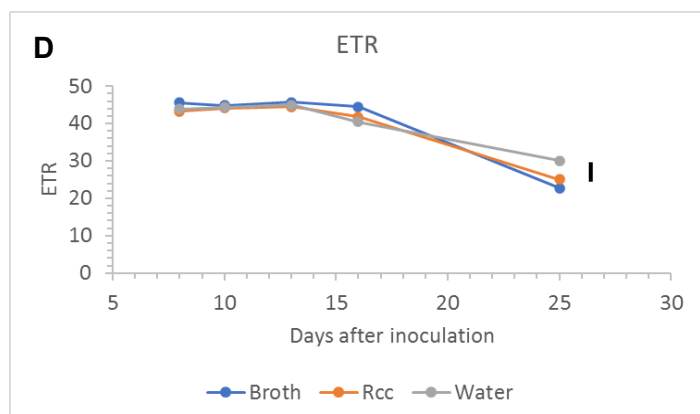
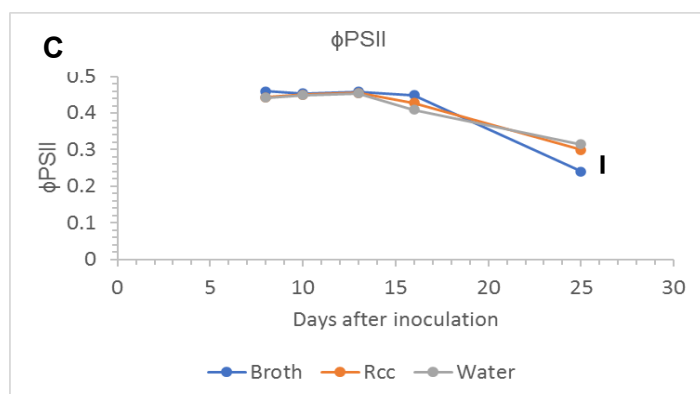
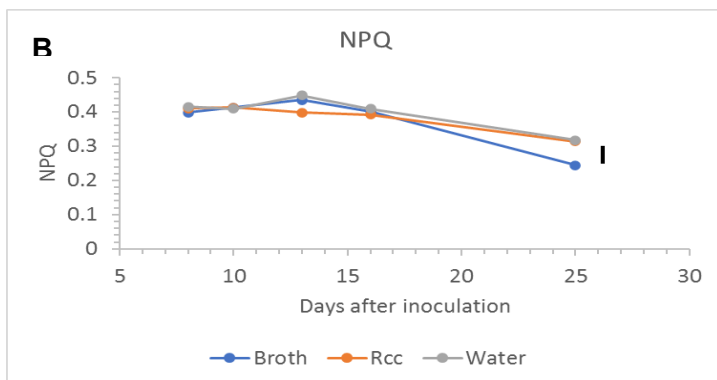
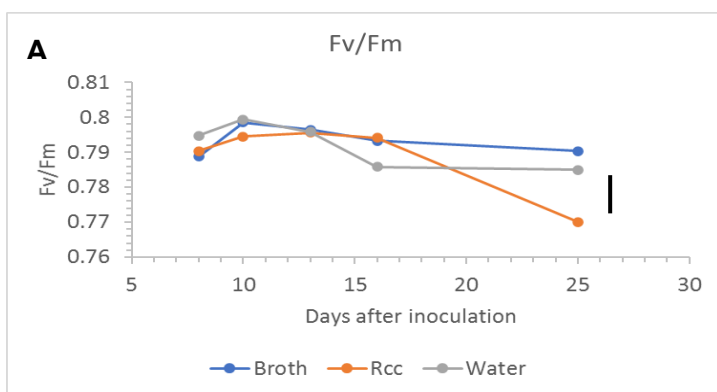


Figure 7. Chlorophyll fluorescence parameters: A) Maximal efficiency of PSII (F_v/F_m); B) Non-photochemical quenching (NPQ); C) Operating efficiency of PSII (ϕ PSII); D) Electron Transport Rate (ETR) at steady state photosynthesis ($230 \mu\text{mol m}^{-2}\text{s}^{-1}$ PAR), measured in second leaves of barley seedlings over an infection time course.

Table 7. Mean values for chlorophyll fluorescence parameters at steady state ($230 \mu\text{mol m}^{-2} \text{s}^{-1}$), measured in second leaves of barley seedlings over an infection time course.

	Days after inoculation				
	8	10	13	16	25
Fv/Fm					
Broth	0.79	0.80	0.80	0.79	0.79
Rcc	0.79	0.79	0.80	0.79	0.77
Water	0.79	0.80	0.80	0.79	0.79
NPQ					
Broth	0.40	0.41	0.44	0.40	0.24
Rcc	0.41	0.41	0.40	0.39	0.31
Water	0.42	0.41	0.45	0.41	0.32
ϕPSII					
Broth	0.46	0.45	0.46	0.45	0.24
Rcc	0.44	0.45	0.46	0.43	0.30
Water	0.44	0.45	0.45	0.41	0.31
ETR					
Broth	45.61	44.91	45.71	44.52	22.69
Rcc	43.24	44.13	44.44	41.83	25.09
Water	43.82	44.32	44.96	40.44	30.03

Table 8. Chlorophyll fluorescence imaging – quenching analysis

	P value	l.s.d.
Fv/Fm		
Treatment	0.053	0.005
Days after inoculation	<0.001	0.006
Treatment.Days after inoculation	0.069	0.010
NPQ		
Treatment	0.233	0.026
Days after inoculation	<0.001	0.033
Treatment.Days after inoculation	0.329	0.058
ϕPSII		
Treatment	0.962	0.020
Days after inoculation	<0.001	0.026
Treatment.Days after inoculation	0.058	0.044
ETR		
Treatment	0.578	2.101
Days after inoculation	<0.001	2.712
Treatment.Days after inoculation	0.114	4.697

An analysis of the whole light induction curve was conducted at each sampling time (days after inoculation) to investigate whether inoculation treatments had any effect on chlorophyll fluorescence variables not observed after steady state had been reached. The analysis was by repeated measures ANOVA using time after the actinic light was switched on as the repeated

measure factor. For each of the fluorescence variables, Φ PSII, NPQ and ETR, there was a significant ($P < 0.001$) effect of time, but no significant effect of treatment nor interaction between treatment and time for any of the sampling dates (Table 8). This indicates that the induction kinetics were similar across all treatments regardless of the date the leaves were sampled after inoculation. Mean induction curves for days 8, 13 and 25 are presented in Figure 8, 9 and 10 as examples. They illustrate changes in the induction kinetics with leaf ageing.

In leaves sampled eight days after inoculation, Φ PSII values rose steadily after the actinic light was switched on, before levelling out once steady state photosynthesis was reached (Figure 8). A slight dip in Φ PSII values was observed for all treatments around 200 s. A similar pattern occurred at subsequent sampling points (13 and 25 dai), although no dip was observed during the induction period. By 25 days after inoculation, Φ PSII values increased less rapidly through the induction period and the final values were substantially lower than at previous sampling points in both infected and control plants.

Eight days after inoculation, NPQ values rose rapidly for all treatments until around 80 s after the actinic light was switched on, at which point a transient drop to lower values was observed, before values rose again more slowly until steady state was achieved (Figure 9). Steady state was reached at around 320 s after the actinic light was switched on. As leaves aged, this pattern of NPQ changed. The initial peak and transient drop in NPQ between 80 and 180 s were less pronounced and the slow rise in NPQ after 180 s continued for the entire measurement period, suggesting a steady state was not achieved for NPQ in the older leaves. By 25 days after inoculation, NPQ values throughout the induction curve were lower than at previous sampling points in both infected and control plants.

The induction kinetics for ETR followed the same pattern as Φ PSII (Figure 15). Thus, there was an initial peak at 140 s followed by a transient dip at 200s before the rise to steady state by the end of the measurement period. As leaves aged, the transient changes were lost and the increase in ETR was less rapid.

Table 9. P values from repeated measures ANOVA during photosynthetic induction of dark-adapted plants over an infection time course.

Number of reps	Days after inoculation	ϕ PSII P values		
		Time	Treatment	Time.Treatment
4	8	<0.001	0.941	0.469
6	10	<0.001	0.650	0.864
5	13	<0.001	0.981	0.955
4	16	<0.001	0.068	0.381
3	25	<0.001	0.602	0.497
Number of reps	Days after inoculation	NPQ P values		
		Time	Treatment	Time.Treatment
4	8	<0.001	0.876	0.838
6	10	<0.001	0.533	0.826
5	13	<0.001	0.510	0.666
4	16	<0.001	0.352	0.676
3	25	<0.001	0.578	0.750
Number of reps	Days after inoculation	ETR P values		
		Time	Treatment	Time.Treatment
4	8	<0.001	0.997	0.422
6	10	<0.001	0.916	0.771
5	13	<0.001	0.982	0.955
4	16	<0.001	0.066	0.386
3	25	<0.001	0.722	0.672

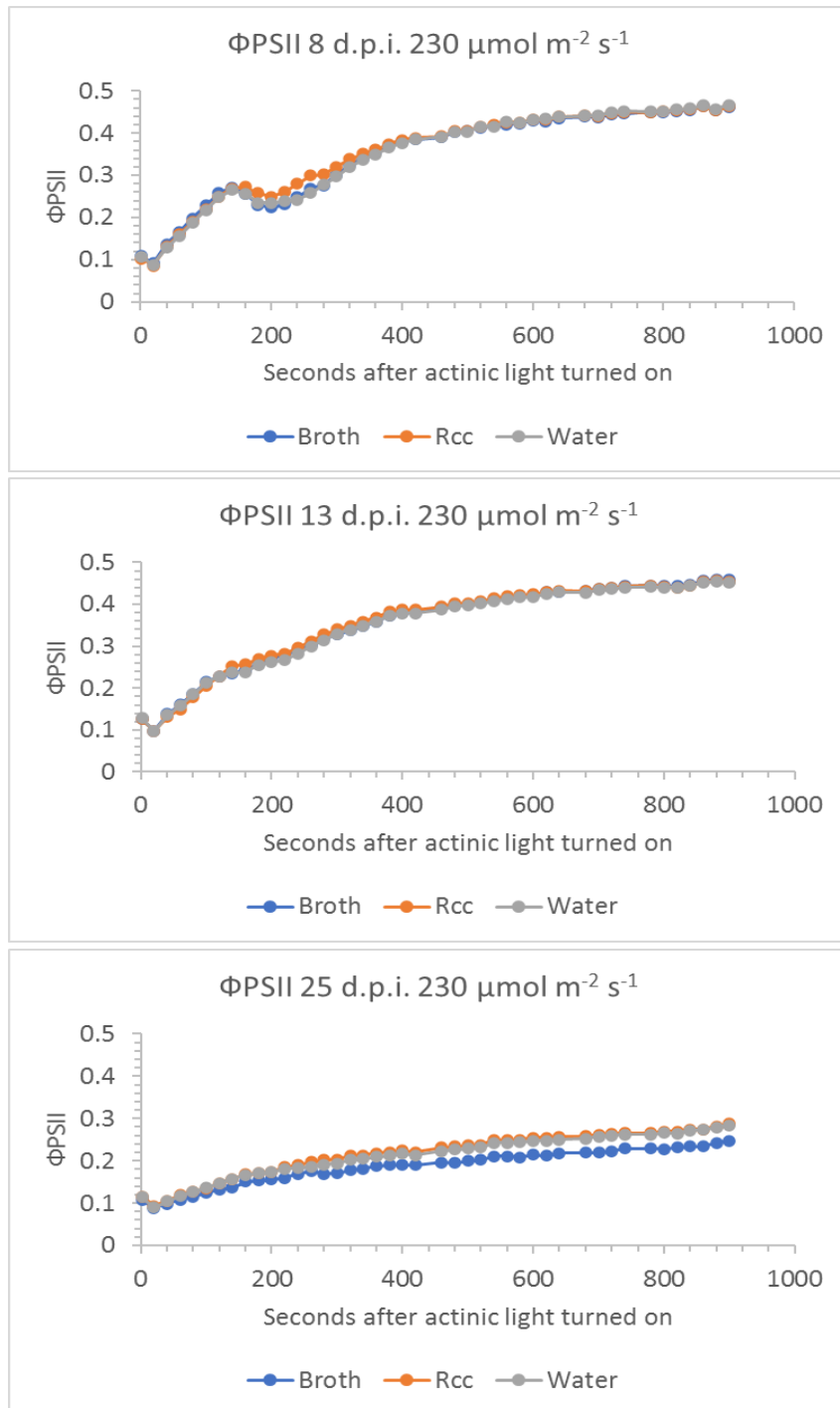


Figure 8. Photosynthetic operating efficiency (Φ_{PSII}) measured during photosynthetic induction of dark-adapted leaves with an actinic irradiance of $230 \mu\text{mol m}^{-2} \text{s}^{-1}$ PAR. Each point is the mean of 4 (8 dpi), 5 (13 dpi) and 3 (25 dpi) replicates. Error bars are omitted for clarity.

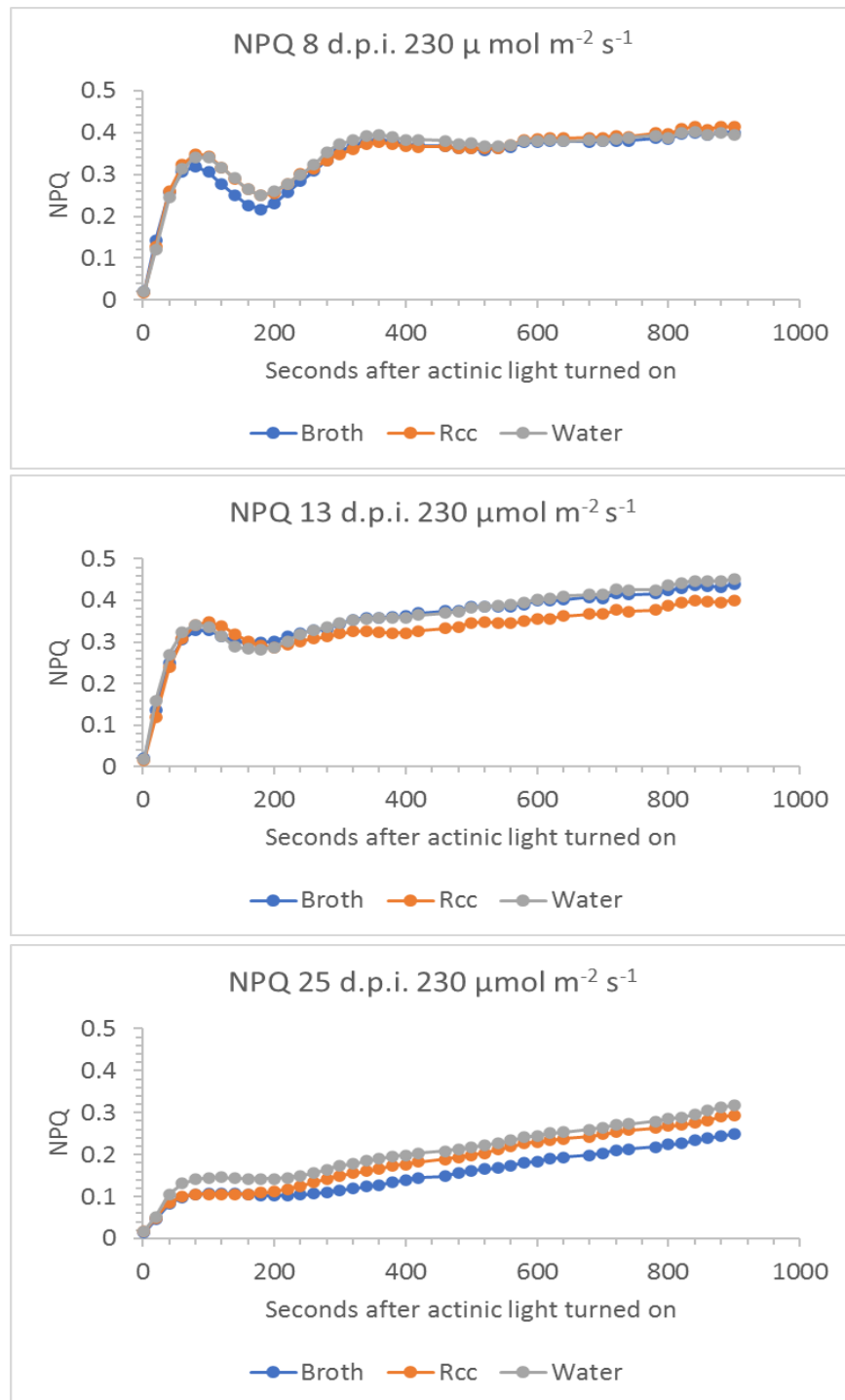


Figure 9. Non-photochemical quenching (NPQ) measured during photosynthetic induction of dark-adapted leaves with an actinic irradiance of $230 \mu\text{mol m}^{-2} \text{s}^{-1}$ PAR. Each point is the mean of 4 (8 dpi), 5 (13 dpi) and 3 (25 dpi) replicates. Error bars are omitted for clarity.

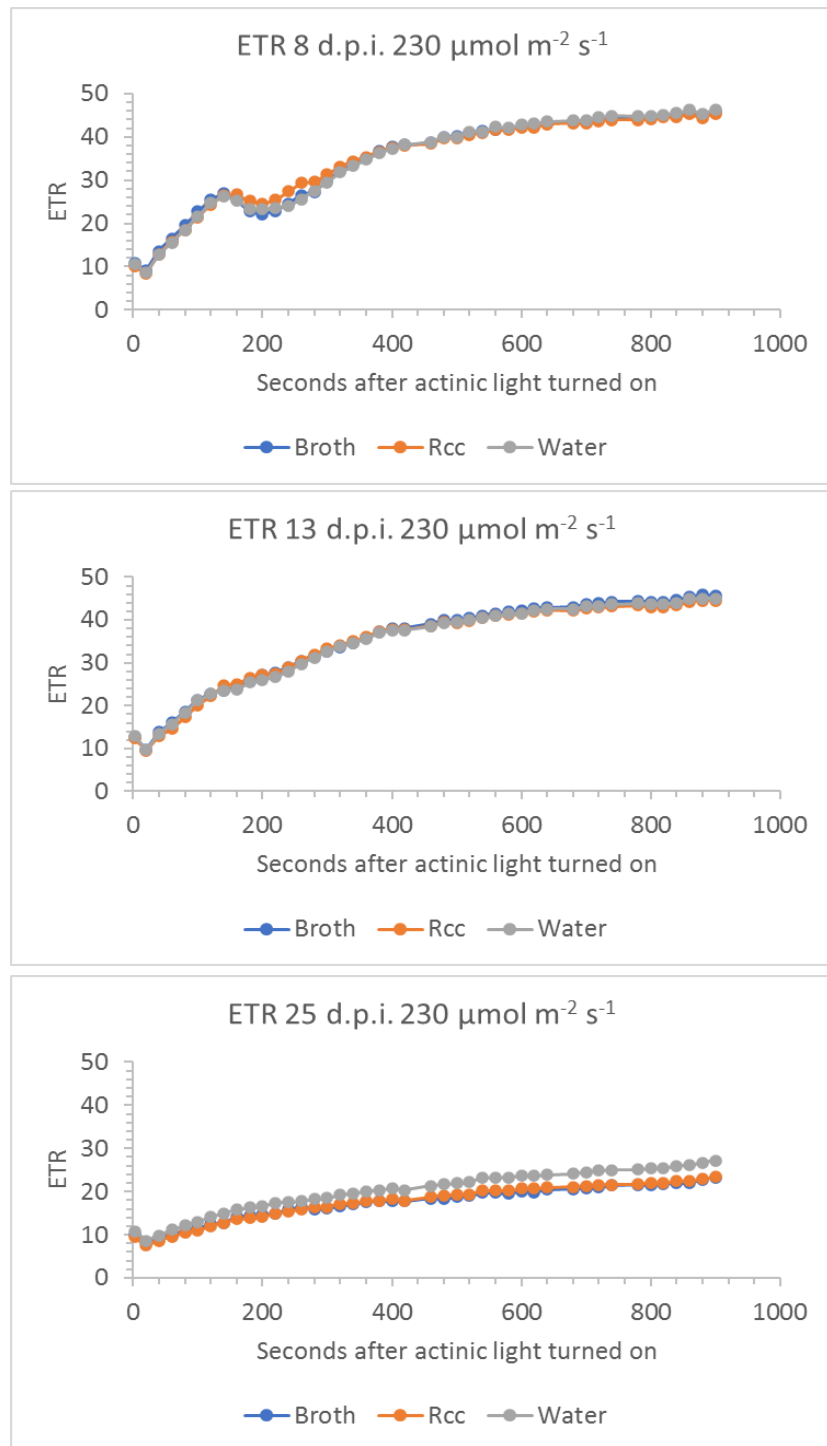


Figure 10. Electron transport rate (ETR) measured during photosynthetic induction of dark-adapted leaves with an actinic irradiance of $230 \mu\text{mol m}^{-2} \text{s}^{-1}$ PAR. Each point is the mean of 4 (8 dpi), 5 (13 dpi) and 3 (25 dpi) replicates. Error bars are omitted for clarity.

4.1.2. Experimental series 2

Experimental series 2 used barley seedlings cv. Fairing. In this experimental series, the same set of leaves were measured at each time point. Chlorophyll fluorescence imaging and infra-red gas analysis were both used to measure the same set of leaves. A higher actinic light intensity period was included in the chlorophyll fluorescence imaging protocol, in addition to the PAR $230 \mu\text{mol m}^{-2} \text{s}^{-1}$ used in experimental series 1, and an additional analysis was conducted on transects taken across chlorophyll fluorescence images of leaves.

4.1.2.1 Visible symptom development and green leaf area

In Experimental series 2, the first symptoms were observed on infected leaves around 18 days after inoculation. Between 18 and 26 days after inoculation, the mean percentage of the infected leaves covered by lesions increased from 2 % to 5 %. The mean % green leaf area of infected leaves fell from 100 % to 86 %, between 18 and 26 days after inoculation. The control treatments did not develop any symptoms. Overall, visible symptom expression was quite low in this experiment.

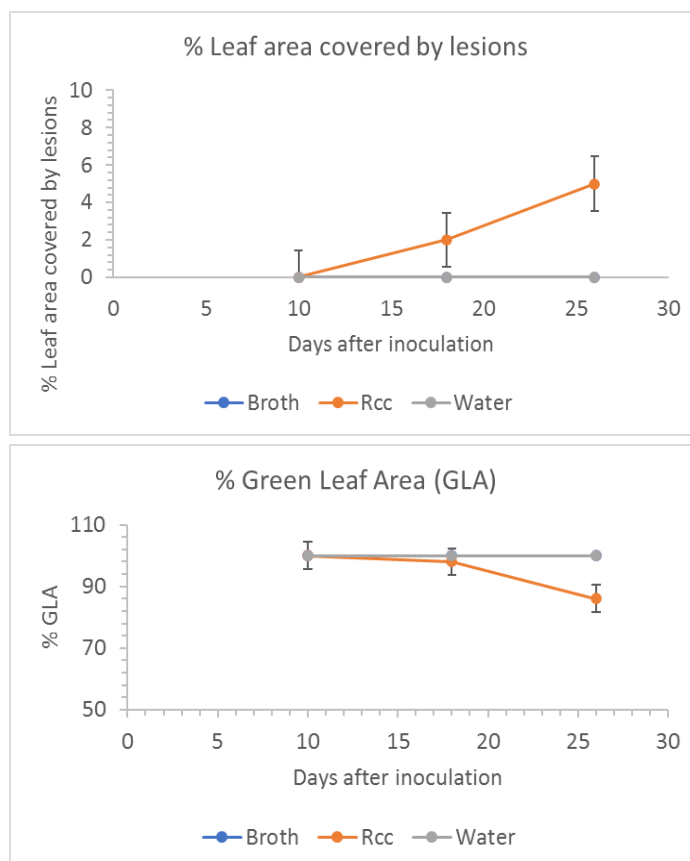


Figure 11. *Ramularia* leaf spot severity (%) and % green leaf area (GLA) of second leaves of barley seedlings cv. Fairing over the time course of an infection. Values are means \pm SEM of 6 replicates. Treatments: Rcc = plants inoculated with *R. collo-cygni* mycelial suspension grown in Potato Dextrose Broth (PDB). Broth = plants inoculated with a control treatment of PDB. Water = plants inoculated with a control treatment of sterile distilled water. Symbols for broth treated plants are hidden by those for water controls.

4.1.2.2 Chlorophyll fluorescence imaging

Results from 10 d.p.i do not include measurements taken at the higher light level, as leaf movement during the time these measurements were being taken rendered them invalid. Fv/Fm value averages for all treatments decreased slightly over time, although none dropped below 0.801, and the treatments did not differ significantly ($P>0.05$) from each other at any of the three time points when measurements were taken (Figure 12 and Table 10). There was a greater decrease in Fv/Fm value for infected leaves between 18 and 26 d.p.i., after symptom appearance, than for control treatments. Fv/Fm values decreased by 0.009, 0.002 and 0.001 for infected, broth-control, and water-control treatments, respectively between 18 and 26 d.p.i.

Chlorophyll fluorescence imaging – steady state

Steady state Φ_{PSII} values did not differ ($P>0.05$) between treatments at either actinic irradiance or measurement occasion (Figure 18 and Table 10). The operating efficiency (Φ_{PSII}) was greater at the growth irradiance of $230 \mu\text{mol m}^{-2} \text{s}^{-1}$ PAR than $530 \mu\text{mol m}^{-2} \text{s}^{-1}$ PAR. For all treatments Φ_{PSII} also decreased over time.

Steady state NPQ values did not differ ($P>0.05$) between treatments at either actinic irradiance or measurement occasion (Figure 19 & Table 10). NPQ was greater at an irradiance of $530 \mu\text{mol m}^{-2} \text{s}^{-1}$ PAR than the growth irradiance of $230 \mu\text{mol m}^{-2} \text{s}^{-1}$ PAR on all measurement occasions. Similarly, ETR did not differ ($P>0.05$) between treatments at either actinic irradiance or measurement occasion (Figure 20 and Table 10). The electron rate was greater at an irradiance of $530 \mu\text{mol m}^{-2} \text{s}^{-1}$ PAR than the growth irradiance of $230 \mu\text{mol m}^{-2} \text{s}^{-1}$ PAR. As with Φ_{PSII} , ETR declined with leaf age (d.p.i).

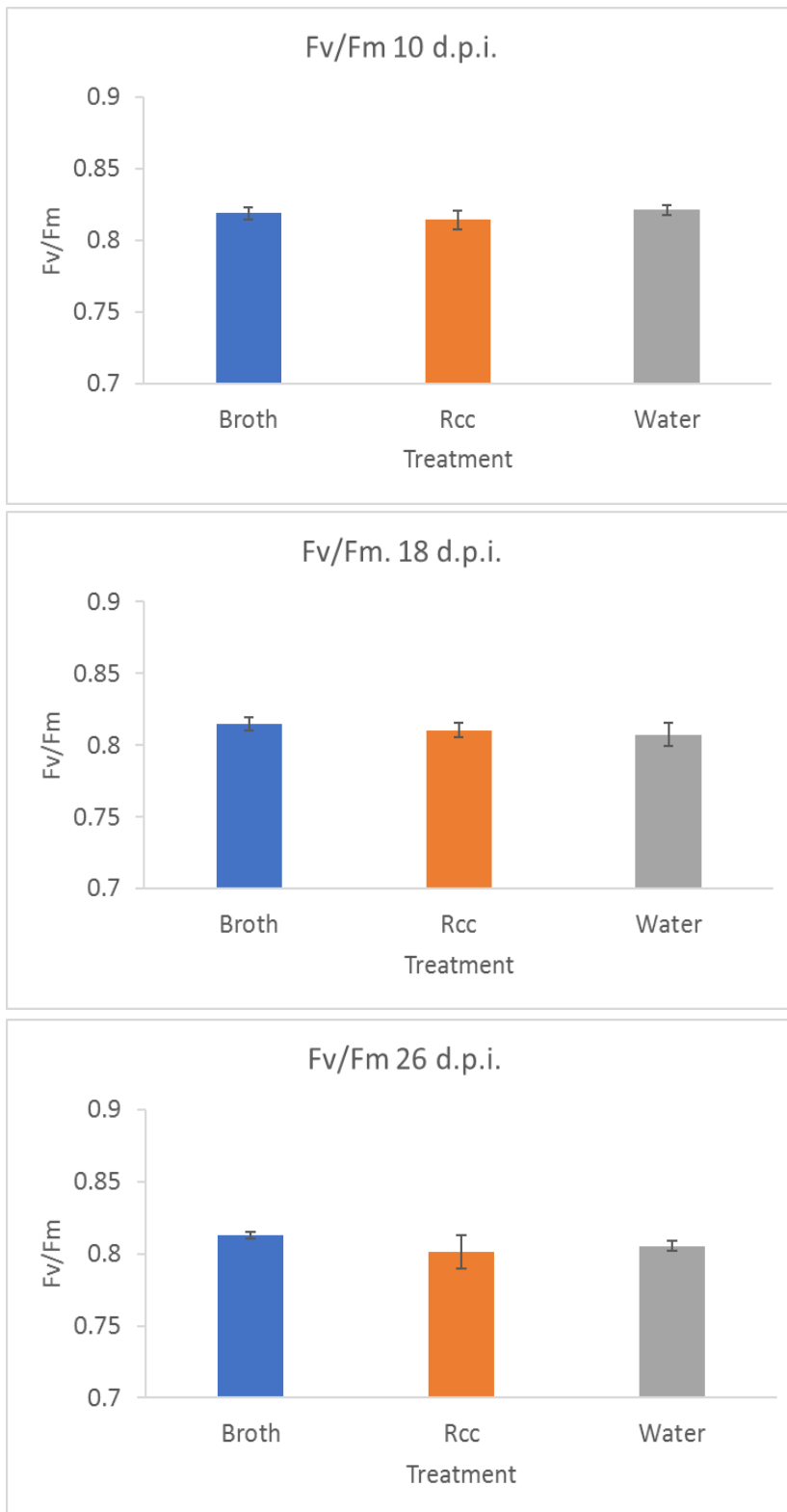


Figure 12. Maximal efficiency of PSII (Fv/Fm). N = at least 5.

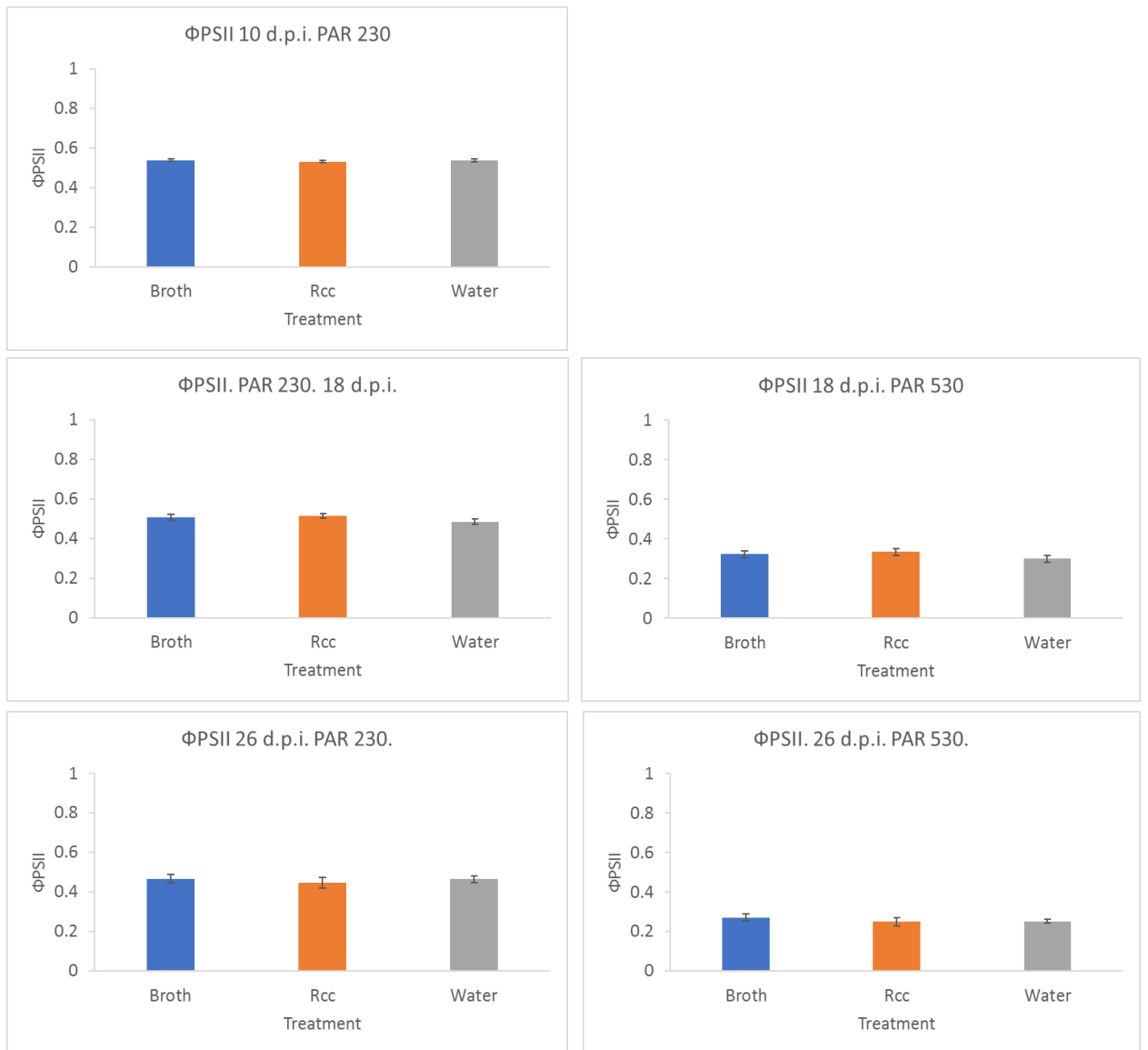


Figure 13. Φ_{PSII} at steady state photosynthesis. At 10 d.p.i. $n =$ at least 4. At 18 d.p.i. $n =$ 6 for both light intensities. At 26 d.p.i. $n =$ at least 5 for $230 \mu\text{mol m}^{-2} \text{s}^{-1}$ and at least 4 for $530 \mu\text{mol m}^{-2} \text{s}^{-1}$.

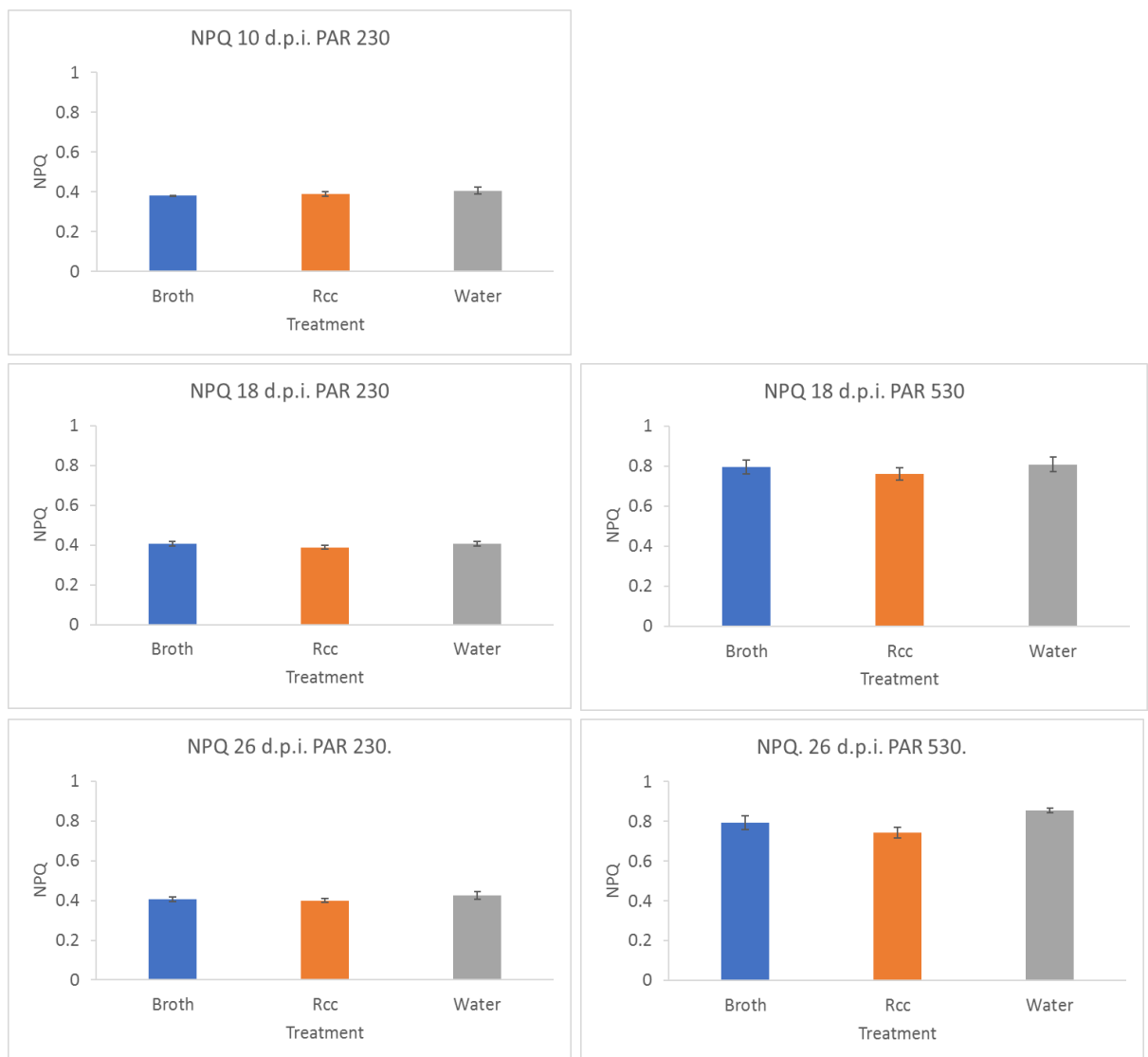


Figure 14. NPQ at steady state photosynthesis. At 10 d.p.i. $n =$ at least 4. At 18 d.p.i. $n = 6$ for both light intensities. At 26 d.p.i. $n =$ at least 5 for $230 \mu\text{mol m}^{-2} \text{s}^{-1}$ and at least 4 for $530 \mu\text{mol m}^{-2} \text{s}^{-1}$.

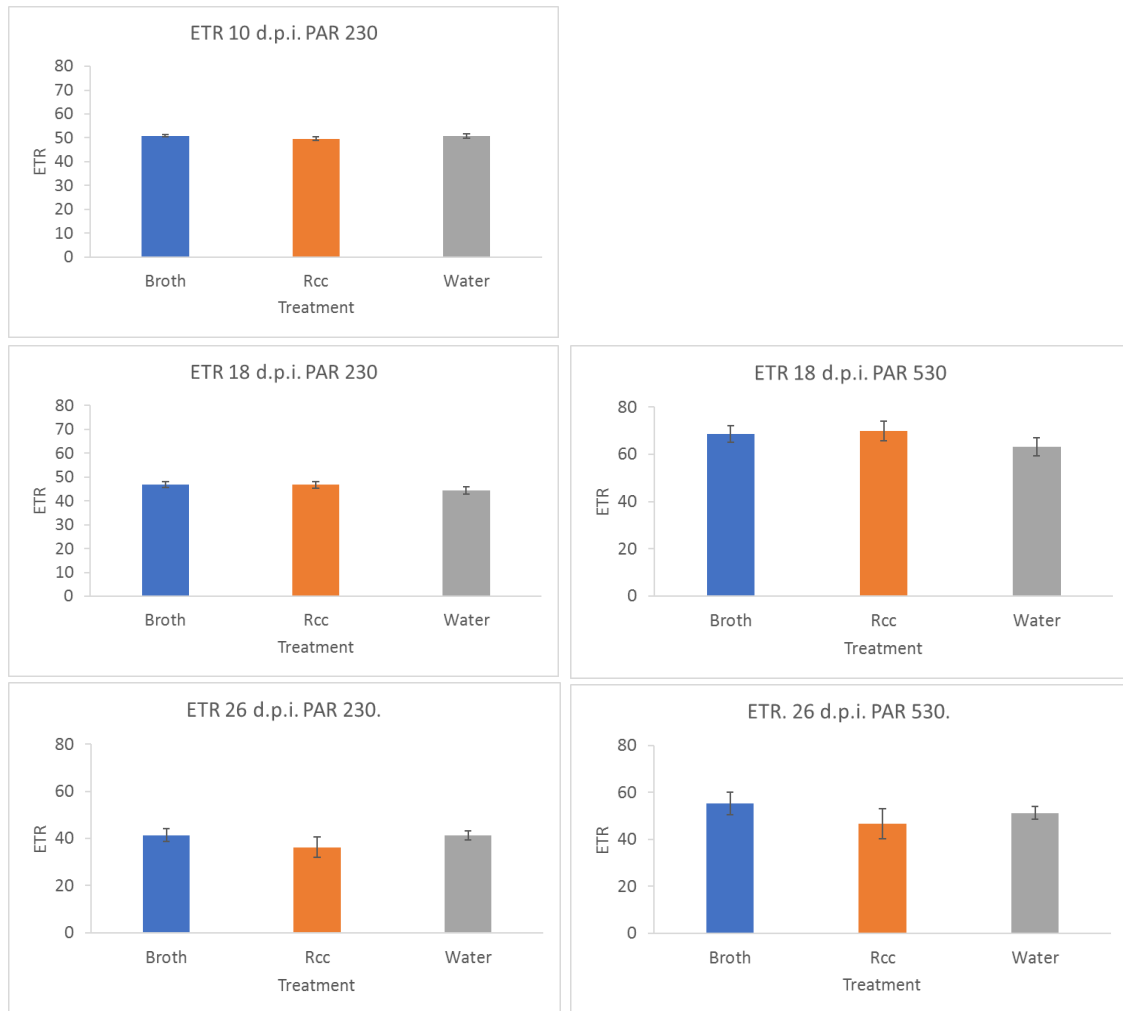


Figure 15. ETR at steady state photosynthesis. At 10 d.p.i. $n =$ at least 4. At 18 d.p.i. $n =$ 6 for both light intensities. At 26 d.p.i. $n =$ at least 5 for $230 \mu\text{mol m}^{-2} \text{s}^{-1}$ and at least 4 for $530 \mu\text{mol m}^{-2} \text{s}^{-1}$.

Table 10. Mean values for chlorophyll fluorescence parameters at steady state photosynthesis.

Treatment	PAR ($\mu\text{mol m}^{-2} \text{s}^{-1}$)	Days after inoculation		
		10	18	26
Fv/Fm				
Broth	NA	0.82	0.81	0.81
Rcc	NA	0.82	0.81	0.80
Water	NA	0.81	0.81	0.81
NPQ				
Broth	230	0.38	0.41	0.41
Broth	530	NA	0.80	0.79
Rcc	230	0.39	0.39	0.40
Rcc	530	NA	0.76	0.74
Water	230	0.41	0.41	0.43
Water	530	NA	0.81	0.85
ϕPSII				
Broth	230	0.54	0.51	0.47
Broth	530	NA	0.32	0.27
Rcc	230	0.53	0.51	0.45
Rcc	530	NA	0.33	0.25
Water	230	0.54	0.48	0.46
Water	530	NA	0.30	0.25
ETR				
Broth	230	50.83	46.71	41.45
Broth	530	NA	68.60	55.40
Rcc	230	49.67	46.74	36.24
Rcc	530	NA	69.90	46.70
Water	230	50.64	44.37	41.30
Water	530	NA	63.20	51.20

Table 11. P values for chlorophyll fluorescence parameters at steady state photosynthesis.

Days after inoculation	Minimum number of reps	Actinic light intensity ($\mu\text{mol m}^{-2} \text{s}^{-1}$)	Variable	P value
10	4	230	Fv/Fm	0.614
10	4	230	ΦPSII	0.704
10	4	230	NPQ	0.376
10	4	230	ETR	0.584
18	6	230	Fv/Fm	0.697
18	6	230	ΦPSII	0.355
18	6	230	NPQ	0.466
18	6	230	ETR	0.412
18	6	530	ΦPSII	0.386
18	6	530	NPQ	0.604
18	6	530	ETR	0.443
26	5	230	Fv/Fm	0.530
26	5	230	ΦPSII	0.789
26	5	230	NPQ	0.402
26	5	230	ETR	0.465
26	4	530	ΦPSII	0.647
26	4	530	NPQ	0.070
26	4	530	ETR	0.501

4.1.2.3 Chlorophyll fluorescence imaging – quenching analysis

An analysis of each stage of the induction curve (i.e. after the initial actinic light was switched on and again after its irradiance was increased to $530 \mu\text{mol m}^{-2} \text{s}^{-1}$) was conducted by repeated measures ANOVA, where time during induction was the repeated measure. The aim was to determine whether treatments had discernible effects on the induction kinetics prior to the attainment of steady state. The analysis did not reveal any significant treatment effects or interactions between treatment and time at either light intensity for ΦPSII , NPQ or ETR at any stage of this experiment (Table 12). The full induction curves are shown in Figure 16, 17 and 18 .

Following dark adaptation and switching on the actinic light, ΦPSII , NPQ and ETR demonstrated similar kinetics to those described in experiment 1. However, the changes observed with leaf age appeared to be less pronounced in experiment 2, especially for NPQ. Thus, the initial peak and transient drop in NPQ was apparent in leaves at all days after inoculation in experiment 2.

After increasing the irradiance there was an immediate decrease in ΦPSII and increase in ETR with values remaining relatively constant thereafter. By contrast NPQ showed a rapid initial increase followed by a more gradual rise over the course of the measurement period.

Table 1. ANOVA table repeated measures experiment 2.

Number of reps	PAR	Days after inoculation	ϕ PSII P values		
			Time	Treatment	Time.Treatment
4	230	10	<.001	0.367	0.601
6	230	18	<.001	0.291	0.719
5	230	26	<.001	0.596	0.753
6	530	18	<.001	0.391	0.999
4	530	26	<.001	0.641	0.987
Number of reps	PAR	Days after inoculation	NPQ P values		
			Time	Treatment	Time.Treatment
4	230	10	<.001	0.375	0.078
6	230	18	<.001	0.950	0.399
5	230	26	<.001	0.122	0.290
6	530	18	<.001	0.730	0.384
4	530	26	<.001	0.102	0.261
Number of reps	PAR	Days after inoculation	ETR P values		
			Time	Treatment	Time.Treatment
4	230	10	<.001	0.406	0.581
6	230	18	<.001	0.364	0.696
5	230	26	<.001	0.371	0.464
6	530	18	<.001	0.443	0.999
4	530	26	<.001	0.592	0.991

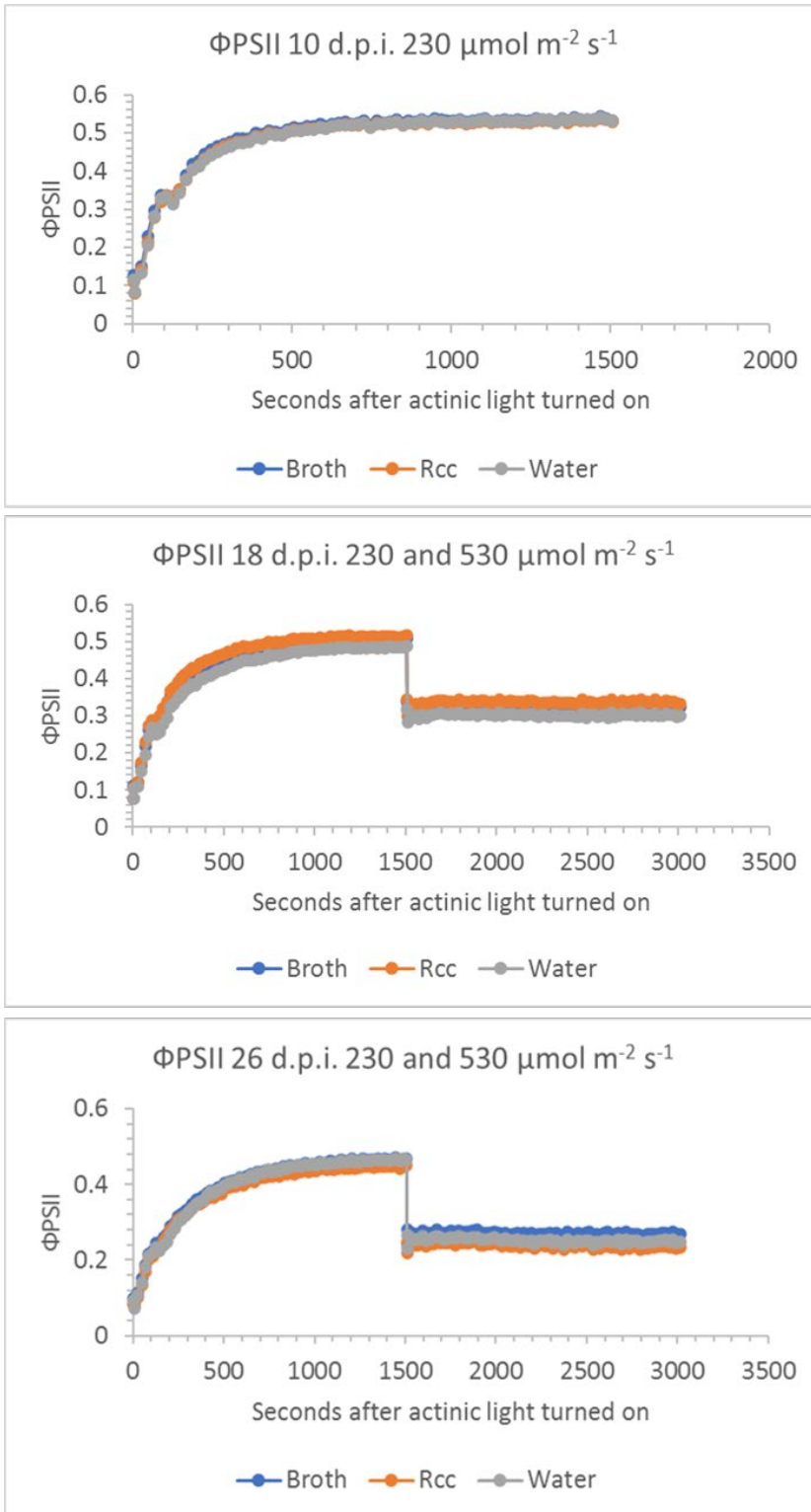


Figure 1 Operating efficiency of PSII (Φ PSII). Actinic light applied at $230 \mu\text{mol m}^{-2} \text{s}^{-1}$ for 1507 seconds, then increased to $530 \mu\text{mol m}^{-2} \text{s}^{-1}$.

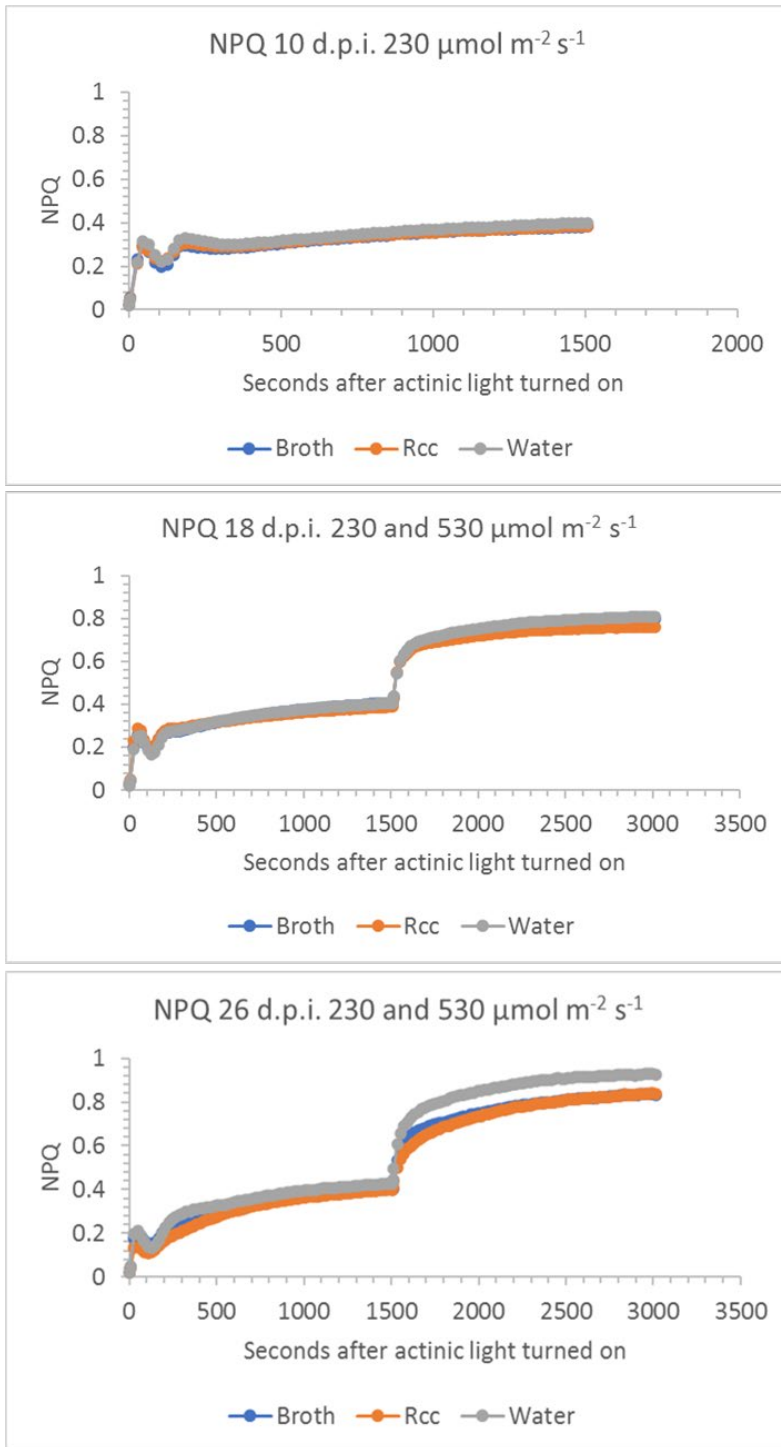


Figure 17. Experimental series 2. Quenching. NPQ. Actinic light applied at $230 \mu\text{mol m}^{-2} \text{s}^{-1}$ for 1507 seconds, then increased to $530 \mu\text{mol m}^{-2} \text{s}^{-1}$.

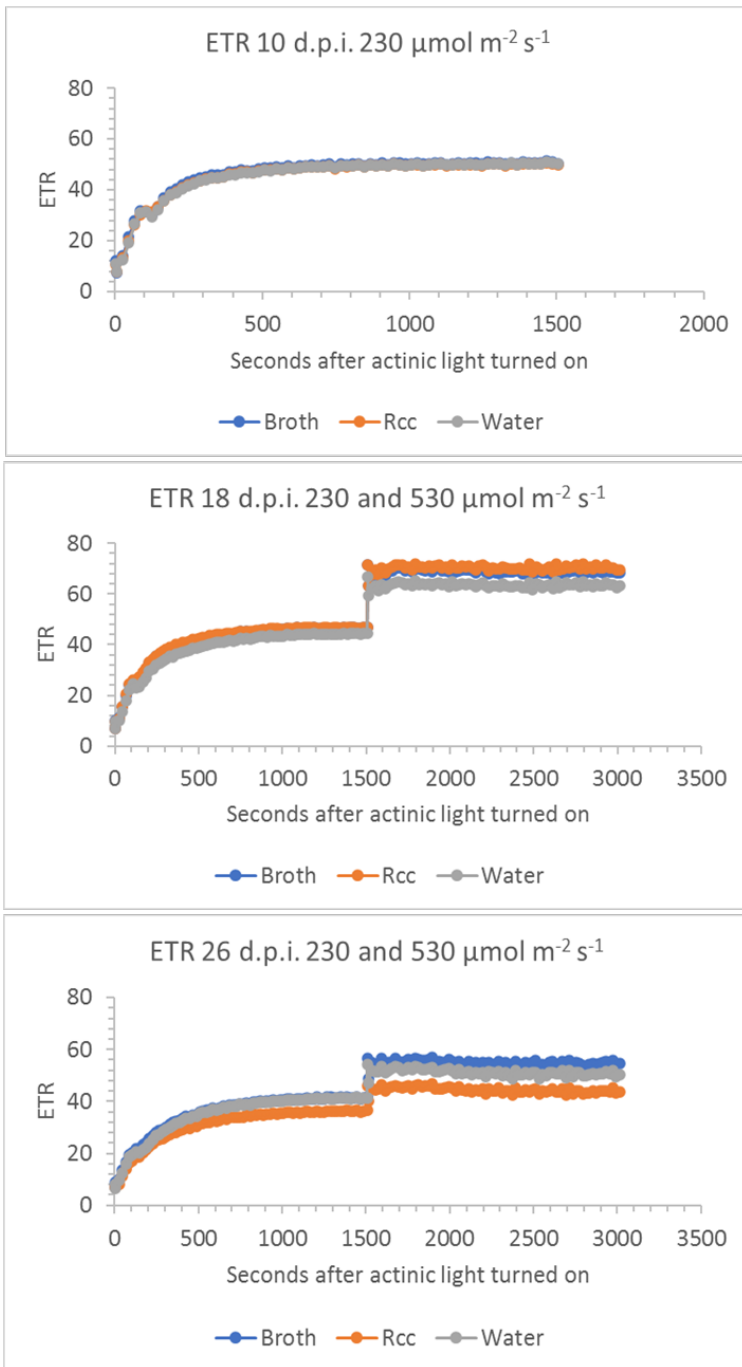


Figure 18. Experimental series 2. Quenching. ETR. Actinic light applied at $230 \mu\text{mol m}^{-2} \text{s}^{-1}$ for 1507 seconds, then increased to $530 \mu\text{mol m}^{-2} \text{s}^{-1}$.

4.1.2.4 Combined infra-red gas analysis and chlorophyll fluorescence

Rates of dark respiration were comparable over the course of the experiment and did not differ significantly between inoculated plants and controls. Rates of net CO₂ fixation measured at both the growth irradiance and at saturating irradiance, declined with leaf age. However, before and after the appearance of visible ramularia symptoms there was no significant effect ($P > 0.05$) of treatment on the rate. Chlorophyll fluorescence parameters (Φ PSII and ETR) did not differ significantly between inoculated plants and controls at any of the time points, in agreement with the results obtained using the imaging fluorometer.

Table 2. CO₂ flux. Ramularia leaf spot symptom severity (% of measured leaf area) and net CO₂ flux ($\mu\text{mol CO}_2 \text{ m}^{-2} \text{ s}^{-1}$) with days after inoculation and measurement irradiance ($\mu\text{mol PAR m}^{-2} \text{ s}^{-1}$).

Days after inoculation	Symptom severity (%)	PAR ($\mu\text{mol m}^{-2} \text{ s}^{-1}$)	CO ₂ Flux			P value
			Broth control	Ramularia	Water control	
6	0	0	-1.795	-1.445	-1.161	0.676
6		230	9.665	10.956	11.018	0.240
6		1250	15.044	16.590	16.970	0.223
16	0.8	0	-0.967	-1.718	-0.741	0.302
16		230	9.480	8.581	9.773	0.587
16		1250	13.500	12.021	13.680	0.514
27	1.4	0	-0.898	-0.788	-1.012	0.511
27		230	4.830	4.389	5.208	0.537
27		1250	6.160	5.682	6.491	0.752

Table 3 ETR. Means and P values from one-way ANOVA at each time point. Ramularia leaf spot symptom severity (% of measured leaf area) and ETR with days after inoculation and measurement irradiance ($\mu\text{mol PAR m}^{-2} \text{ s}^{-1}$).

Days after inoculation	Symptom severity (%)	PAR ($\mu\text{mol m}^{-2} \text{ s}^{-1}$)	ETR			P value
			Broth control	Ramularia	Water control	
6	0	230	56.318	56.302	57.676	0.434
6		1250	98.361	102.347	103.402	0.789
16	0.8	230	51.943	48.219	50.750	0.301
16		1250	75.062	70.016	67.652	0.558
27	1.4	230	35.111	34.289	36.050	0.860
27		1250	37.819	35.349	38.641	0.785

Table 4 Φ PSII. Means and P values from one-way ANOVA at each time point. *Ramularia* leaf spot symptom severity (% of measured leaf area) and Φ PSII with days after inoculation and measurement irradiance ($\mu\text{mol PAR m}^{-2} \text{s}^{-1}$).

Days after inoculation	Symptom severity (%)	PAR ($\mu\text{mol m}^{-2} \text{s}^{-1}$)	Φ PSII			P value
			Broth control	Ramularia	Water control	
6	0	230	0.563	0.561	0.575	0.477
6		1250	0.181	0.187	0.189	0.828
16	0.8	230	0.516	0.497	0.503	0.788
16		1250	0.137	0.128	0.136	0.704
27	1.4	230	0.353	0.341	0.358	0.855
27		1250	0.070	0.067	0.071	0.919

4.1.2.5 Analysis of transects across leaves

Replicates from Experimental series 2 which had developed lesions on infected leaves by 18 or 26 days after inoculation were used in this analysis. The chlorophyll fluorescence images used were captured at steady state photosynthesis at $230 \mu\text{mol m}^{-2} \text{s}^{-1}$ PAR.

Transects were drawn across infected leaves, through one lesion in the upper leaf area (towards the leaf tip) and one lesion in the lower leaf area (towards the base), and in corresponding areas of control leaves (Figure 18). Transects were also drawn across areas of infected leaves which had no lesions, close to each transect through a lesion. Eighteen days after inoculation, three replicates had developed lesions on infected leaves (reps 1, 3 and 6). By 26 days after inoculation, an additional replicate had developed lesions on the infected leaf (rep 4). Prior to analysis of chlorophyll fluorescence outputs, each lesion was visually categorised as being either a small, developing lesion (category A) or a lesion at a more advanced stage of development (category B) (Table 16). Lesions that were selected for analysis at 18 days post inoculation were reanalysed at 26 days.

Table 5. Lesion categories

D.p.i.	Rep	Lesion position	Lesion category
18	1	Upper leaf	A
18	1	Lower leaf	A
18	3	Upper leaf	B
18	3	Lower leaf	A
18	6	Upper leaf	B
18	6	Lower leaf	B
26	1	Upper leaf	B
26	1	Lower leaf	A
26	2	Upper leaf	A
26	2	Lower leaf	A
26	3	Upper leaf	B
26	3	Lower leaf	A
26	6	Upper leaf	B
26	6	Lower leaf	B

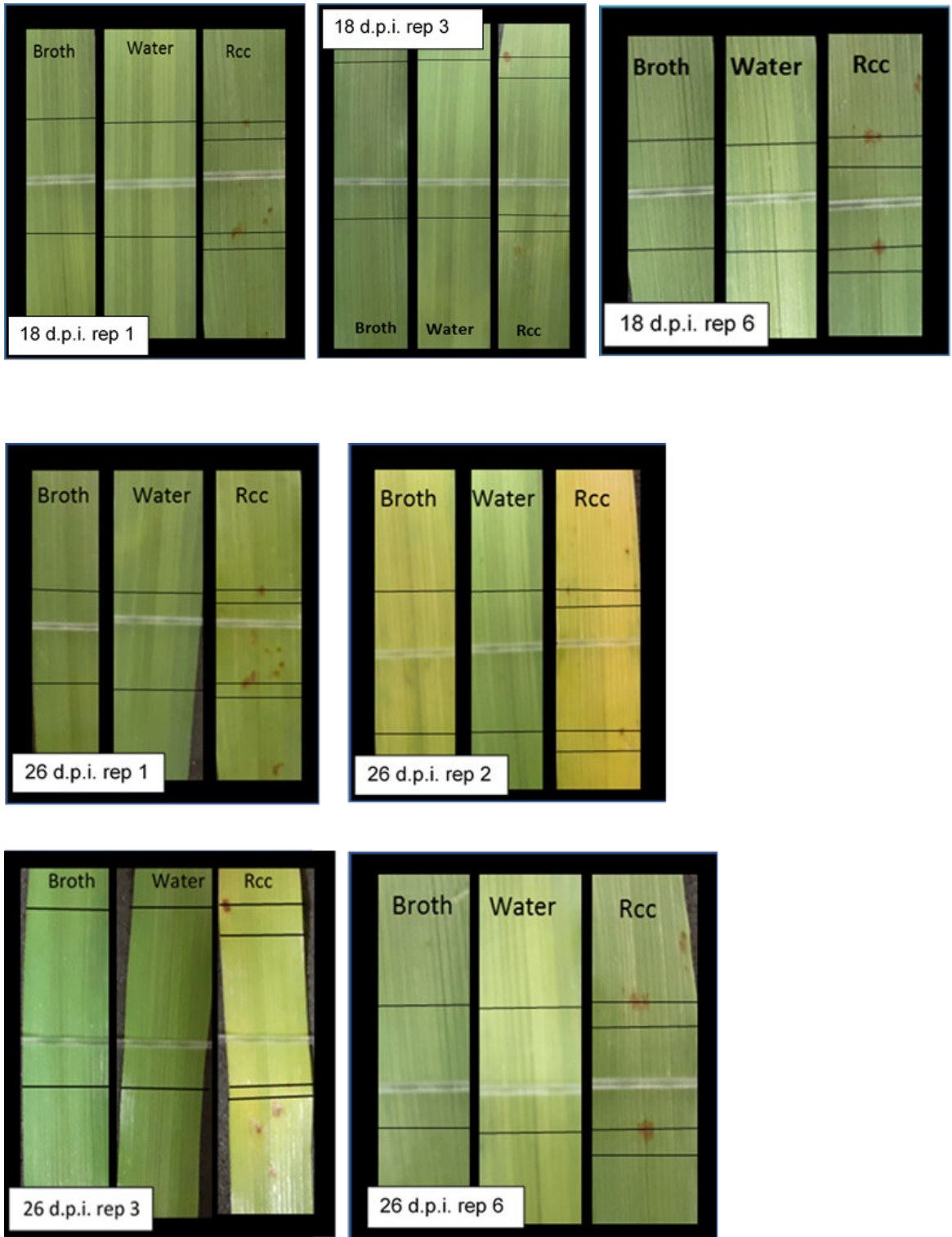


Figure 19. Leaves showing positions of upper and lower transects at 18 days and 26 days post-inoculation (d.p.i.).

4.2.1.6 Chlorophyll fluorescence imaging transect analysis – steady state photosynthesis

Values for the chlorophyll fluorescence outputs of Fv/Fm, NPQ, Φ PSII and ETR were recorded pixel by pixel along each transect (Figure 20). The three black arrows on the graphs indicate the left edge, centre, and right edge of the lesions on infected leaves. The direction and relative scale of the effects observed are summarised qualitatively in Table 17.

At 18 d.p.i., in small and developing lesions (category A) the most pronounced effect observed was a reduction in NPQ within the lesion. Smaller reductions in Fv/Fm were also seen in some, but not all lesions. By contrast, Φ PSII and ETR values within lesions were similar to those in non-symptomatic areas of infected leaves or in control leaves. In the more developed category B lesions, a small reduction in Φ PSII and ETR was also often observed. In the most developed lesions, e.g. replicate 3 upper and replicate 6 upper, a 'spike' in NPQ was visible towards the edge of the lesions, displaying higher values than those in non-symptomatic areas of infected leaves or in control leaves, while reduced NPQ was observed in the central part of these lesions.

All lesions which were in category B at 18 d.p.i. continued to develop further (replicate 3 upper lesion, and replicate 6 upper and lower lesions). In these lesions, by 26 d.p.i., values for all the measured chlorophyll fluorescence outputs had dropped to zero or close to zero within the lesions. A spike displaying higher Φ PSII values than those in non-symptomatic areas of infected leaves or in control leaves was observed in rep 3 upper lesion and rep 6 lower lesion, close to the edge of the lesions.

By 26 d.p.i., replicate 1 upper lesion (R1 U) appeared to have developed slightly, growing marginally darker and was re-categorised as a type B lesion. However, there was little change in its fluorescence characteristics. Thus, NPQ showed a decrease within the lesion, whilst Φ PSII and ETR remained comparable to that in non-symptomatic regions. A spike in NPQ values, similar to those displayed by category B lesions at 18 d.p.i., was observed close to the edge of the lesion. Other category A lesions (R1 L and R3 L) showed no further development after 18 d.p.i., although the infected leaf for rep 3 had started to display some chlorosis by 26 d.p.i (Figure 20m). A new replicate (2) was added to the analysis at 26 d.p.i. as lesions had appeared on this infected leaf between 18 and 26 d.p.i. For this replicate, the infected leaf, and the broth control leaf both displayed some chlorosis. This was more advanced in the infected leaf than in the broth control leaf. As with other small developing lesions, a reduction in NPQ was found, but only marginal or no effect on Fv/Fm, Φ PSII and ETR.

Table 6. Direction and scale of change in fluorescence variables within the visible lesions on infected leaves compared to regions outside the lesion on the same leaves. Variables decreased (↓) or increased (↑) with the number of arrows indicating the relative scale from small (↓) to major (↓↓↓) change. ~ indicates a possible marginal or uncertain effect. Where no effect was observed, the cell has been left empty. Lesions are identified by leaf replicate number (R1, R2 etc) and whether the lesion was on the upper (U) or lower (L) transect. Variables are: Fv/Fm, maximal photochemical efficiency; NPQ, non-photochemical quenching; Φ PSII, operating photochemical efficiency; ETR, Electron Transport Rate.

Days after inoculation	Category	Lesion	Fluorescence variable			
			Fv/Fm	NPQ	Φ PSII	ETR
18	A	R1 U	↓	↓↓		
	A	R1 L		↓↓		
	A	R3 L	↓	↓↓		~↓
18	B	R3 U	↓	↓↓	↓	↓
	B	R6 U	↓	↓↓	~↓	↓
	B	R6 L	↓↓	↓↓↓		↓
26	A	R1 L		~↑	↑	
	A	R2 U		↓		
	A	R2 L		↓	~↑	~↑
	A	R3 L		↓↓		
26	B	R1 U		↓↓		
	B	R3 U	↓↓↓	↓↓↓	↓↓↓	↓↓↓
	B	R6 U	↓↓↓	↓↓↓	↓↓↓	↓↓↓
	B	R6 L	↓↓↓	↓↓↓	↓↓↓	↓↓↓

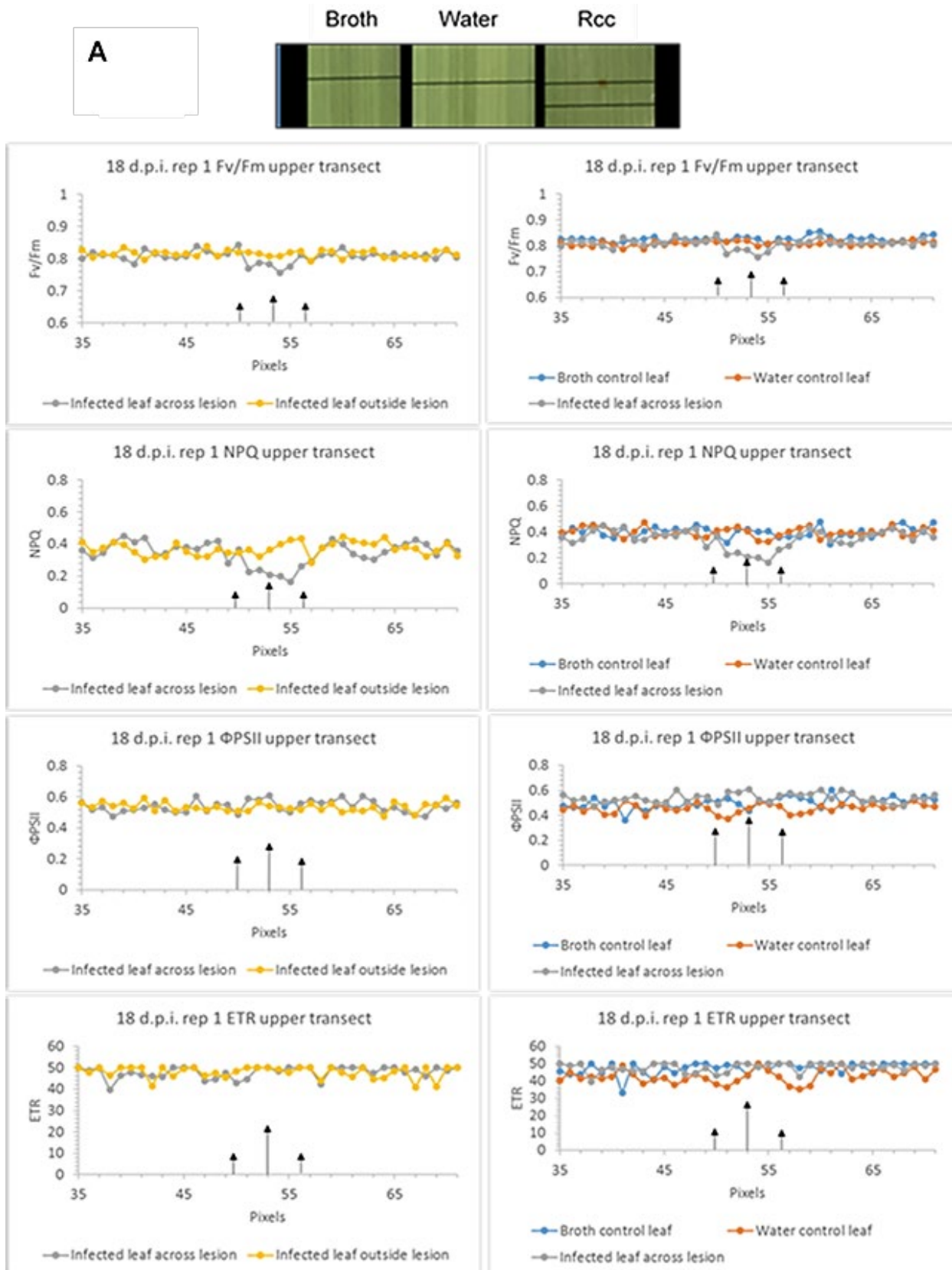


Figure 20 (a). Chlorophyll fluorescence measured across leaf transects. Photographs show location of upper and lower leaf transects graphs show chlorophyll fluorescence parameters along the transects. Left hand panels show parameters for transects across lesions and across nearby non-symptomatic areas of infected leaves. Right hand panels show parameters for transects across lesions and across equivalent areas of control leaves. Measurements taken at 18 and 26 days after inoculation. Replicates categorised as group A = small, developing lesion. Replicates categorised as Group B = lesion at more advanced stage of development.

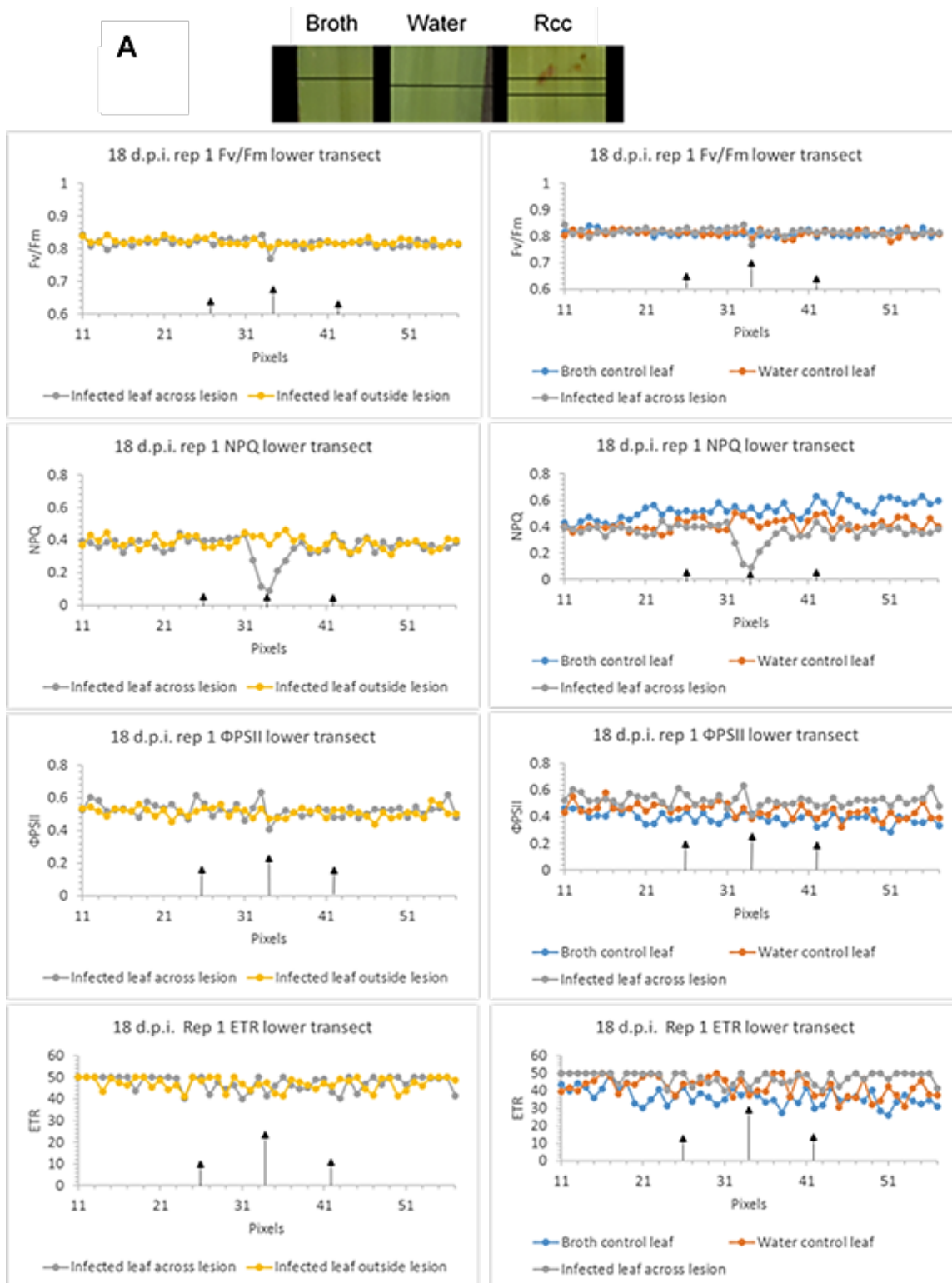


Figure 20 (b). Chlorophyll fluorescence measured across leaf transects. Photographs show location of upper and lower leaf transects graphs show chlorophyll fluorescence parameters along the transects. Left hand panels show parameters for transects across lesions and across nearby non-symptomatic areas of infected leaves. Right hand panels show parameters for transects across lesions and across equivalent areas of control leaves. Measurements taken at 18 and 26 days after inoculation. Replicates categorised as group A = small, developing lesion. Replicates categorised as Group B = lesion at more advanced stage of development.

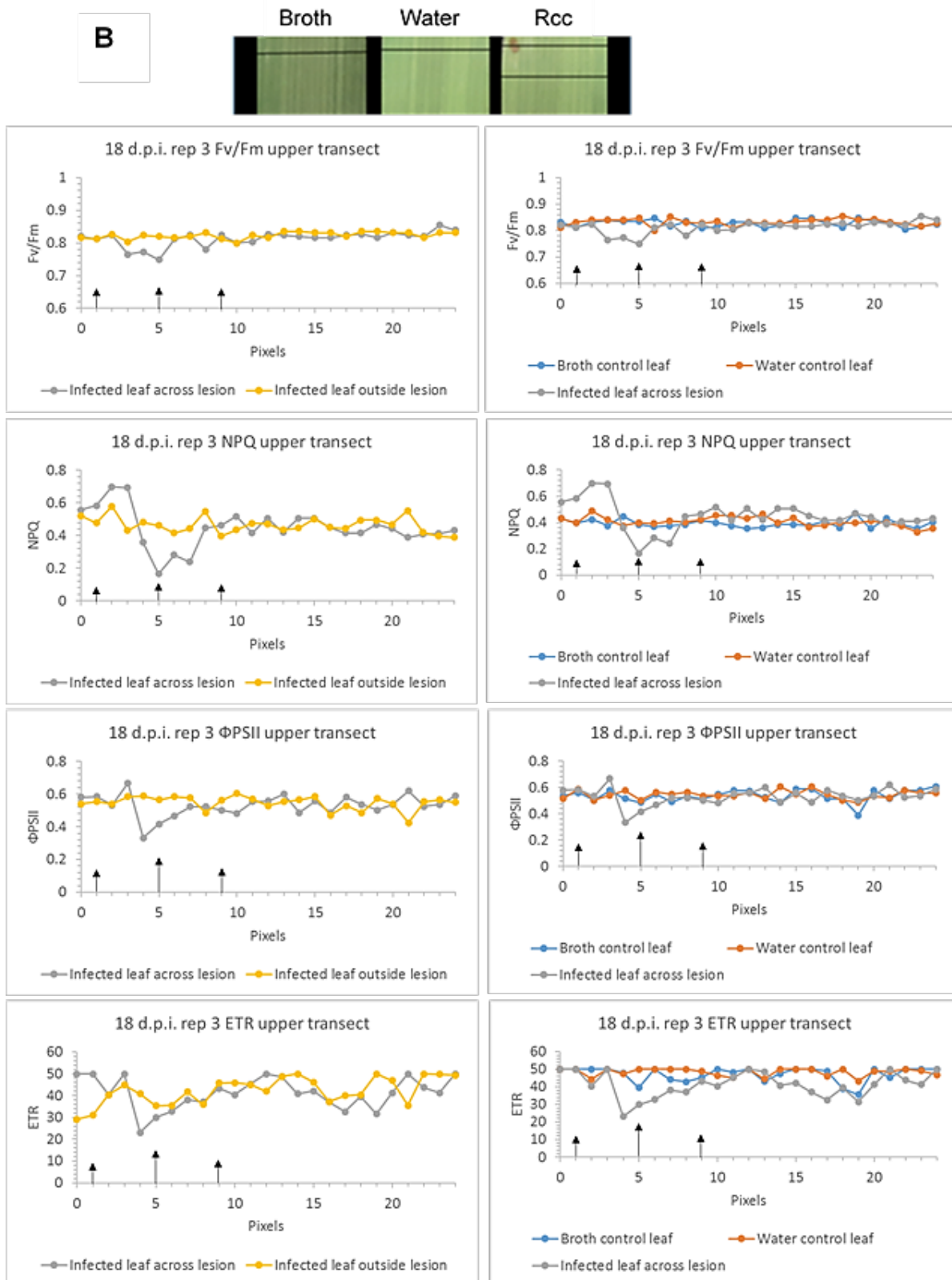


Figure 20 (c). Chlorophyll fluorescence measured across leaf transects. Photographs show location of upper and lower leaf transects graphs show chlorophyll fluorescence parameters along the transects. Left hand panels show parameters for transects across lesions and across nearby non-symptomatic areas of infected leaves. Right hand panels show parameters for transects across lesions and across equivalent areas of control leaves. Measurements taken at 18 and 26 days after inoculation. Replicates categorised as group A = small, developing lesion. Replicates categorised as Group B = lesion at more advanced stage of development.

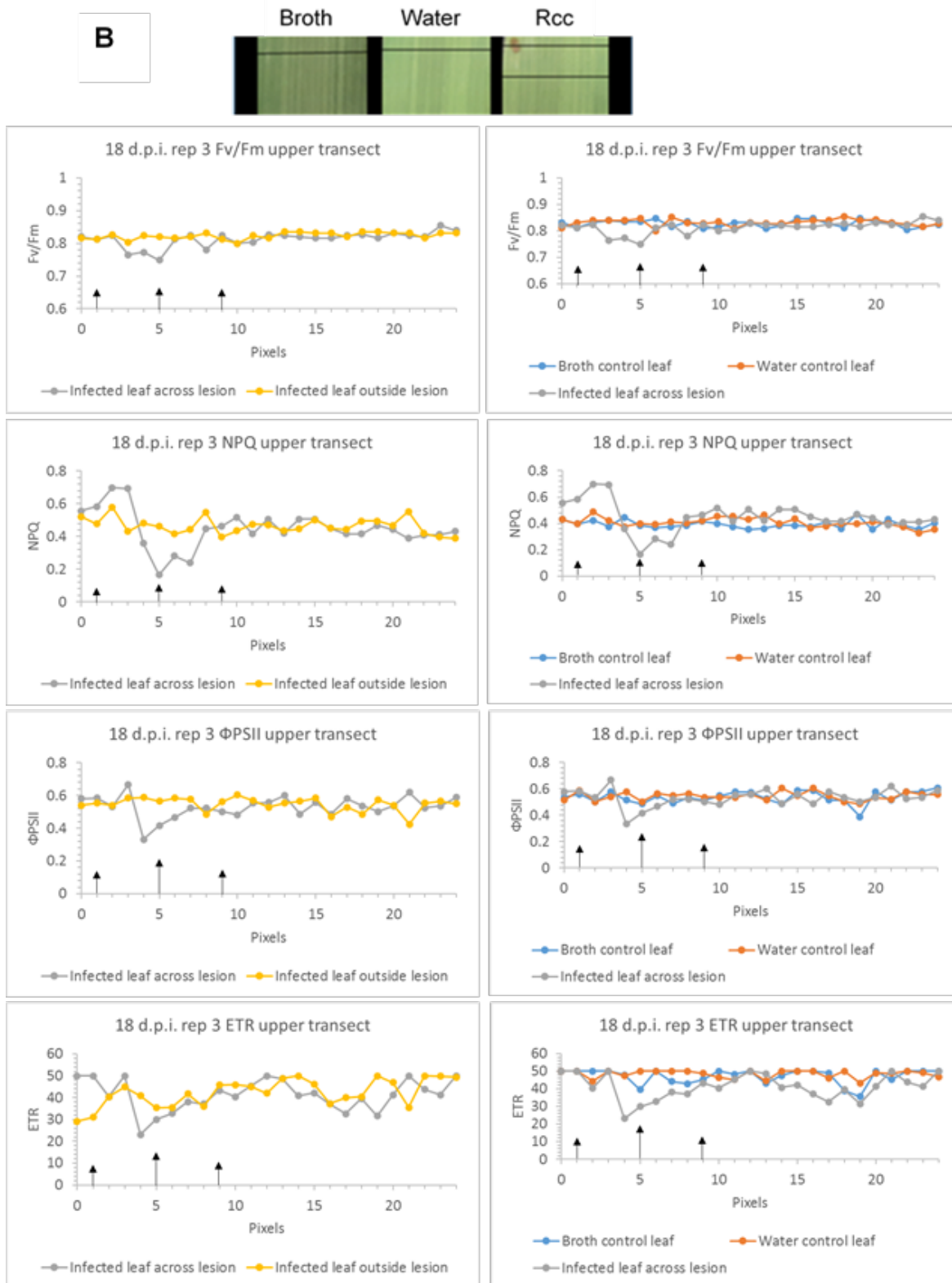


Figure 20 (d). Chlorophyll fluorescence measured across leaf transects. Photographs show location of upper and lower leaf transects graphs show chlorophyll fluorescence parameters along the transects. Left hand panels show parameters for transects across lesions and across nearby non-symptomatic areas of infected leaves. Right hand panels show parameters for transects across lesions and across equivalent areas of control leaves. Measurements taken at 18 and 26 days after inoculation. Replicates categorised as group A = small, developing lesion. Replicates categorised as Group B = lesion at more advanced stage of development.

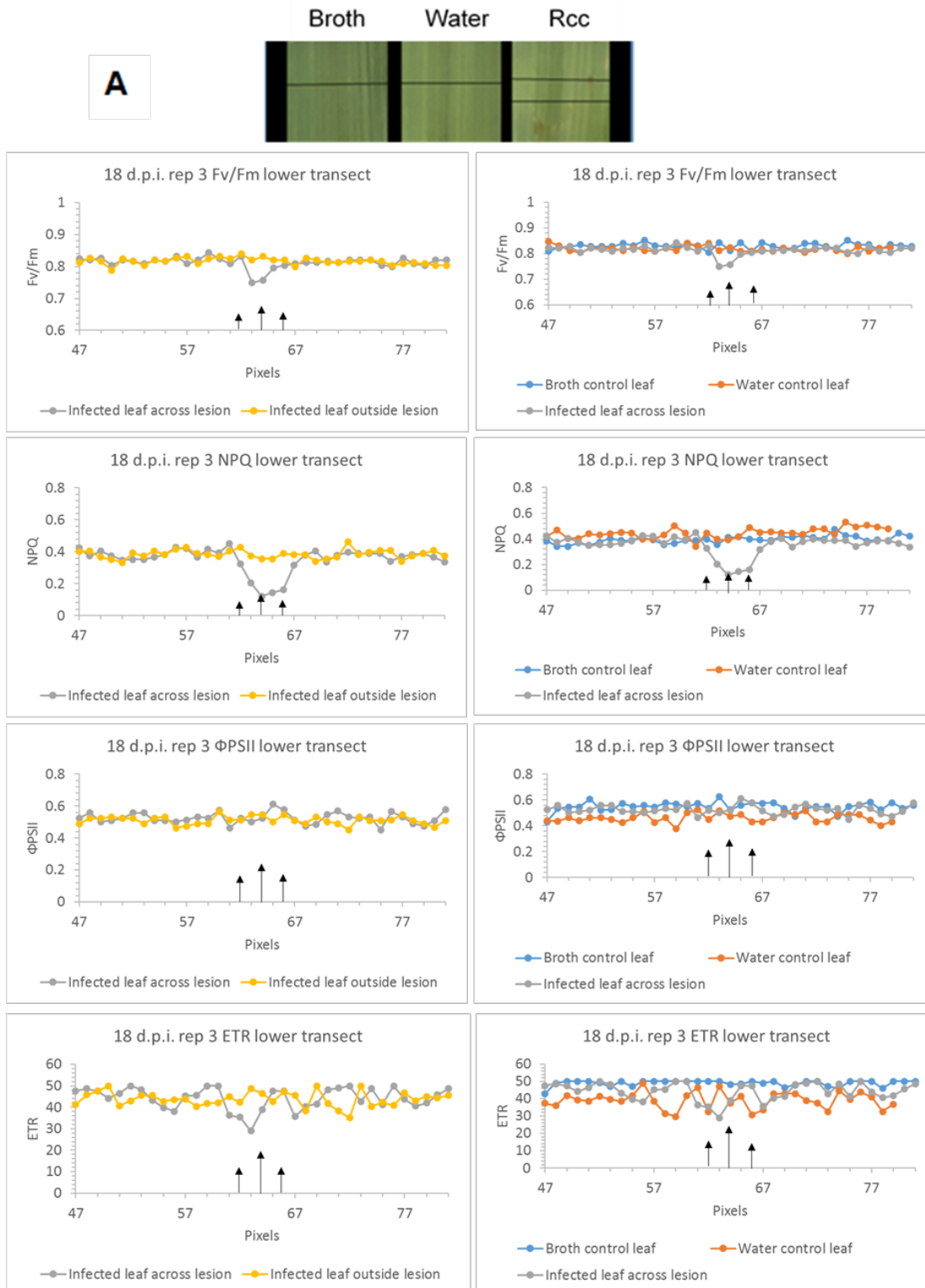


Figure 20 (e). Chlorophyll fluorescence measured across leaf transects. Photographs show location of upper and lower leaf transects graphs show chlorophyll fluorescence parameters along the transects. Left hand panels show parameters for transects across lesions and across nearby non-symptomatic areas of infected leaves. Right hand panels show parameters for transects across lesions and across equivalent areas of control leaves. Measurements taken at 18 and 26 days after inoculation. Replicates categorised as group A = small, developing lesion. Replicates categorised as Group B = lesion at more advanced stage of development.

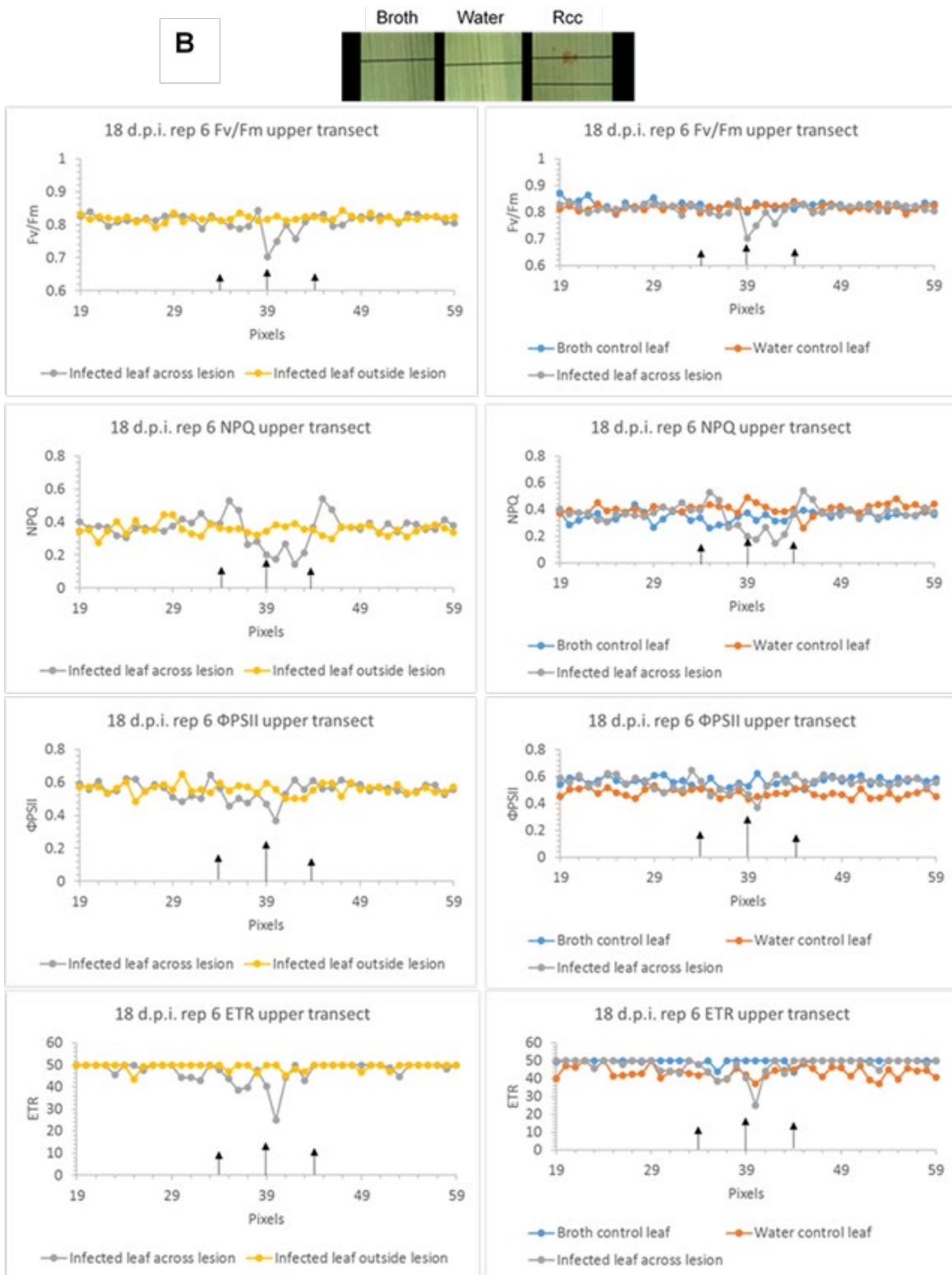


Figure 20 (f). Chlorophyll fluorescence measured across leaf transects. Photographs show location of upper and lower leaf transects graphs show chlorophyll fluorescence parameters along the transects. Left hand panels show parameters for transects across lesions and across nearby non-symptomatic areas of infected leaves. Right hand panels show parameters for transects across lesions and across equivalent areas of control leaves. Measurements taken at 18 and 26 days after inoculation. Replicates categorised as group A = small, developing lesion. Replicates categorised as Group B = lesion at more advanced stage of development.

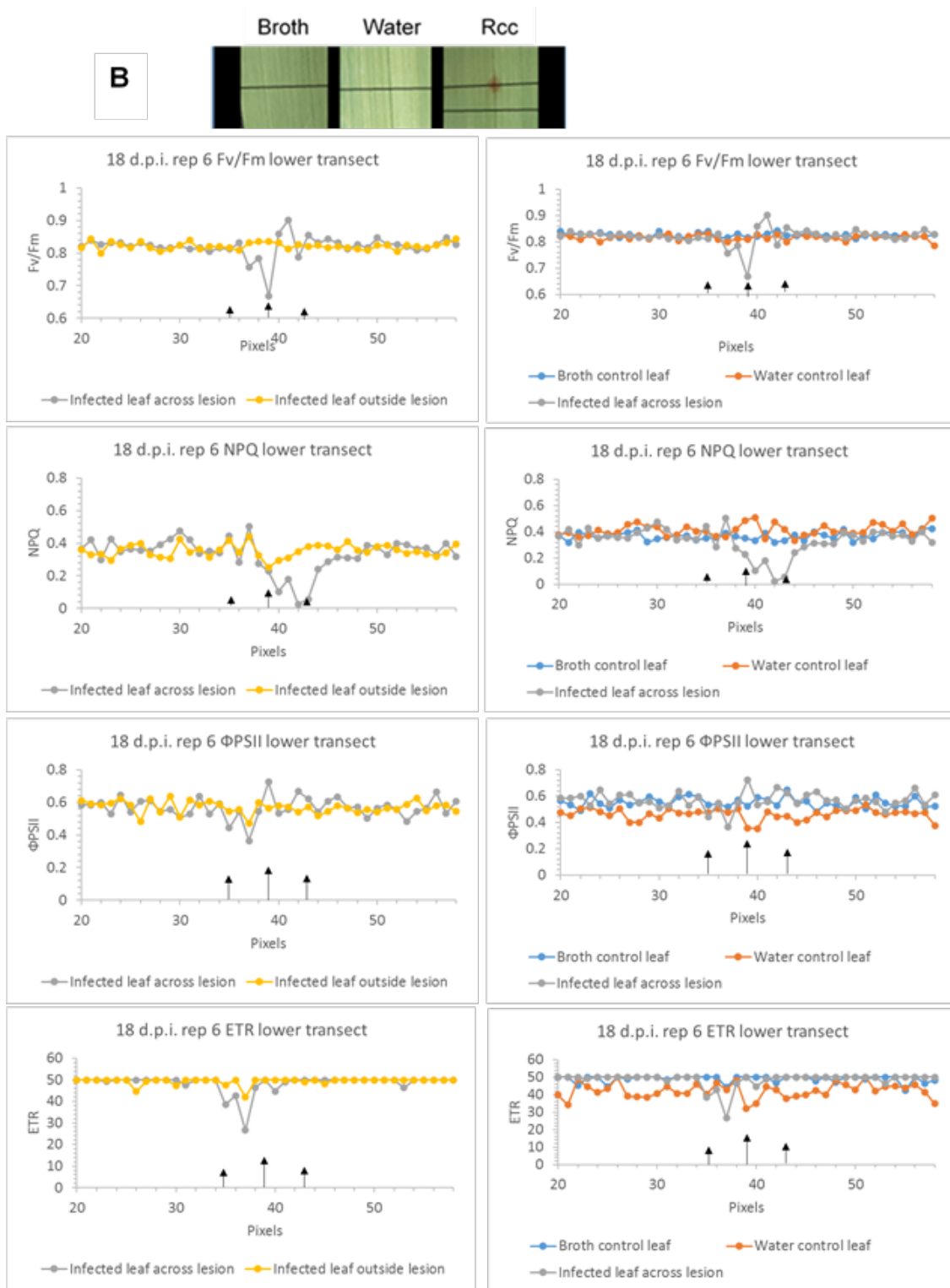


Figure 20 (g). Chlorophyll fluorescence measured across leaf transects. Photographs show location of upper and lower leaf transects graphs show chlorophyll fluorescence parameters along the transects. Left hand panels show parameters for transects across lesions and across nearby non-symptomatic areas of infected leaves. Right hand panels show parameters for transects across lesions and across equivalent areas of control leaves. Measurements taken at 18 and 26 days after inoculation. Replicates categorised as group A = small, developing lesion. Replicates categorised as Group B = lesion at more advanced stage of development.

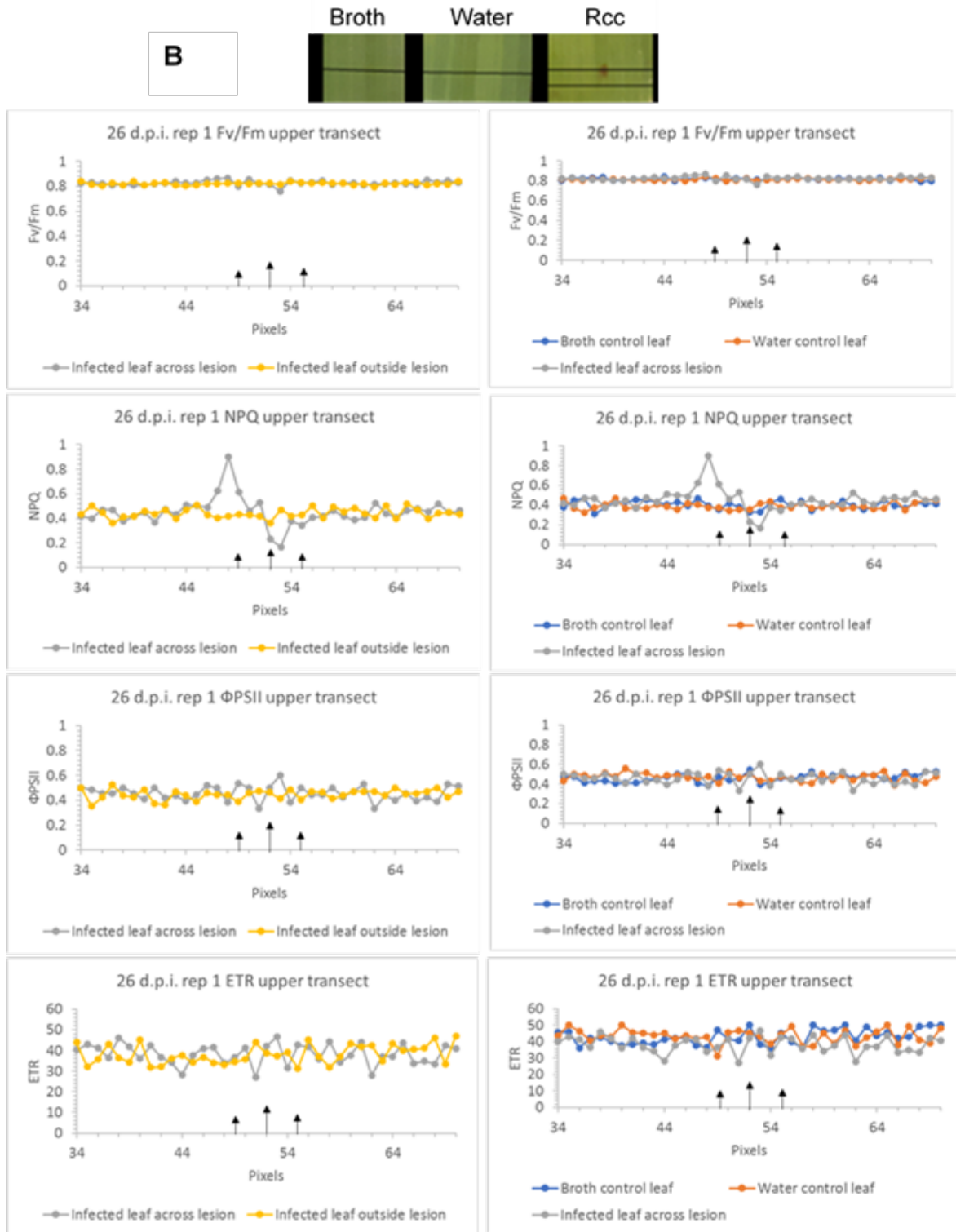


Figure 20 (h). Chlorophyll fluorescence measured across leaf transects. Photographs show location of upper and lower leaf transects graphs show chlorophyll fluorescence parameters along the transects. Left hand panels show parameters for transects across lesions and across nearby non-symptomatic areas of infected leaves. Right hand panels show parameters for transects across lesions and across equivalent areas of control leaves. Measurements taken at 18 and 26 days after inoculation. Replicates categorised as group A = small, developing lesion. Replicates categorised as Group B = lesion at more advanced stage of development.

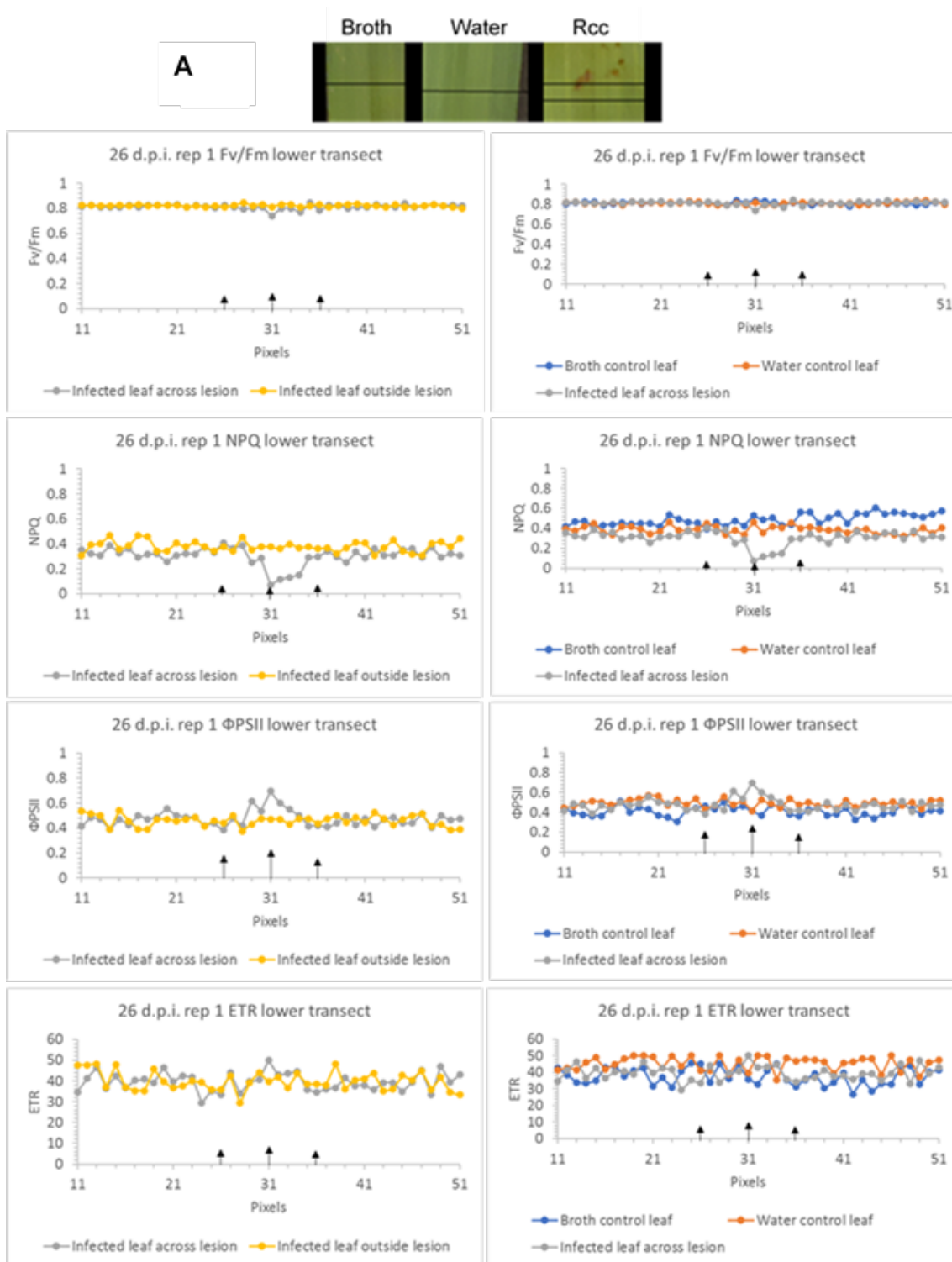


Figure 20 (i). Chlorophyll fluorescence measured across leaf transects. Photographs show location of upper and lower leaf transects graphs show chlorophyll fluorescence parameters along the transects. Left hand panels show parameters for transects across lesions and across nearby non-symptomatic areas of infected leaves. Right hand panels show parameters for transects across lesions and across equivalent areas of control leaves. Measurements taken at 18 and 26 days after inoculation. Replicates categorised as group A = small, developing lesion. Replicates categorised as Group B = lesion at more advanced stage of development.

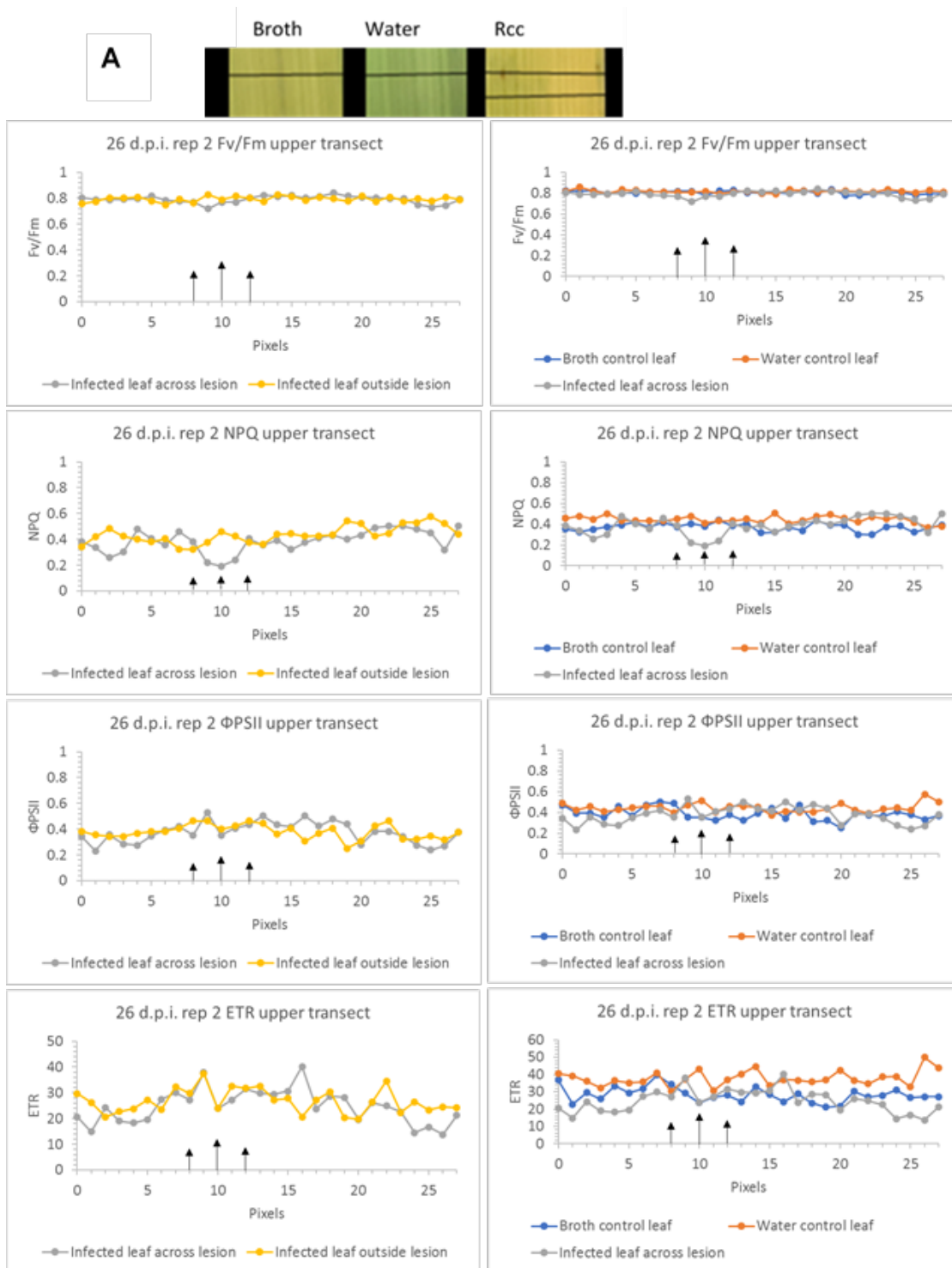


Figure 20 (j). Chlorophyll fluorescence measured across leaf transects. Photographs show location of upper and lower leaf transects graphs show chlorophyll fluorescence parameters along the transects. Left hand panels show parameters for transects across lesions and across nearby non-symptomatic areas of infected leaves. Right hand panels show parameters for transects across lesions and across equivalent areas of control leaves. Measurements taken at 18 and 26 days after inoculation. Replicates categorised as group A = small, developing lesion. Replicates categorised as Group B = lesion at more advanced stage of development.

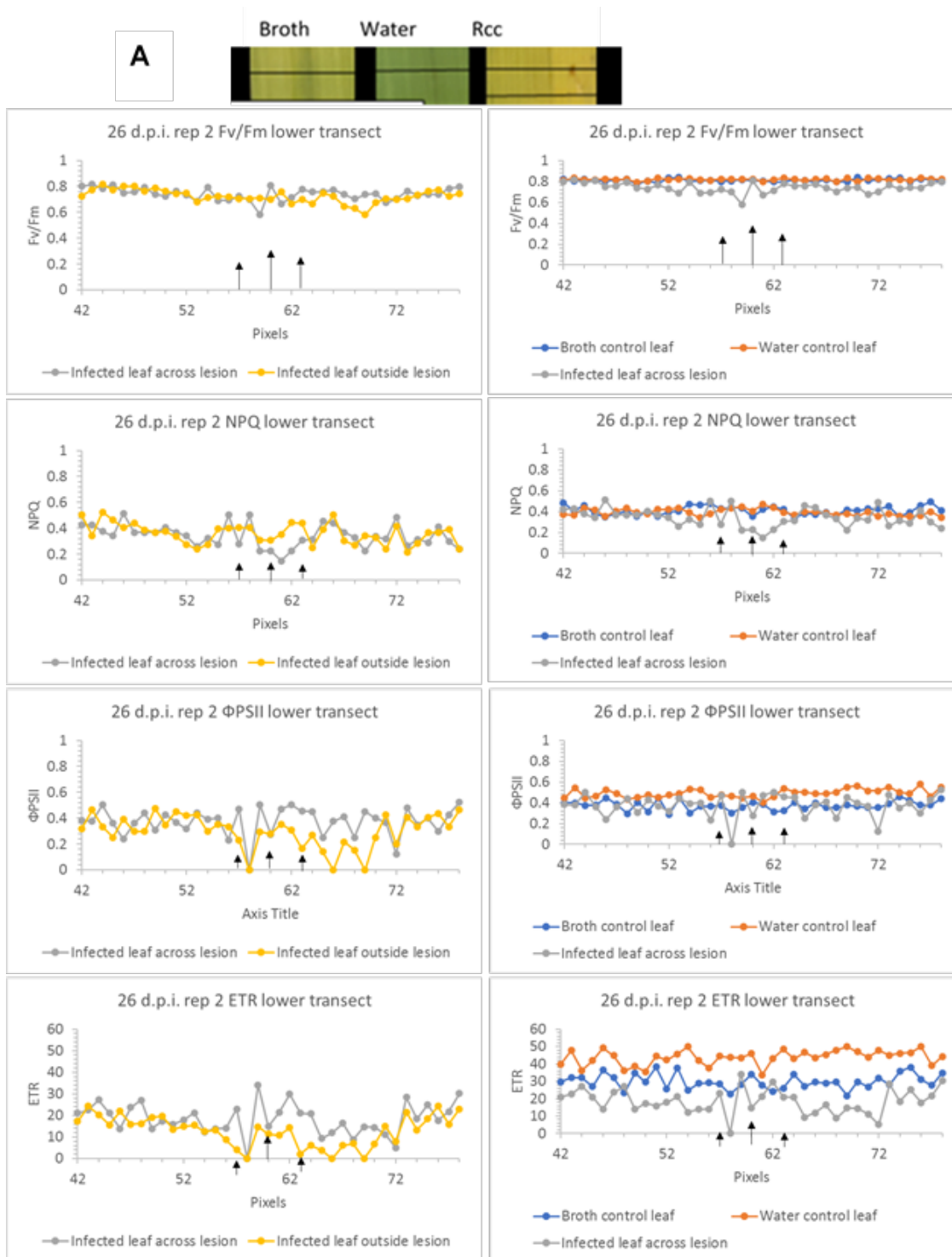


Figure 20 (k). Chlorophyll fluorescence measured across leaf transects. Photographs show location of upper and lower leaf transects graphs show chlorophyll fluorescence parameters along the transects. Left hand panels show parameters for transects across lesions and across nearby non-symptomatic areas of infected leaves. Right hand panels show parameters for transects across lesions and across equivalent areas of control leaves. Measurements taken at 18 and 26 days after inoculation. Replicates categorised as group A = small, developing lesion. Replicates categorised as Group B = lesion at more advanced stage of development.

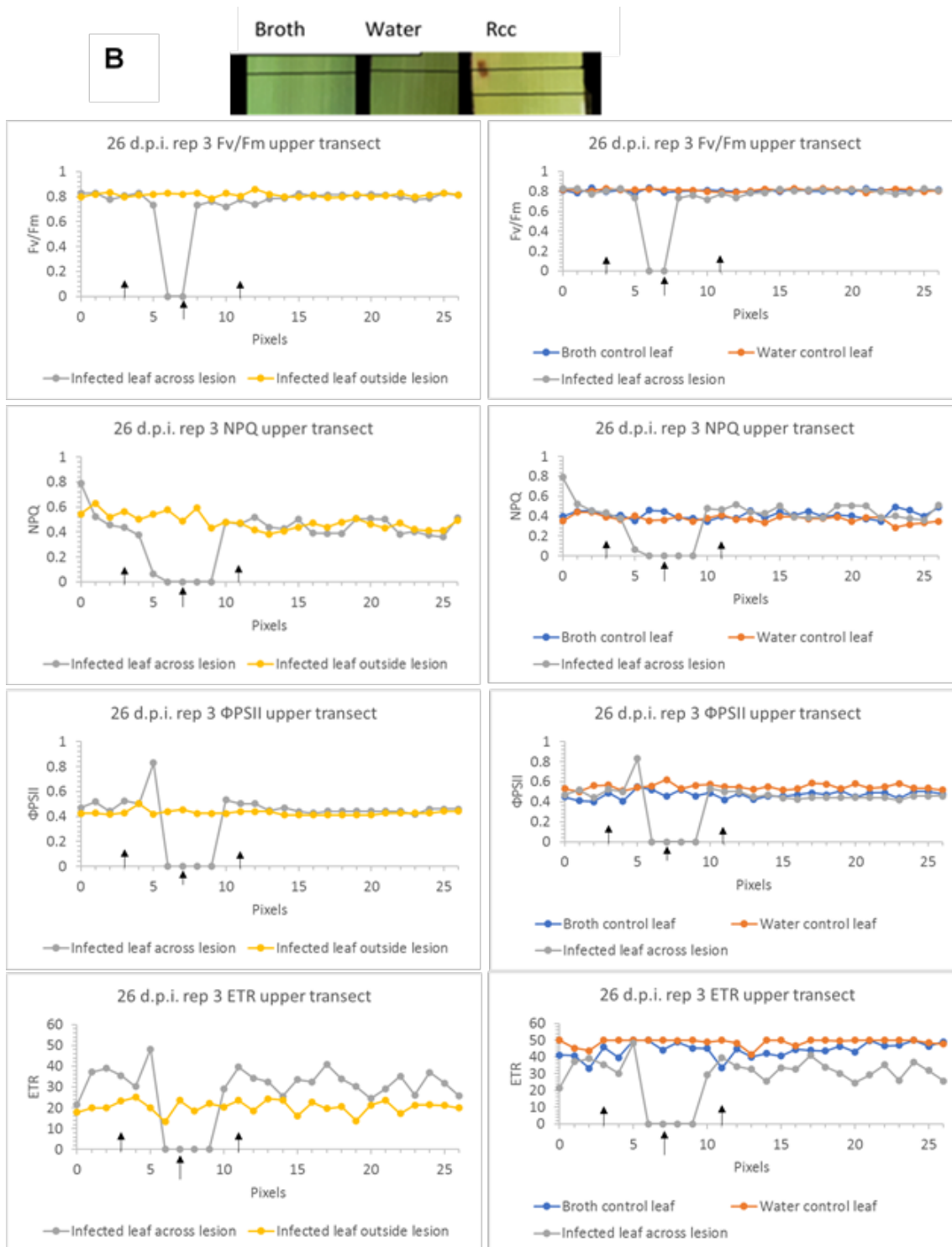


Figure 20 (I). Chlorophyll fluorescence measured across leaf transects. Photographs show location of upper and lower leaf transects graphs show chlorophyll fluorescence parameters along the transects. Left hand panels show parameters for transects across lesions and across nearby non-symptomatic areas of infected leaves. Right hand panels show parameters for transects across lesions and across equivalent areas of control leaves. Measurements taken at 18 and 26 days after inoculation. Replicates categorised as group A = small, developing lesion. Replicates categorised as Group B = lesion at more advanced stage of development

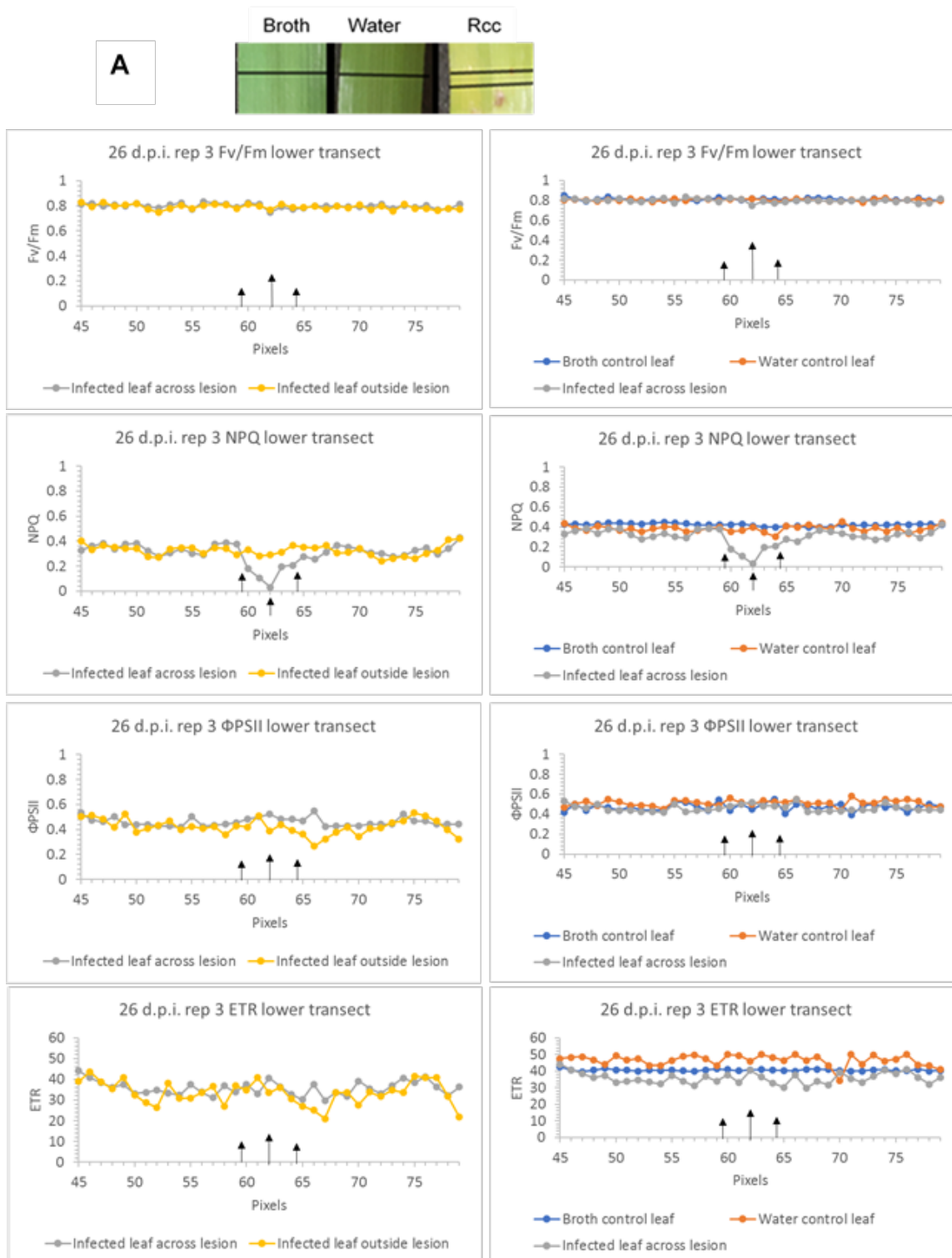


Figure 20 (m). Chlorophyll fluorescence measured across leaf transects. Photographs show location of upper and lower leaf transects graphs show chlorophyll fluorescence parameters along the transects. Left hand panels show parameters for transects across lesions and across nearby non-symptomatic areas of infected leaves. Right hand panels show parameters for transects across lesions and across equivalent areas of control leaves. Measurements taken at 18 and 26 days after inoculation. Replicates categorised as group A = small, developing lesion. Replicates categorised as Group B = lesion at more advanced stage of development

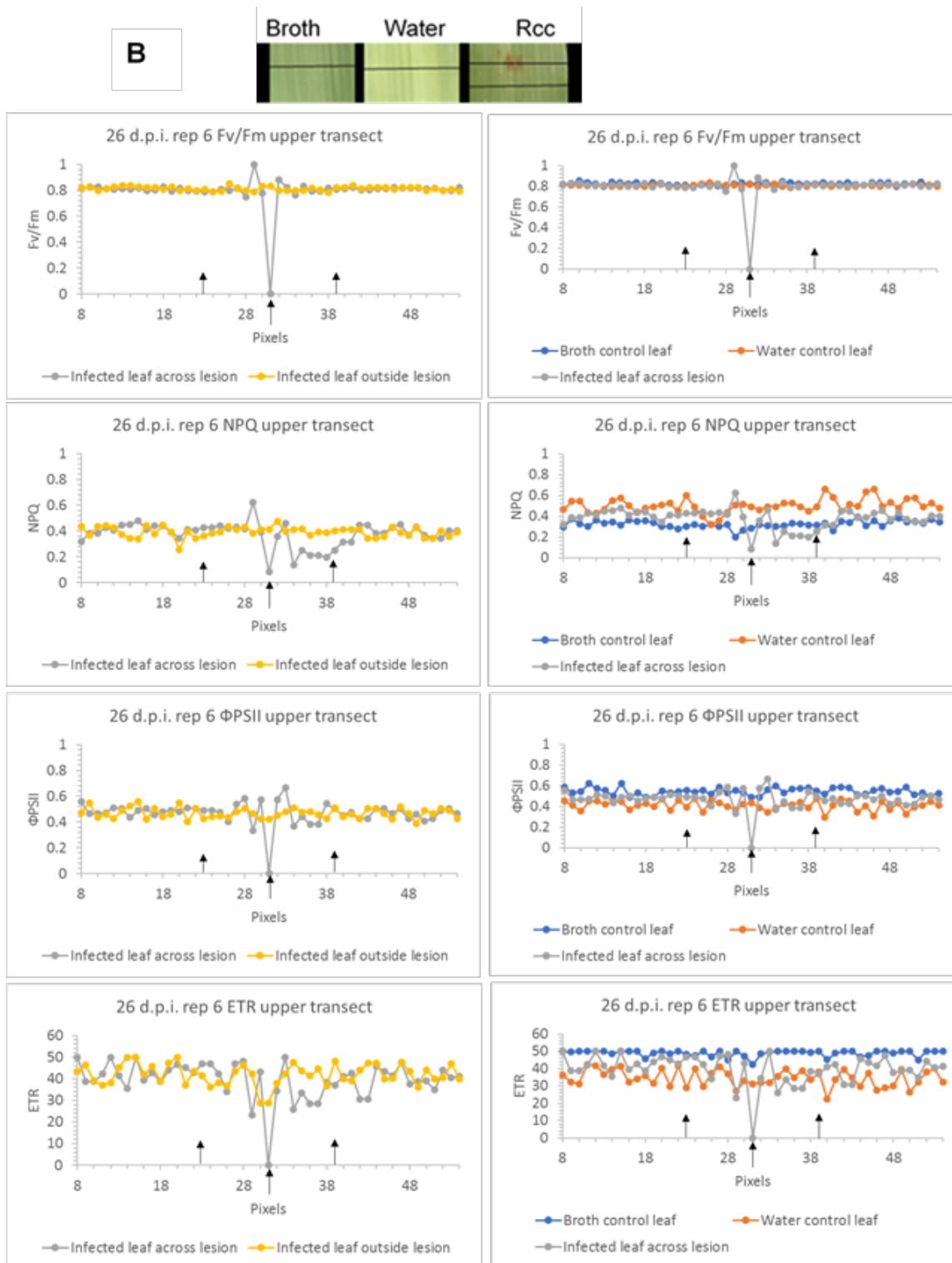


Figure 20 (n). Chlorophyll fluorescence measured across leaf transects. Photographs show location of upper and lower leaf transects graphs show chlorophyll fluorescence parameters along the transects. Left hand panels show parameters for transects across lesions and across nearby non-symptomatic areas of infected leaves. Right hand panels show parameters for transects across lesions and across equivalent areas of control leaves. Measurements taken at 18 and 26 days after inoculation. Replicates categorised as group A = small, developing lesion. Replicates categorised as Group B = lesion at more advanced stage of development

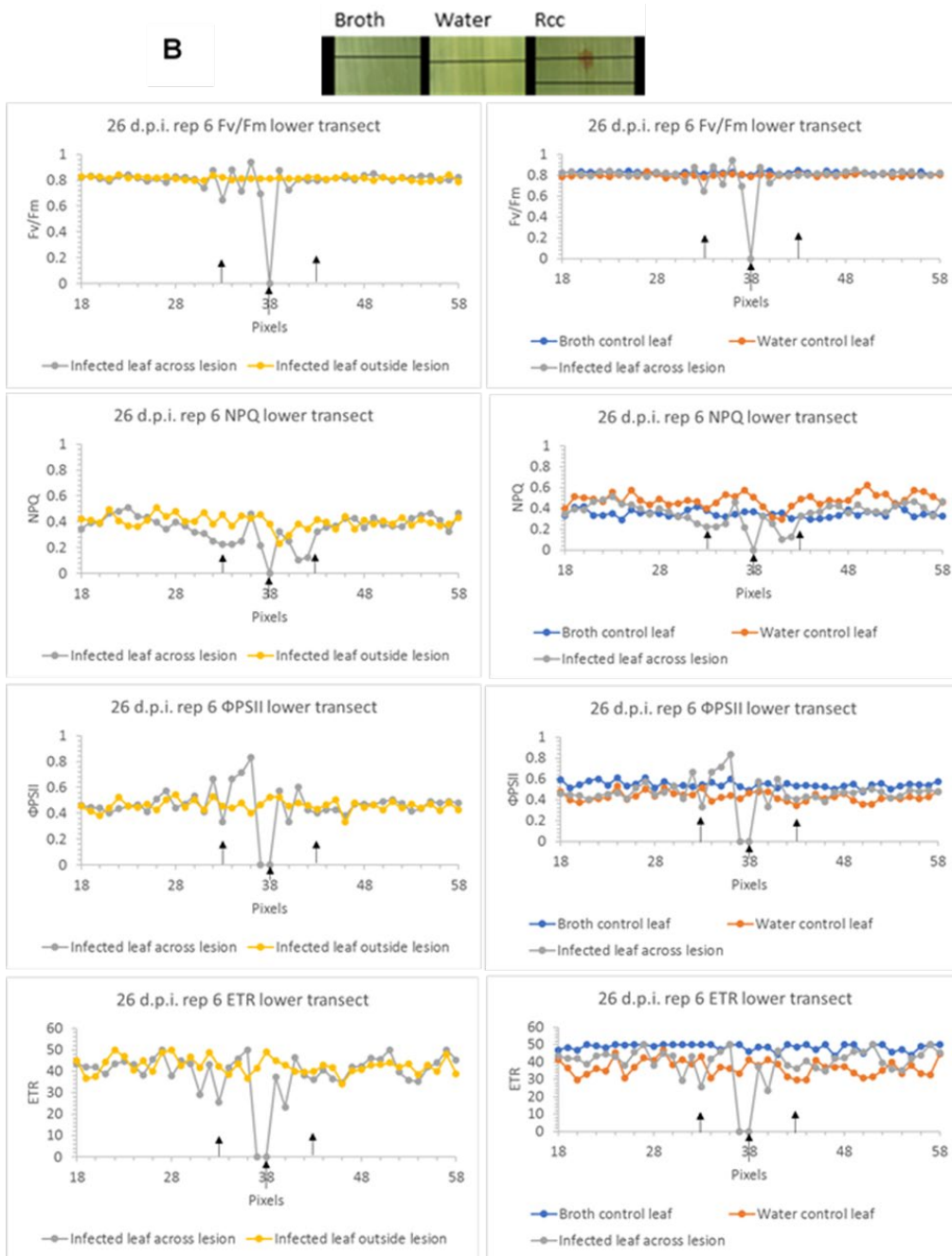


Figure 20 (o). Chlorophyll fluorescence measured across leaf transects. Photographs show location of upper and lower leaf transects graphs show chlorophyll fluorescence parameters along the transects. Left hand panels show parameters for transects across lesions and across nearby non-symptomatic areas of infected leaves. Right hand panels show parameters for transects across lesions and across equivalent areas of control leaves. Measurements taken at 18 and 26 days after inoculation. Replicates categorised as group A = small, developing lesion. Replicates categorised as Group B = lesion at more advanced stage of development

4.2. Impact of Rcc life phases on barley yield

4.2.1. Disease severity and % green area

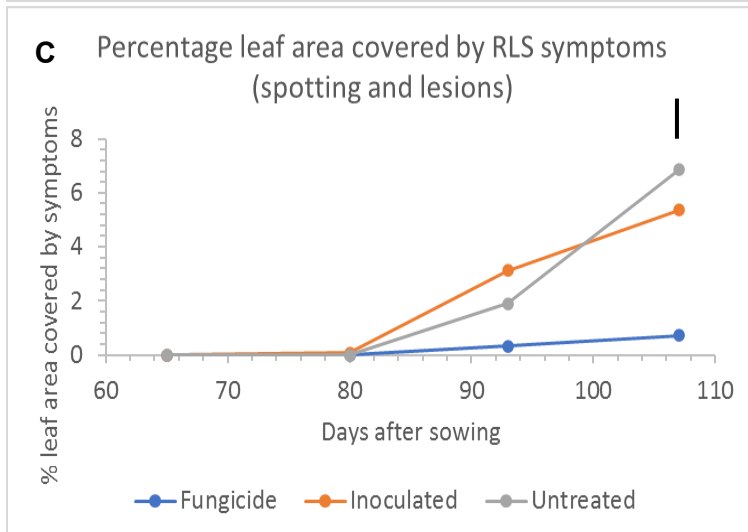
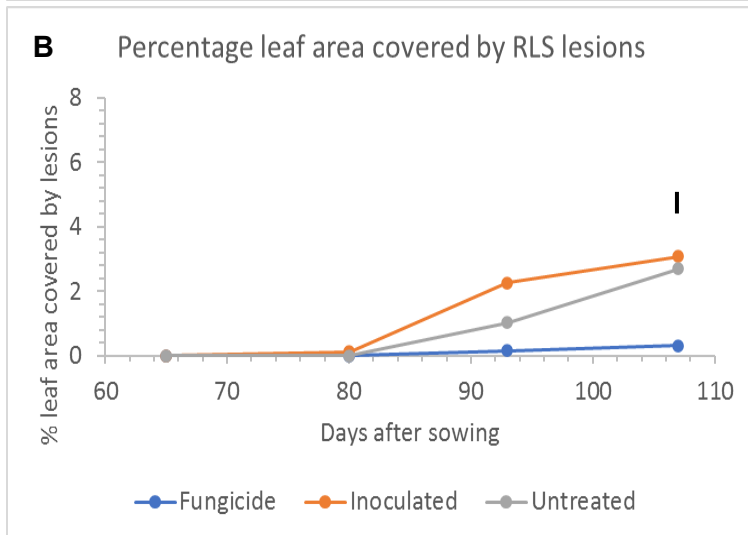
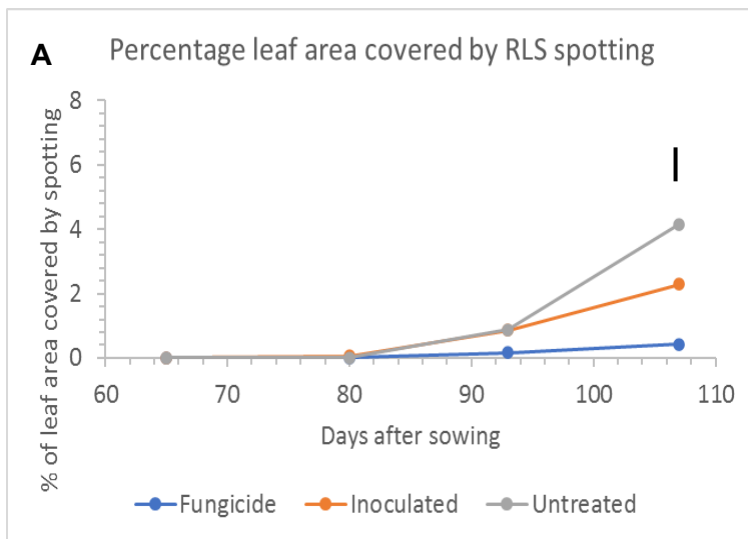
Graphs showing the progress over time of the % area of leaves covered by spotting, lesions, and chlorotic, necrotic, or green tissue (averaged over the top three leaves of plants; flag leaf, F-1 and F-2) are presented in Figure 21. (These data are from the detailed disease progress assessments of plants sampled at 65 days after sowing and at four further two-week intervals thereafter).

Beyond 107 days after sowing, the extent of necrotic tissue meant accurate visual estimates of spotting and lesion coverage were not always possible, so these data are not presented for the final sampling date. The spotting and lesion coverage data presented for 107 days after sowing excludes F-2 leaves for the same reason. The untreated plot from one of the randomised blocks became infested with couch grass early in this experiment which meant that accurate measurements of crop light interception were not possible and was, therefore, excluded from all data analysis.

At 65 days after sowing, no differences in leaf health were observed between the three treatment groups. Plants showed no spotting, lesions, or green leaf area loss. A slight increase in mean chlorotic leaf area was observed in inoculated plants by 80 days after sowing and in untreated plants by 93 days after sowing, and *Ramularia* leaf spot symptoms had begun to develop on inoculated and untreated plants by 93 days after sowing (around a week after flowering). However, at this point an analysis of variance showed no significant differences between treatments for any of the measured parameters (Table 18).

By 107 days after sowing (GS 73), the percentage of leaf area covered by symptoms (spotting plus lesions) varied significantly ($P < 0.001$) between treatments. At this point untreated plants had a higher level of symptoms overall than either of the other treatment groups; however, the composition of the symptom type observed differed, as inoculated leaves displayed on average more lesions relative to spotting, and untreated leaves displayed on average more spotting relative to lesions. By 107 days after sowing, mean necrotic leaf area was significantly greater ($P < 0.001$) in both inoculated and untreated plants, and mean green leaf area was significantly higher ($P < 0.001$) in fungicide treated plants than in either of the other treatment groups.

By 123 days after sowing (GS 83), the mean area of chlorotic leaf tissue had increased slightly on fungicide treated plants, while both inoculated and untreated plants were, on average, almost completely necrotic and had lost all, or almost all, remaining chlorotic or green leaf area. At this point, fungicide treated leaves retained a significantly higher ($P < 0.001$) percentage of green leaf area (~30%) compared to both inoculated and untreated plants, which retained 1.7% and 0%, respectively.



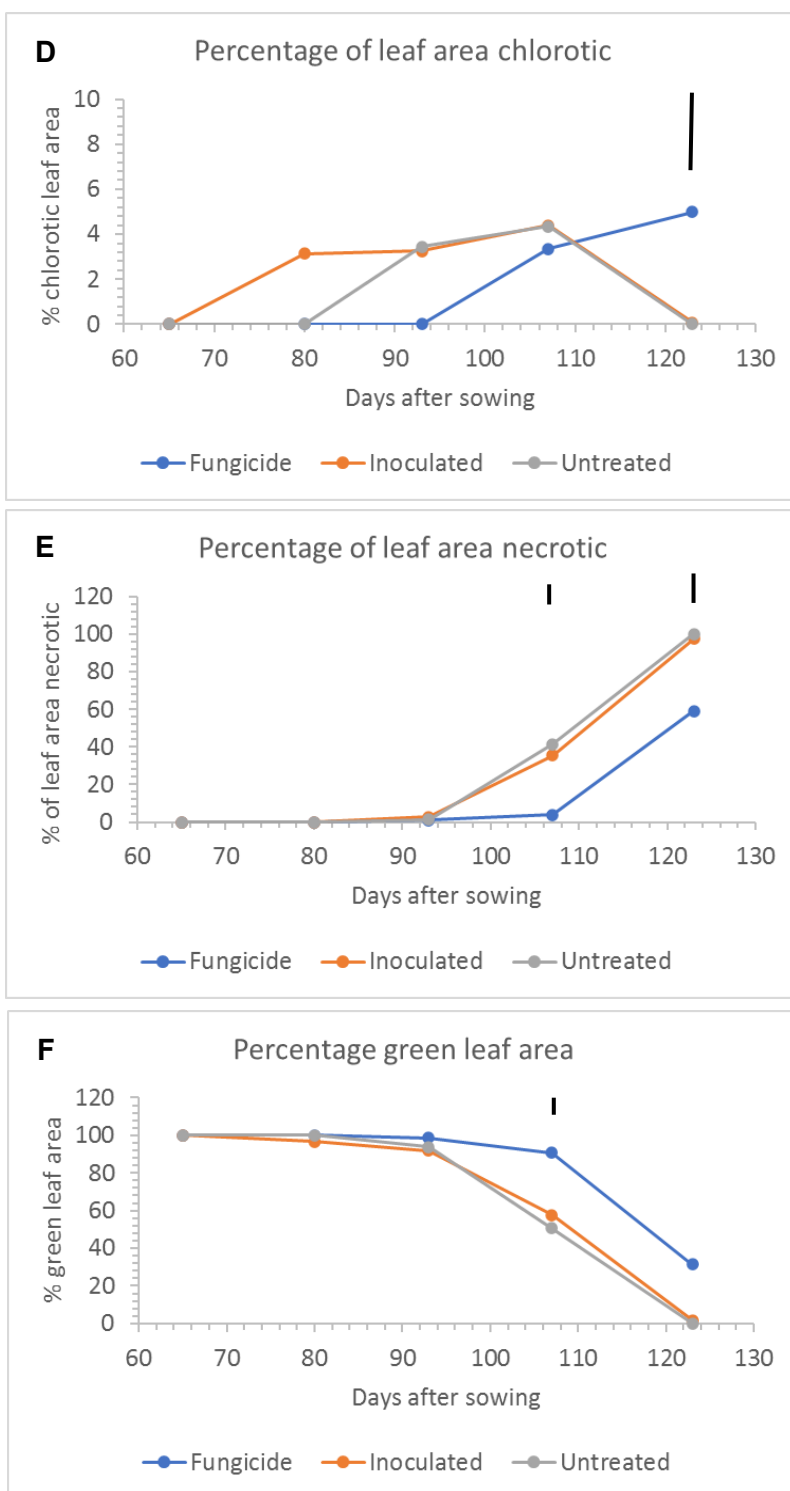


Figure 21. RLS symptom development and green leaf area in field grown barley cv Concerto. Each point at 65, 80, 107 and 123 days after sowing represents the mean of 4 replicates for fungicide treated and inoculated plots, and 3 replicates for untreated plots (10 plants per replicate). Each point at 93 days after sowing represents the mean of 2 replicates (10 plants per replicate). The mean value of the top 3 leaves (Flag leaf, F-1 and F-2) is presented, with the exception of points at 107 days after sowing for the symptom graphs (A, B and C), for which the mean of the top 2 leaves only (Flag and F-1) is presented. Black vertical lines above the graphs represent the l.s.d. for treatment effect from an analysis of variance at that time point. L.s.d. bars are only shown where significant ($P < 0.050$) differences were found between any of the three treatment groups.

Table 18. Analysis of variance results for disease severity and % green area. P values and l.s.d. values from analysis of variance at each time point.

Days after sowing	P value	l.s.d.
Spotting		
65	NA	NA
80	0.230	0.094
93	0.396	1.629
107	<0.001	0.854
123	NA	NA
Lesions		
65	NA	NA
80	0.204	0.157
93	0.290	3.426
107	<0.001	0.642
123	NA	NA
Spotting plus lesions		
65	NA	NA
80	0.213	0.251
93	0.309	4.739
107	<0.001	1.185
123	NA	NA
Leaf chlorosis		
65	NA	NA
80	0.073	3.082
93	0.447	8.430
107	0.845	4.646
123	0.010	3.194
Leaf necrosis		
65	NA	NA
80	NA	NA
93	0.731	6.843
107	<0.001	8.130
123	<0.001	14.320
Leaf Green area (GA)		
65	NA	NA
80	0.075	3.284
93	0.483	16.280
107	<0.001	7.430
123	<0.001	12.160

4.2.2. Fungal growth in planta

R. collo-cygni DNA was extracted from leaves directly below the flag leaf (the F-1 leaf). A low level of *R. collo-cygni* DNA (0.4 ng on average across the first four sampling dates) was found to be present in fungicide-treated plants. *R. collo-cygni* remained low on average for all treatment groups up to and including 107 days after sowing, although by 93 days after sowing the average *R. collo-cygni* DNA quantity in both inoculated and untreated plants was more than double that in fungicide-treated plants, and by 107 days after sowing the average quantity of *R. collo-cygni* DNA in fungicide-treated plants was just 3 % and 0.2 % of that in inoculated and untreated plants, respectively. By 120 days after sowing, the quantity of *R. collo-cygni* DNA in all treatment groups had increased, and was significantly higher ($P < 0.05$ as shown by the l.s.d. for the time x treatment interaction) in both inoculated and untreated plants than in fungicide-treated plants (Table 19), as analysed by ANOVA with time as a factor; however, there was no significant difference between treatment groups prior to this point, meaning that the overall treatment effect was not found to be significant ($P = 0.067$).

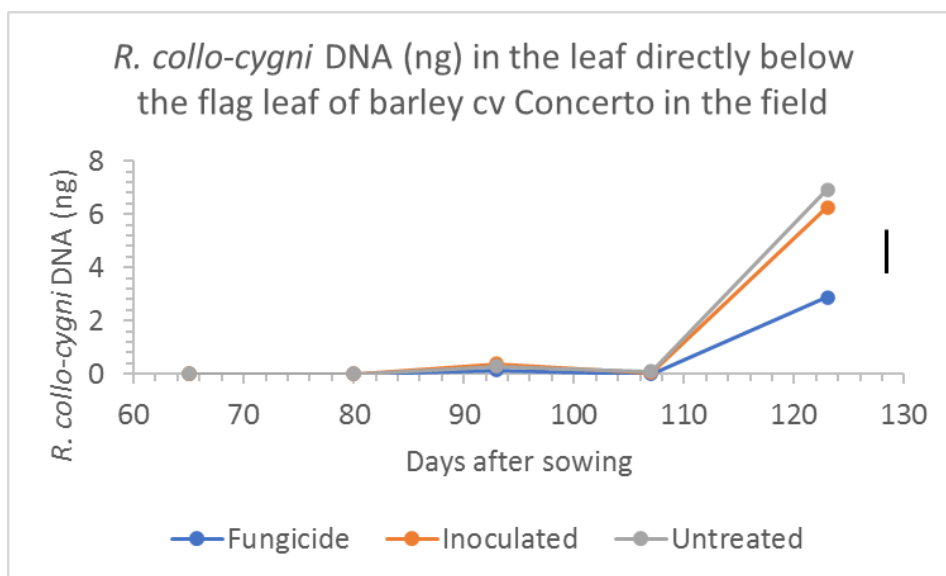


Figure 22. *R. collo-cygni* DNA (ng) in F-1 leaves of field-grown barley cv Concerto. Each point represents the mean of 4 replicates for fungicide treated and inoculated plots and 3 replicates for untreated plots (10 plants per replicate). The black bar to the right of the graph represents the l.s.d. for Treatment.Days after sowing from an analysis of variance.

Table 19. Analysis of Variance results for an analysis of the quantity of *R. collo-cygni* DNA in F-1 leaves of field-grown barley cv Concerto. L.s.d at 5% level.

	P value	l.s.d.
Treatment	0.067	0.781
Days after sowing	<0.001	1.008
Treatment.Days after sowing	0.028	1.746

4.2.3. Crop biomass

R. collo-cygni infection was not found to affect above-ground biomass (dry weight m⁻²) in this experiment (Figure 23 and Table 20). An analysis of variance including time as a factor showed no significant treatment effect ($P = 0.632$) and no significant interaction between treatment and time ($P = 0.882$). Crop biomass was measured at 85, 99 and 113 days after sowing, incorporating the period from anthesis to late grain fill, but not end of grain fill and the period of major canopy senescence.

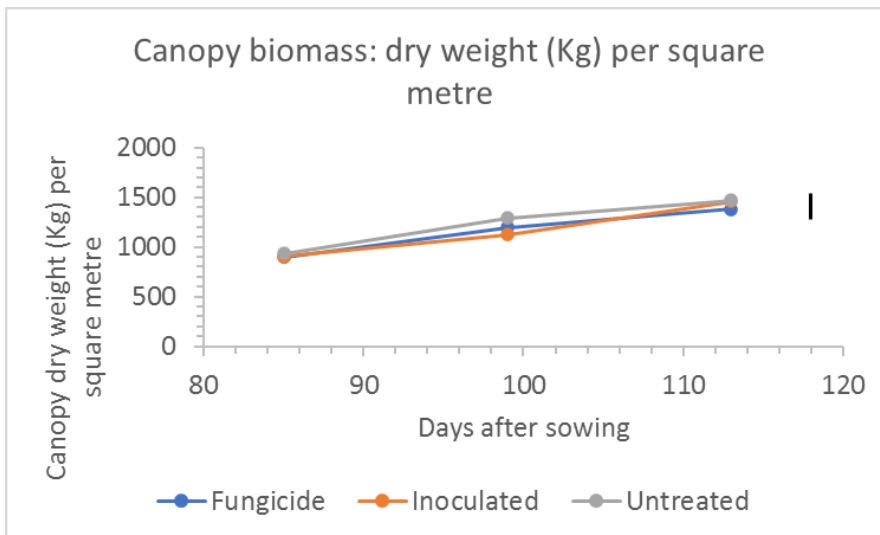


Figure 23. Canopy biomass of field-grown barley cv Concerto. Each point represents the mean of 4 replicates for fungicide treated and inoculated plots and 3 replicates for untreated plots. The black line to the right of the graph represents the l.s.d. (5% level) for the Treatment.Days after sowing interaction from an analysis of variance.

Table 20. Analysis of variance results for above-ground biomass of field-grown barley cv Concerto.

	P value	l.s.d.
Treatment	0.632	142.7
Days after sowing	<0.001	142.7
Treatment.Days after sowing	0.882	247.1

4.2.4. Chlorophyll fluorescence

An analysis of variance with time as a factor detected no significant differences in maximal chlorophyll fluorescence (F_v/F_m) between treatments until 111 days after sowing, by which point symptoms and associated green leaf area loss on inoculated and untreated leaves were well-developed. At this point, F_v/F_m was significantly ($P = 0.007$) reduced in both inoculated and untreated plots, relative to fungicide treated plots (Table 21 and Figure 24).

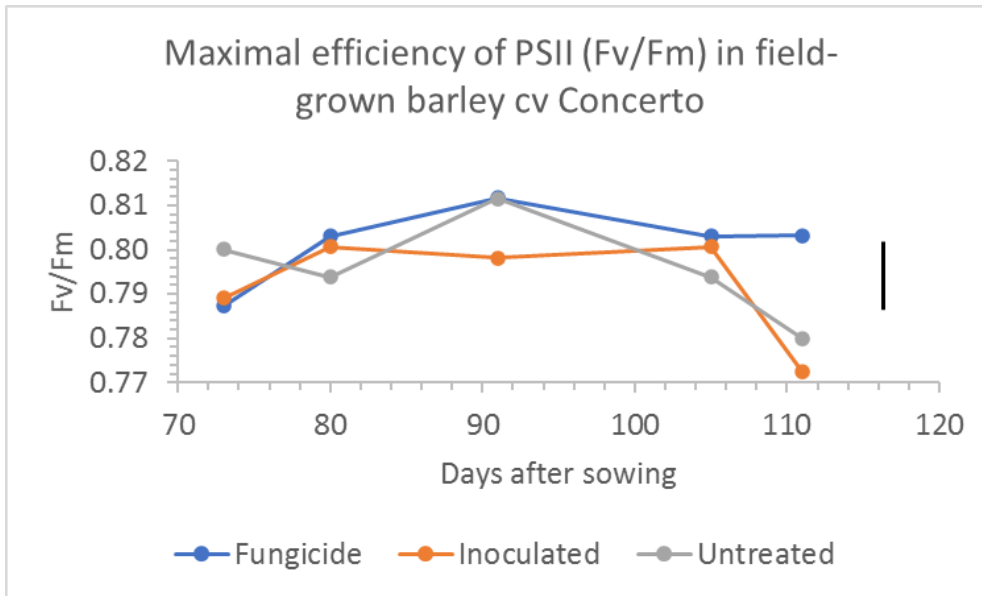


Figure 24. Maximal efficiency of PSII (Fv/Fm) measured on F-1 leaves of field-grown barley. Each point represents the mean of 4 replicates for fungicide treated and inoculated plots and 3 replicates for untreated plots (5 plants per replicate).

Table 21. Analysis of variance results for maximal efficiency of PSII (Fv/Fm) measured on F-1 leaves of field-grown barley.

	P value	I.s.d.
Treatment	0.013	0.006
Days after sowing	<0.001	0.008
Treatment.Days after sowing	0.007	0.014

4.2.5. Healthy area light interception

The fraction of the incident PAR intercepted by plants that was intercepted by healthy (green) tissue was calculated from measurements taken at three time points during grain filling at 85, 99 and 113 days after sowing. The data were analysed using analysis of variance for each time point (Table 22). At 85 days after sowing, no significant differences were found between treatment groups.

At 99 days after sowing, inoculated and untreated plots were found to be significantly different ($P = 0.005$) to fungicide treated plots. At this point, the fraction of PAR intercepted by healthy tissue for fungicide treated plots remained the same as it had been at 85 days after sowing (0.97); however, that for both inoculated and untreated plots had fallen to 0.94.

At 113 days after sowing, the fraction of PAR intercepted by healthy tissue had fallen again for inoculated and untreated plots (to 0.83 and 0.81, respectively), significantly lower ($P < 0.001$) than that for fungicide treated plots (0.93).

The total PAR (MJ m^{-2}) intercepted by healthy (green) tissue during grain filling was also analysed using analysis of variance (Table 24). Significant differences were found between all treatment groups ($P < 0.001$). PAR intercepted by healthy tissue was reduced relative to fungicide treated plots for both inoculated and untreated plots (~18% and ~23% reduction, respectively). The difference between inoculated and untreated plots was also found to be significant ($P < 0.001$). PAR intercepted by healthy tissue was reduced by ~ 5% for untreated plots relative to inoculated plots.

Table 22. Treatment means and analysis of variance results for the fraction of incident PAR that was intercepted by healthy (green) tissue of field grown barley plants cv Concerto at 3 time points during grain filling.

Days after sowing	Treatment means for the fraction of total light intercepted by plants that was intercepted by healthy (green) tissue			P value	l.s.d.
	Fungicide	Inoculated	Untreated		
85	0.97	0.96	0.96	0.805	0.018
99	0.97	0.94	0.94	0.005	0.018
113	0.93	0.82	0.81	<0.001	0.040

Table 23. Treatment means and analysis of variance results for total PAR (MJ m^{-2}) intercepted by healthy (green) tissue of field grown barley plants cv Concerto during grain filling

Treatment means for total PAR (MJ m^{-2}) intercepted by healthy (green) tissue during grain filling			P value	l.s.d.
Fungicide	Inoculated	Untreated		
289.80	236.70	223.90	<0.001	5.810

4.2.6. Crop yield

2.1.6.1 Yield components

An analysis of variance (Table 23) detected significant differences between the three treatment groups for grain number m^{-2} and yield (t ha^{-1} at 15% moisture content); ($P < 0.001$ and $P = 0.001$ respectively). Yield and grain number m^{-2} for both inoculated and untreated plots were reduced relative to fungicide treated plots; however, inoculated plots had a higher grain number relative to untreated plots (a difference of ~1000 grains m^{-2}) and a higher yield (a difference of ~1 t ha^{-1}).

Table 24. Yield components. I.s.d. values are for 5% level

	Mean treatment value			P value	I.s.d.
	Fungicide	Inoculated	Untreated		
Grain number m ⁻²	15571	13899	12689	<0.001	978.400
Mean grain weight (mg)	46.90	45.63	43.17	0.115	3.651
Yield (t ha ⁻¹ at 15% Moisture Content)	7.30	6.34	5.49	0.001	0.715

4.2.6.2 Radiation use efficiency

Radiation use efficiency (RUE) was estimated by plotting the biomass gain during the first half of grain filling against the cumulative healthy PAR interception over the same period. Simple linear regression with groups was used to compare the slopes and the intercepts for the different treatments. The slopes were not significantly different. The slope for fungicide was 2.30, for inoculated it was 2.83 and for untreated it was 2.05 g DM MJ⁻¹ PAR. The slope of the initial single regression applied to all data, assuming slopes and constants to be equal, was 2.41 g DM MJ⁻¹. This was used in the yield loss prediction equation as the constant value for RUE (g biomass per MJ of light intercepted).

4.2.6.3 Predicted and observed yield loss

The reduction in yield relative to fungicide-treated plots predicted from the loss of green leaf area and healthy area PAR interception (Figure 25) was 1.51 t ha⁻¹ for inoculated plots and 1.87 t ha⁻¹ for untreated plots. These were found not to be significantly different from the observed yield losses at harvest when analysed by paired t-test (P = 0.126 and P = 0.881, respectively).

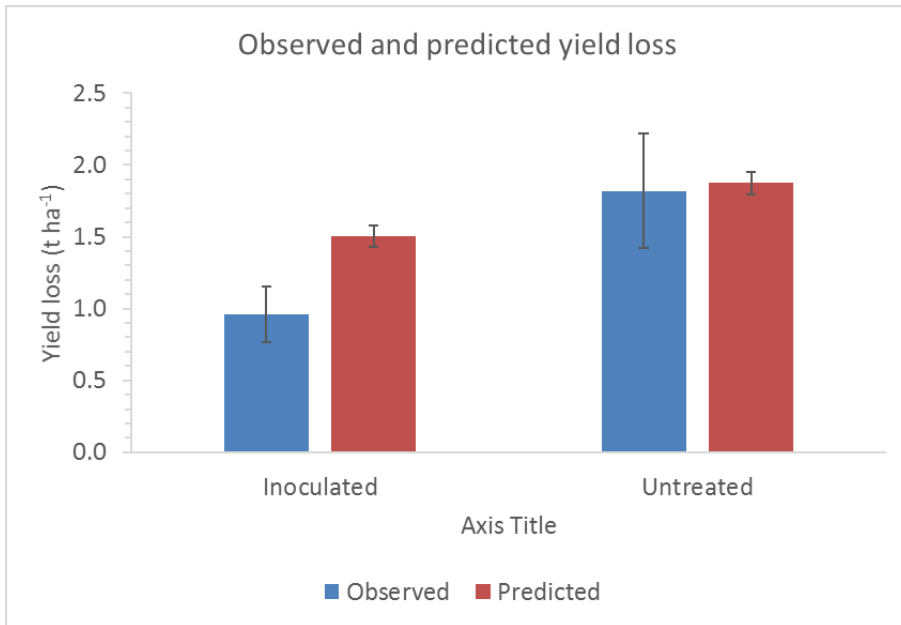


Figure 25. Reduction in yield of inoculated and untreated plots relative to fungicide treated plots. Blue columns = observed reduction. Red columns = reduction predicted from the loss of green leaf area and healthy area PAR interception. Each column represents the average of 4 replicates (inoculated) and 3 replicates (untreated). Error bars are \pm SEM.

4.3. Effects of varying rates of leaf senescence on RLS disease development

4.3.1. Senescence and visible symptom progression

4.3.1.1 *Relative chlorophyll content*

Relative leaf chlorophyll content reduced over time in all treatment groups (Figure 26). The rate and extent of decline was greater in plants that were not treated with cytokinin. A repeated measures analysis of variance (Table 27) revealed a significant ($P < 0.001$) main effect of cytokinin treatment on relative chlorophyll content, and a significant interaction ($P < 0.001$) between cytokinin treatment and time (days after inoculation). The analysis did not reveal a statistically significant main effect of fertiliser treatment ($P = 0.181$), and there was no significant interaction between fertiliser treatment and time ($P = 0.122$), between fertiliser treatment and cytokinin treatment ($P = 0.332$), or between fertiliser treatment, cytokinin treatment and time ($P = 0.403$). Leaving fertiliser treatment out of consideration, therefore, plants in the treatment groups that did not receive cytokinin had, on average, significantly lower ($P < 0.001$) relative chlorophyll content than those that did from 21 days after inoculation onwards.

4.3.1.2 *Green Leaf Area*

A repeated measures analysis of variance revealed a significant ($P = 0.003$) main effect of cytokinin treatment on % Green Leaf Area, and a significant interaction ($P < 0.001$) between cytokinin treatment and time (days after inoculation) (Figure 26 and Table 27). The analysis did not reveal a statistically significant main effect of fertiliser treatment ($P = 0.064$), and there was no significant interaction between fertiliser treatment and time ($P = 0.081$) or between fertiliser treatment and cytokinin treatment ($P = 0.086$). There was a borderline significant ($P = 0.052$) interaction between fertiliser treatment, cytokinin treatment and time. By 24 days after inoculation, plants that received neither fertiliser nor cytokinin (treatment group 1) had lower % GLA ($P = 0.052$) than plants in all the other treatment groups (Figure 26). There were no significant differences between plants in any of the other treatment groups at this stage. This pattern remained stable up to and including 28 days after inoculation. By 33 days after inoculation, plants in both the treatment groups that did not receive cytokinin (groups 1 and 3) displayed lower ($P = 0.052$) % GLA than those that did (treatment groups 2 and 4). By this stage there was no longer a statistically significant difference between plants that received fertiliser but no cytokinin and plants that received neither fertiliser nor cytokinin (groups 1 and 3). There were no significant differences between plants in either of the treatment groups that received cytokinin (groups 2 and 4) at any point throughout the experiment, regardless of fertiliser status. Thus, fertiliser application delayed

decline in % GLA temporarily compared to plants that were not treated with either cytokinin or additional fertiliser (controls – treatment group 1). Plants treated with cytokinin maintained a greater percentage of green leaf area over a longer period than those that did not, irrespective of the fertiliser treatment (Figure 26).

4.3.1.3 RLS symptoms

In inoculated plants that were not treated with either cytokinin or additional fertiliser (controls – treatment group 1), the first symptoms of RLS appeared 9 days after inoculation. Symptom severity steadily increased reaching around 9% by the end of the experiment. Application of additional fertiliser significantly reduced the severity of symptoms compared to controls from around day 17 onwards such that symptom severity at the end of the experiment was ~5%. Treatment of plants with cytokinin either on its own or in combination with additional fertiliser had a greater effect on symptom development than fertiliser alone. The final disease severity was <3% in plants treated with cytokinin alone.

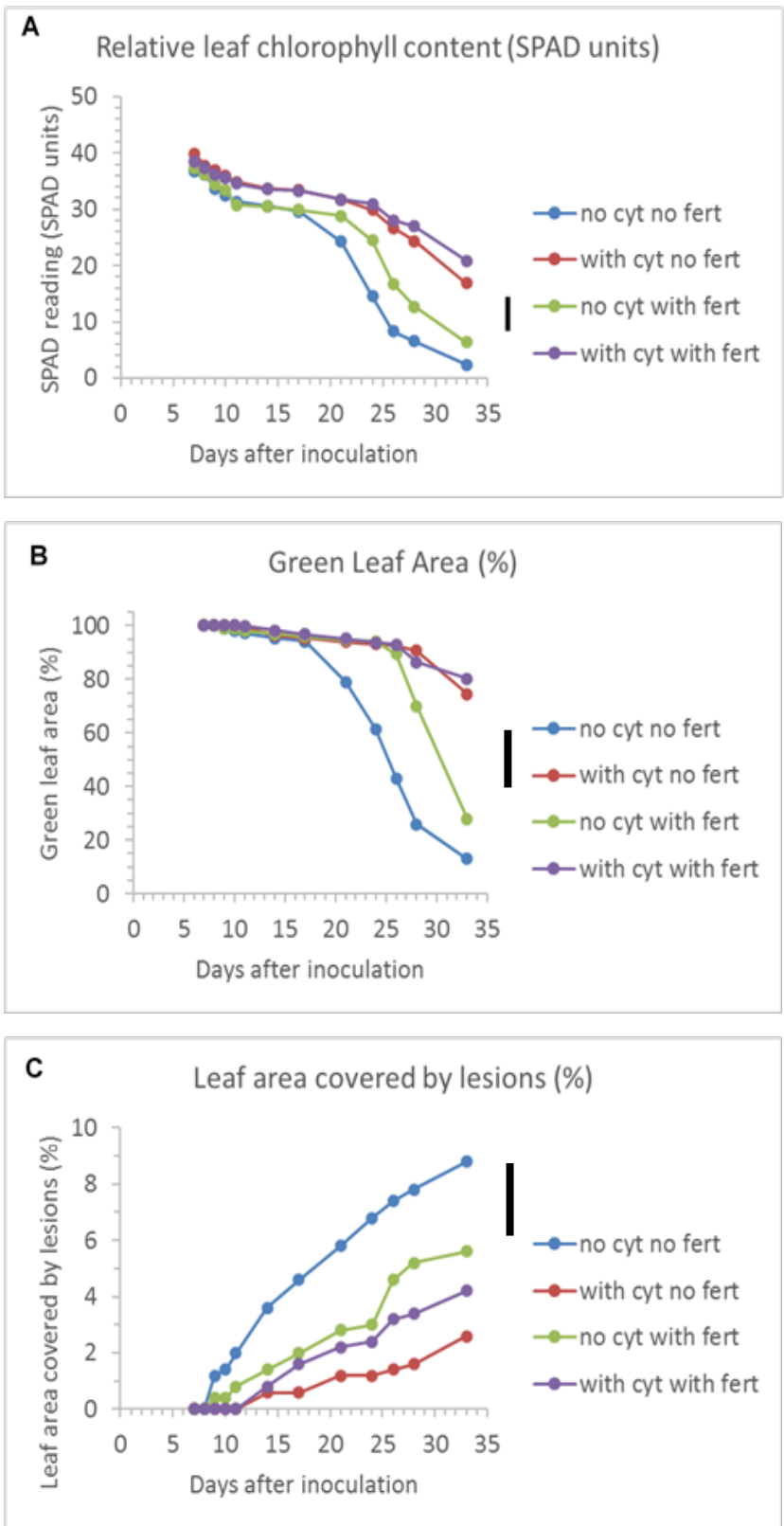


Figure 26. Effects of cytokinin and additional fertiliser treatments on leaf senescence and RLS symptom development on barley cv Fairing seedlings over time (days after inoculation). **A**) Relative leaf chlorophyll content (SPAD units): average value of measurements taken in distal and basal leaf sections. **B**) Green Leaf Area (%) **C**) Leaf area covered by RLS lesions (%). Points are means of 5 replicates. All data is from second leaves of barley seedlings. Vertical black lines to the right of the graphs represent the least significant difference (l.s.d. 5%) value for the interaction between cytokinin, fertiliser treatment, and time (days after inoculation) from a repeated measures ANOVA.

Table 25. P values from repeated measures ANOVA of effects of cytokinin treatment (yes or no), fertiliser treatment (yes or no) and time (days after inoculation) on the relative chlorophyll content (SPAD readings), % Green Leaf Area, and % area of leaf covered by RLS lesions of second leaves of barley seedlings N = 5.

	SPAD reading leaf average	Green area of leaf (%)	Area of leaf covered by lesions (%)
Cyt	<0.001	0.003	0.004
Fert	0.181	0.064	0.310
Cyt.Fert	0.332	0.086	0.039
Time	<0.001	<0.001	<0.001
Time.Cyt	<0.001	<0.001	0.003
Time.Fert	0.122	0.081	0.523
Time.Cyt.Fert	0.403	0.052	0.045

4.3.2. Fungal growth in planta

4.3.2.1 *Rcc* DNA levels in leaves during the experiment

R. collo-cygni DNA was quantified from unique sets of plants destructively sampled at 7, 11, 17 and 21 days after inoculation (1, 5, 11 and 15 days after cytokinin application). An analysis of variance using cytokinin treatment (yes or no), fertiliser treatment (yes or no) and time (days after inoculation) as factors detected significant main effects of cytokinin treatment ($P < 0.001$), fertiliser treatment ($P = 0.023$) and time ($P < 0.001$). All interactions tested were also found to be significant (Figure 27 and Table 26). By 21 days after inoculation, *R. collo-cygni* DNA levels were significantly higher ($P = 0.023$) in plants that received neither cytokinin nor fertiliser treatment than in all other treatment groups.

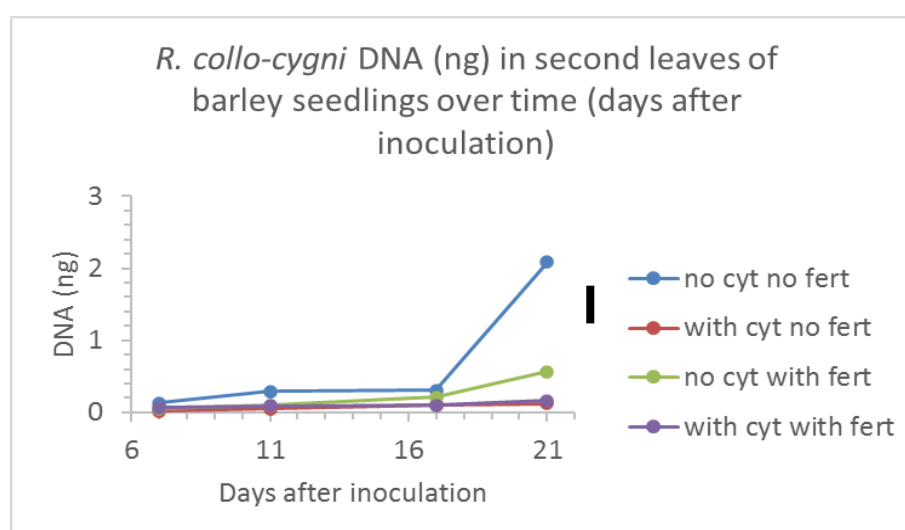


Figure 27. *R. collo-cygni* DNA (ng) in second leaves of barley seedlings cv Fairing over time. From an experiment to compare the effects of cytokinin and fertiliser treatments on green leaf area retention and RLS disease development. Each point shows the average of 5 replicates. The black, vertical bar to the right of the graph represents the least significant difference (l.s.d. 5%) for the interaction between cytokinin treatment, fertiliser treatment and time from an analysis of variance.

Table 26. ANOVA results for fungal growth in planta. P values and l.s.d. values from ANOVA with cytokinin treatment (yes or no, fertiliser treatment (yes or no) and time (days after inoculation) as factors. N = 5. From an experiment to compare the effects of cytokinin and fertiliser treatments on green leaf area retention and RLS disease development

	P value	l.s.d.
Cytokinin	<0.001	0.185
Fertiliser	0.023	0.185
Days after inoculation	<0.001	0.262
Cytokinin.Fertiliser	0.010	0.262
Cytokinin.Days after inoculation	<0.001	0.371
Fertiliser.Days after inoculation	0.027	0.371
Cytokinin.Fertiliser.Days after inoculation	0.023	0.524

4.3.3. Rcc DNA levels in leaves at the end of the experiment

The same set of plants which had been measured repeatedly and non-destructively throughout the experiment to monitor leaf senescence and RLS symptom development were destructively sampled at 33 days after inoculation, and the *R. collo-cygni* DNA level in second leaves was quantified.

A one-way ANOVA comparing the four treatment groups showed that *R. collo-cygni* DNA levels were significantly higher ($P = 0.025$) in the plants that received no cytokinin and no fertiliser treatment than in any of the other groups (Figure 28). No significant differences were found between any of the other treatment groups ($P > 0.05$).

A two-way ANOVA including the interaction between fertiliser treatment and cytokinin treatment (Table 27) found no significant effect of fertiliser treatment ($P = 0.093$) and a weak interaction between fertiliser and cytokinin treatment ($P = 0.059$). This method of analysis showed a significant main effect of cytokinin treatment ($P = 0.032$).

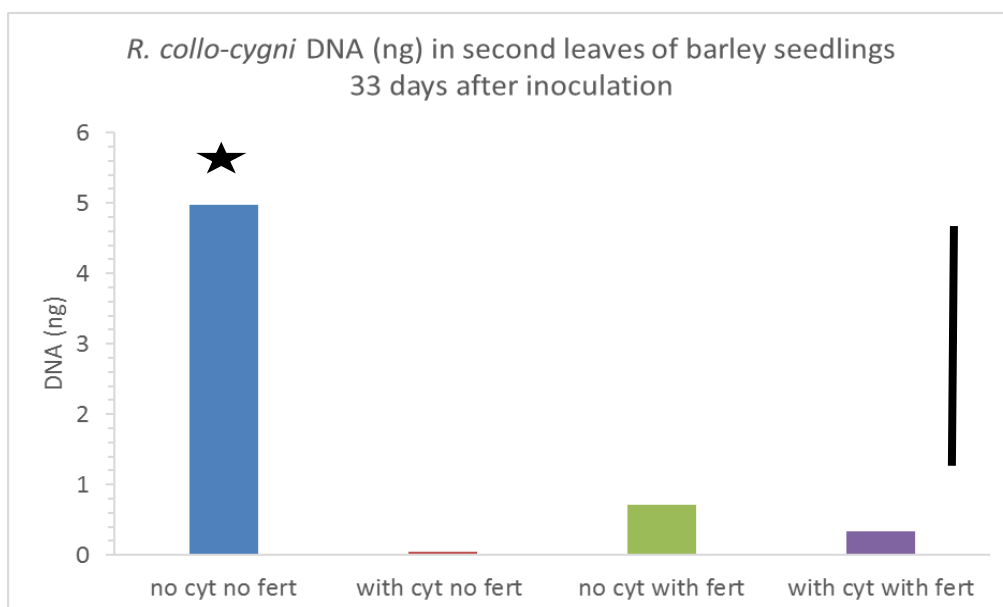


Figure 28. *R. collo-cygni* DNA (ng) in second leaves of barley seedlings Cv Fairing at 33 days after inoculation. Bars show average of 5 replicates. The black, vertical line to the right of the graph represents the l.s.d. (3.39) for Cytokinin.Fertiliser from a two-way ANOVA. The star above treatment group 1 (no cytokinin or fertiliser treatment) indicates that the plants in this treatment group had significantly higher *R. collo-cygni* DNA levels than those in any of the other treatment groups ($P = 0.025$), when analysed using one-way ANOVA.

Table 27. ANOVA results for fungal DNA in plants at the end of the experiment. P values from a two-way ANOVA including interaction between fertiliser and cytokinin treatment. $N = 5$.

	P value
Cytokinin	0.032
Fertiliser	0.093
Cytokinin.Fertiliser	0.059

5. Discussion

5.1. Effect of Rcc infection on photosynthesis

Inoculation of barley seedlings with *R. collo-cygni* mycelial suspension achieved fewer and smaller lesions than are typical of Ramularia leaf spot symptoms in the field on both the spring barley varieties used in the experiments (cv Concerto and cv Fairing). Fungal biomass in infected leaves, as detected by DNA quantification, remained relatively static throughout asymptomatic growth and onset of disease symptoms when analysed in cv Concerto seedlings (this analysis was not conducted in cv Fairing). Analyses of leaf photosynthesis and dark respiration using chlorophyll fluorescence imaging and infra-red gas analysis did not detect any significant differences between infected and control leaves prior to the development of visible symptoms. As visible symptoms developed, effects on photosynthesis were localised to lesions on otherwise green leaves. After symptom development, rates of net CO₂ fixation and photochemical efficiency were still not found to be significantly reduced when averaged over the wider leaf measurement area. The apparent

lack of a significant disease effect at this scale would seem to be a result of the low severity of disease symptoms as finer scale chlorophyll fluorescence image analyses revealed a progressive reduction in photosynthetic activity within lesions as they matured. Analysis of photosynthetic induction kinetics provided additional evidence that photochemical processes were not affected by asymptomatic infection. Induction kinetics can be altered by some factors as shown by effects of leaf age in Experimental series 1, in particular. However, *R. collo-cygni* infection was not found to affect induction kinetics.

The results indicate that *R. collo-cygni* does not impact leaf photosynthesis in asymptomatic leaves or green areas of symptomatic leaves, suggesting that asymptomatic infection or low levels of symptom expression do not necessarily have a negative impact on barley.

These results are similar in some respects to those for some previous studies of hemibiotrophic crop pathogens. Robert *et al.* (2006) reported no significant effect on net photosynthesis in wheat leaves inoculated with *Zymoseptoria tritici* prior to the appearance of visible symptoms. Thereafter, net leaf photosynthesis was found to be increasingly reduced as visible symptoms developed from chlorotic to necrotic damage. Studies of bean anthracnose disease associated with *Colletotrichum lindemuthianum* (Bassanezi *et al.*, 2001; Meyer *et al.*, 2001) also found no effect on net photosynthesis prior to visible symptom appearance. In that pathosystem, once necrotic lesions appeared, greater reductions in net leaf photosynthesis were observed than could be accounted for by the extent of visible symptoms. Bassanezi *et al.* (2001) attributed this to a reduction of intercellular CO₂ due to stomatal resistance. However, Meyer *et al.* (2001) argued that metabolic inhibition of photosynthesis, possibly mediated through inhibition of Ribulose 1·5-bisphosphate (RuBP) regeneration, was also involved as a decrease in the photosynthetic electron transport rate was maintained under high CO₂ exposure.

The results presented in this chapter did not suggest any effect on photosynthesis in non-symptomatic tissue. Chlorophyll fluorescence images of developing lesions indicated a pattern whereby Φ PSII and ETR values were initially maintained in young lesions, while NPQ and Fv/Fm values were usually reduced. Fv/Fm values were often particularly or solely reduced in a small area towards the centre of developing lesions at this early stage. As symptoms matured, all photosynthetic parameters were normally reduced, reaching near zero in the most developed lesions, presumably indicating physical damage to cells or cell death.

An analysis of the infection process of *R. collo-cygni* in barley using confocal microscopy and transgenic fungal isolates (Kaczmarek *et al.*, 2017) also found no evidence of physical damage to host cells until the appearance of visible symptoms on leaves. Host cells appeared to remain undamaged during leaf penetration via stomata, fungal growth in the substomatal cavity, and the

earlier stages of intercellular growth of hyphae in the mesophyll tissue. Development and maturation of lesions was associated with localised mesophyll cell death and fungal sporulation through stomata and collapsed mesophyll cells. A loss of chlorophyll fluorescence signal was observed within necrotic lesions. Some red discolouration of the tissue immediately surrounding developing lesions was also observed, which the authors suggested could be related to the production of rubellin toxins by the fungus.

NPQ (non-photochemical quenching), observed in the current experiments to be lower within lesions than in green areas of infected leaves or control leaves from the early stages of lesion development onwards, has a role in preventing damage from reactive oxygen species (ROS) by dissipating excess excitation energy and down-regulating PSII. The apparent loss of, or decrease in, the ability to activate NPQ through generation of a transthylakoid gradient within lesions could increase the likelihood of damage at high light intensities or in any situations where CO₂ dependent electron flow is disrupted, for example due to damage to Calvin-Benson cycle enzymes. Hideg *et al.* (2008) showed that suppression of NPQ could result from inhibition of enzymes involved in the Mehler ascorbate peroxidase (MAP) cycle, and that ROS are formed when the NPQ-generating process is, thus, inhibited. Possibly, the reduced NPQ observed at lesion sites could indicate a direct or indirect effect of *R. collo-cygni* on processes necessary for initiation of NPQ. If this were the case, the initial maintenance of relatively high levels of Φ PSII within developing lesions could possibly be associated with absence or reduction of NPQ-related downregulation, potentially leading to increased ROS production, particularly under environmental stress such as high light intensity.

Interestingly, two recent comparative transcriptomic studies of *Z. tritici* on wheat (Ma *et al.*, 2018) and *R. collo-cygni* on barley (Sjokvist *et al.*, 2018), have reported upregulation of host pathogenesis-related genes and down-regulation of photosynthesis-related genes during asymptomatic infection. Possibly, the down-regulation of photosynthesis-related genes observed in these studies does not result in a significant effect on physiology as analysed in the experiments presented in this study or those presented in the reports of Robert *et al.* (2006) or Scholes and Rolfe (2009). Alternatively, differences in experimental methodology might explain the different outcomes. This reported very active transcriptome response of barley to *R. collo-cygni* contrasts with the comparatively subdued response of *Lolium arundinaceum* (tall fescue) to its fungal endophyte *Epichloë coenophiala* (Dinkins *et al.*, 2017), perhaps casting some doubt on the accuracy of describing *R. collo-cygni* as an endophyte during its asymptomatic growth period in barley.

Two other observations of interest from the study by Sjokvist *et al.* (2018) are the reported upregulation of defence-response genes associated with plant recognition of necrotic pathogens,

for example, associated with the production of jasmonic acid and ethylene, but no regulation of expression of genes associated with the salicylic acid pathway more commonly associated with biotrophic pathogens, and the upregulation of *R. collo-cygni* genes associated with hexose transporters. The latter suggests hexose feeding by the fungus in the apoplast once hyphae entered the mesophyll layer. Some fungal pathogens of plants are capable of utilising different nutritional sources under different conditions (Divon and Fluhr, 2007), so understanding more about the nutritional status of *R. collo-cygni* in its different life stages could be informative in understanding shifts in host responses. Sjokvist *et al.* (2018) reported upregulation of *R. collo-cygni* genes associated with activation of the glyoxylate cycle during asymptomatic infection, which suggests the fungus may utilise fatty acids (either fungal or host-derived) for nutrition at this stage, similar to the early stages of asymptomatic infection of wheat by *Zymoseptoria tritici* as reported by Palma-Guerrero *et al.* (2016). However, both these studies were conducted in artificially inoculated seedlings, while the period prior to symptom appearance was short (~ 10 days). As fatty acid metabolism is common in fungal pathogens of plants during leaf surface growth and leaf penetration (Divon and Fluhr, 2007), evidence pointing to fatty acid metabolism in this context does not necessarily reflect the nutritional strategy adopted during the much longer asymptomatic phase of *R. collo-cygni* observed in the field, particularly, where infected seed is the source of fungal growth *in planta*, or the context of a mature plant and the onset of senescence associated with the typical timing of *Ramularia* leaf spot symptoms.

In summary, the results found no effect on host photosynthesis of *R. collo-cygni* infection prior to symptom appearance or in green areas of infected leaves, and low levels of visible disease symptoms were not found to affect net leaf photosynthesis. However, it is important to bear in mind that these experiments were conducted in seedlings using inoculation with mycelial suspension. The conditions were quite different to those of a field epidemic of *Ramularia* leaf spot. It is possible that plant developmental stage, interaction with environment, infection route (via seed or spore), or other factors could lead to a different outcome in a field situation.

5.2. Impact of Rcc infection on barley yield

The timing of symptom appearance and disease development observed during the experiment were consistent with those previously described as typical for RLS (see section one of the report). Symptoms had begun to develop on the upper three leaves of inoculated and untreated plants by 93 days after sowing (around a week after flowering), increasing significantly relative to fungicide treated plots by 107 days after sowing (GS 73), at which point symptom severity, assessed as the percentage of leaf area covered by symptoms including both spotting and lesions, was greater in untreated plots than in inoculated.

At GS 73, fungicide treated plants retained >90% of green leaf area on average across the upper three leaves, while inoculated and untreated plants had lost ~50% and ~60% of green leaf area, respectively. Fungicide treated plants retained ~30% green leaf area on average across the upper three leaves at 123 days after sowing (GS 83), when inoculated and untreated plants were nearing total senescence. Total canopy senescence occurred at approximately 123, 127 and 135 days after sowing for untreated, inoculated and fungicide treated plots, respectively. These effects of treatments on post-anthesis green leaf area duration resulted in associated changes in PAR interception by healthy tissue during grain filling.

Maximal chlorophyll fluorescence (F_v/F_m) was not found to be affected by *R. collo-cygni* infection in asymptomatic leaves or green areas of symptomatic leaves. It was significantly reduced in symptomatic tissue after lesions developed indicating damage to photosystem II reaction centres. These results reflect those found in barley seedlings inoculated with *R. collo-cygni*, described in previously. The lack of any significant effect on photosynthetic activity prior to symptom development is consistent with whole canopy measurements of RUE (radiation use efficiency). In the current work, RUE was estimated from the relationship between light interception by green (healthy) tissue and above ground biomass gain. There was no significant difference in RUE between fungicide treated, untreated or inoculated plants implying that RUE was not affected by *R. collo-cygni* infection when necrotic lesions are excluded from estimates of light interception and the analysis confined to non-symptom expressing tissue. When RUE is estimated this way, it measures the efficiency of conversion of light energy intercepted by healthy tissue into biomass and is, thus, the net outcome of effects of environment and experimental treatments on photosynthesis, respiration and partitioning of biomass between shoots and roots. These data, therefore, support the conclusion that there is no discernible effect of asymptomatic *R. collo-cygni* infection on RUE.

untreated plots relative to that of fungicide treated plots in this experiment. However, the yield of inoculated plots was significantly higher than that of untreated plots. If the effects of ramularia leaf spot on yield are the simply the result of reductions in green leaf area because of symptom development and tissue necrosis, it should be possible to estimate the difference in yield between diseased and non-diseased plants from the difference in light interception without needing to invoke effects of disease on RUE or remobilisation of soluble carbohydrate reserves for grain filling. The results for the analysis of healthy area light interception and comparison of predicted and observed yield loss indicated that the difference in post-anthesis PAR interception by healthy tissue between fungicide-treated and the inoculated and untreated plots was sufficient to account for the observed yield losses.

The reduction in post-anthesis PAR interception by healthy tissue in inoculated and untreated plots was associated with RLS symptom development; the production of lesions and associated chlorosis and necrosis, and reduced duration of the period between anthesis and complete canopy senescence relative to fungicide treated plots. However, whilst the maintenance of green leaf area following fungicide treatment may be sufficient to account for the yield differences between treatments, the actual mechanisms responsible for increasing yield appear to be more complex. The greater yield of fungicide-treated plots was the result of a larger grain number m^{-2} and not a greater mean grain weight as might be expected were fungicide solely protecting post-anthesis photosynthetic activity.

It is conceivable that loss of post-anthesis assimilation due to disease-associated reduction in healthy area light interception could lead to loss of ears or abortion of grains. However, experiments using shading to reduce light interception in spring barley as a proxy for the effects of foliar disease symptoms (Kennedy *et al.*, 2018) found no evidence of grain abortion, nor a significant reduction in ear number, when shading was imposed 14 days after GS55 to reduce net photosynthesis activity during grain filling.

It is also possible that fungicide treatment increased grain numbers directly and that the increase in grain sink capacity operated in tandem with protection of canopy PAR interception and photosynthesis to provide sufficient assimilate for grain filling and to maintain mean grain weight. Yield effects associated with some fungicide groups extending beyond visible disease control have been a topic of research for some time. SDHI, triazole and strobilurin fungicides have been found to delay leaf senescence in wheat, correlating with increased yields (Wu and Von Tiedemann, 2001; Cromey *et al.*, 2004; Berdugo *et al.*, 2012). Suggested mechanisms for strobilurin-associated delayed leaf senescence in wheat include reduced production of ethylene linked to reduced rates of cytokinin degradation (Grossmann and Retzlaff, 1997; Grossmann *et al.*, 1999) or increased production of antioxidants leading to reduced oxidative stress (Wu and Von Tiedemann, 2001). Bingham *et al.* (2021) reported increased grain numbers m^{-2} in spring barley with applications of triazole and strobilurin fungicides during booting (prothioconazole and pyraclostrobin) in the absence of any visible disease. In the same study, chlorothalonil application provided equivalent disease control, including a reduction in *R. collo-cygni* DNA during asymptotic infection prior to flowering, but did not lead to increased grain number m^{-2} . This suggests that the increased grain number m^{-2} associated with triazole and strobilurin fungicides was a direct physiological effect, and not due, for example, to asymptomatic pathogen control. The authors suggested that increased grain numbers per ear and decreased spikelet mortality could be responsible for the observed effects of triazole and strobilurin fungicides on grain number.

The field experiment described in this report used prothioconazole as part of the full fungicide treatment to achieve disease-free plants and pyraclostrobin to control diseases other than *R. collo-cygni* in the inoculated treatment group (Table 1). Both of these fungicides have been linked to direct effects on grain number m⁻² as described above; therefore, it is possible that this was a contributing factor to the yield differences observed between treatment groups.

In summary, *R. collo-cygni* was not found to impact photosynthesis in field grown barley cv. Concerto prior to the appearance of visible RLS disease symptoms, reflecting the situation observed in inoculated seedlings described in controlled condition experiments, suggesting that the long asymptomatic life stage of *R. collo-cygni* in field grown barley may not have a negative impact. Analysis of healthy area light interception and comparison of predicted and observed yield loss indicated that the difference in post-anthesis PAR interception by healthy tissue between fungicide-treated and the inoculated and untreated plots was sufficient to account for the observed yield losses. This indicates that the symptomatic life stage of *R. collo-cygni* in barley is of primary importance for yield loss to RLS.

5.3. Effect of varying rates of leaf senescence on RLS development

RLS symptom severity and fungal growth in planta was reduced in plants that received treatments designed to delay leaf senescence relative to control plants that did not. Exogenous application of cytokinin was more effective than fertiliser application at maintaining green leaf area and relative leaf chlorophyll content.

Symptom expression and fungal DNA levels were highest in plants that received neither of the senescence-delaying treatments. RLS lesions first appeared, and symptom severity differed significantly between treatments before differences in relative chlorophyll content or % GLA became apparent. *R. collo-cygni* DNA was significantly reduced in all plants relative to controls (treatment group 1), including those treated with fertiliser alone. Symptom severity between treatments differed significantly before significant differences in fungal DNA level were apparent between treatments, so the quantity of fungus within leaves did not appear to be a basis for initial symptom expression or severity. The association between increased symptom severity and higher levels of *R. collo-cygni* DNA observed towards the end of the experiment was similar to that reported by Taylor *et al.* (2010). In the field experiment described in this report, *R. collo-cygni* DNA levels increased significantly in infected plants at the later stages of symptom development once leaves were senescing. It may be that this rise coincides with fungal sporulation.

The early lesion development on control plants observed in the current results, before differences in relative chlorophyll content or % GLA became apparent, could indicate that senescence itself may not act as a trigger for RLS symptom expression, similar to the conclusions of McGrann and

Brown (2018). It could be that symptom expression is triggered by pre-senescence signals or signals associated with the onset of senescence in barley at a very early stage, including potentially changes in ROS status. However, the current results also do not rule out the possibility of the fungal switch to necrotrophy instead acting as a trigger for senescence, as suggested by the results reported in Sjøkvist *et al.*, (2018), in which the authors reported upregulation of cytokinin oxidases and abscisic acid response genes in barley seedlings during infection with *R. collo-cygni*, in the period just before visible symptom appearance, and during early symptom development. In this scenario, the treatments used to delay senescence in the current experiments may have interfered with this process.

5.4. General discussion

RLS epidemics can cause significant yield loss in barley, yet our understanding of the relative impact of different stages of the *R. collo-cygni* lifecycle is limited. This fungus can undergo a long period of asymptomatic growth in barley prior to the appearance of visible foliar disease symptoms, typically late in the growing season after flowering has occurred. It was not previously known with any certainty whether yield loss to RLS is mainly associated with reduced radiation interception after the appearance of visible disease symptoms, or whether the long asymptomatic phase contributes significantly to yield loss, for example, through effects on host radiation use efficiency during plant development and establishment of grain sink capacity.

Physiological responses to infection were examined in barley seedlings inoculated with *R. collo-cygni* during asymptomatic growth and as visible foliar disease symptoms developed. Steady state photosynthesis, photosynthetic induction kinetics of dark-adapted plants, and dark respiration were assessed using chlorophyll fluorescence and infra-red gas analysis techniques.

No evidence was found to indicate an effect of *R. collo-cygni* infection on barley leaf photosynthesis prior to the appearance of visible symptoms. Furthermore, limited lesion development on otherwise green leaves was not found to impact net leaf photosynthesis. Within RLS lesions, as lesions developed and matured, photosynthesis was eventually reduced to near zero, indicating cell damage or death.

Experiments were then scaled-up to field level to determine whether the results shown in inoculated seedlings in controlled environment experiments translated to mature plants in the field environment, and further experiments were undertaken to probe the relative impact on yield loss associated with RLS of the asymptomatic and symptomatic life stages of *R. collo-cygni* in barley. Chlorophyll fluorescence analysis was used to examine photosynthesis in barley leaves during asymptomatic growth and throughout the development of visible foliar disease symptoms, and an analysis of healthy tissue light interception and comparison of predicted and observed yield loss

was used to assess whether differences in post-anthesis PAR interception by healthy tissue between infected and fungicide-treated plots could account for the observed yield loss.

In agreement with the results shown in inoculated seedlings in controlled environment experiments, no evidence was found to indicate an effect of *R. collo-cygni* infection on barley leaf photosynthesis prior to the appearance of visible symptoms in the field. The results for the analysis of healthy area light interception and comparison of predicted and observed yield loss indicated that the difference in post-anthesis PAR interception by healthy tissue between fungicide-treated and the inoculated and untreated plots was sufficient to account for the observed yield losses, without needing to invoke effects of disease on RUE or remobilisation of soluble carbohydrate reserves for grain filling. This suggests that the effects of RLS on yield are largely the result of reductions in green leaf area associated with symptom development and tissue necrosis in diseased plants relative to fungicide-treated plants.

These results indicate that the asymptomatic life stage of *R. collo-cygni* in barley may not negatively affect plants and is, therefore, not in itself an important target for RLS disease control strategies. They suggest that the necrotrophic life stage of *R. collo-cygni* is primarily responsible for yield loss to RLS; therefore, the switch to necrotrophy and development of visible symptoms are the most important target for RLS disease control strategies.

Building on these outcomes, further experiments were designed to investigate whether it was possible to reduce or delay the appearance of RLS symptoms in barley. RLS can be associated with rapid and premature senescence (Oxley *et al.*, 2008), although some uncertainty remains around the mechanisms which link senescence and RLS symptom expression. If the onset of leaf senescence, or other factors such as changes in ROS status that can lead to senescence, are involved in triggering the *R. collo-cygni* switch to necrotrophic growth and RLS symptom development, then it could be possible to delay the appearance of symptoms using treatments that delay leaf senescence. Exogenous cytokinin application and applications of fertiliser were used to treat barley seedlings inoculated with *R. collo-cygni* in order to delay foliar senescence.

Cytokinin application was the most successful treatment in this regard. *R. collo-cygni* growth *in planta* and RLS symptom severity was reduced in barley seedlings displaying delayed foliar senescence. Symptom expression and fungal DNA levels were highest in plants that received neither of the senescence-delaying treatments. RLS lesions first appeared, and symptom severity differed significantly between treatments, before differences in relative chlorophyll content or % GLA became apparent, suggesting that, either the fungal switch to necrotrophy may be involved in triggering senescence, or that the fungus may be sensitive to pre-senescence signals or signals associated with the onset of senescence in barley at a very early stage.

Protection of green canopy light interception against foliar diseases using fungicides is currently an integral part of management strategies for spring barley. However, Bingham *et al.* (2019) demonstrated that maintenance of green canopy for the entire duration of grain filling is not always necessary to protect against yield loss to foliar disease in sink-limited spring barley crops. The current results indicate that the life stage of *R. collo-cygni* that is most damaging to spring barley yield is the period of foliar symptom proliferation after the switch to necrotrophic growth, during which substantial reductions in green canopy area can occur. This normally coincides with grain filling in field epidemics of RLS. As fungicide treatments for RLS are becoming more limited due to both resistance and withdrawal of effective products, there could be merit in further investigation of whether prolonging green canopy area using methods such as exogenous cytokinin application for a portion of the duration of grain filling would result in reduced RLS symptom expression in the field. However, any such strategy would need to take account of overlapping functions of plant hormones and consider possible effects on factors such as remobilisation of nitrogen to the ear for grain filling.

Nitrogen remobilisation from senescing tissues contributes to grain protein content in cereals, and earlier leaf senescence and proteolysis in barley has been associated with high grain protein content (Jukanti and Fischer, 2008). Kichey *et al.* (2007) found that nitrogen remobilised from leaves accounts for 90% of total grain nitrogen content in wheat. Interestingly, Zhao *et al.* (2015) found that delayed leaf senescence in wheat associated with overexpression of a NAC transcription factor increased grain nitrogen content, which the authors ascribed to post-anthesis nitrogen assimilation rather than amino acids remobilised from vegetative tissue. Relatively low grain nitrogen is a preferred trait for malting barley.

As discussed earlier, exposure of barley plants to abiotic stress has been linked to RLS symptom expression and increased disease severity. A recent report from Hoheneder *et al.*, (2021) identified some barley varieties that showed durable quantitative resistance to RLS under different field conditions over three consecutive years. Frequently, however, environment appears to have a strong effect on disease severity year-on-year or across different locations. Genotype-environment interaction is, therefore, a primary consideration in studies of barley resistance to RLS, and further investigation of the relationship between abiotic stress tolerance in barley and RLS disease severity is warranted.

The current results showed that appearance of RLS symptoms was delayed, and RLS symptom severity reduced, relative to control plants in barley seedlings treated with exogenous cytokinin. Further research to understand the way in which the internal environment of the leaf is changed by cytokinin application and how this could affect the activity of *R. collo-cygni* could, therefore, be informative. A useful next step would be to establish whether RLS symptom expression is also

reduced in mature barley plants treated with cytokinin. Thereafter, effects on yield and interaction with environment would be important factors to consider.

The results from this project indicate that the necrotrophic life stage of *R. collo-cygni* in barley is primarily responsible for yield loss to RLS, highlighting the importance of further research to identify factors that may act as triggers for the *R. collo-cygni* transition to necrotrophy. If it were possible to identify and/or control such triggers, this could potentially reduce the need for fungicidal control of *R. collo-cygni* in barley or otherwise, inform a more targeted approach based on understanding of risk factors for transition of the fungus from asymptomatic to symptomatic growth.

6. References

- Baker, N. R. (2008) 'Chlorophyll fluorescence: a probe of photosynthesis in vivo.', Annual review of plant biology, 59, pp. 89–113. doi: 10.1146/annurev.arplant.59.032607.092759.
- Bassanezi, R. B. *et al.* (2001) 'Accounting for photosynthetic efficiency of bean leaves with rust, angular leaf spot and anthracnose to assess crop damage', Plant Pathology, 50(4), pp. 443–452. doi: 10.1046/j.1365-3059.2001.00584.x.
- Behr, M. *et al.* (2010) 'The Hemibiotroph *Colletotrichum graminicola* Locally Induces Photosynthetically Active Green Islands but Globally Accelerates Senescence on Aging Maize Leaves', Molecular plant-microbe interactions. St. Paul, MN: APS Press, 23(7), pp. 879–892. doi: 10.1094/MPMI-23-7-0879.
- Berdugo, C. A. *et al.* (2012) 'Effect of bixafen on senescence and yield formation of wheat', Pesticide Biochemistry and Physiology. Elsevier Inc., 104(3), pp. 171–177. doi: 10.1016/j.pestbp.2012.07.010.
- Biemelt, S. and Sonnewald, U. (2006) 'Plant-microbe interactions to probe regulation of plant carbon metabolism', Journal of Plant Physiology, 163(3), pp. 307–318. doi: 10.1016/j.jplph.2005.10.011.
- Bilgin, D. D. *et al.* (2010) 'Biotic stress globally downregulates photosynthesis genes', Plant, Cell and Environment, 33(10), pp. 1597–1613. doi: 10.1111/j.1365-3040.2010.02167.x.
- Bingham, I. J. *et al.* (2007a) 'Is barley yield in the UK sink limited? I. Post-anthesis radiation interception, radiation-use efficiency and source-sink balance', Field Crops Research, 101(2), pp. 198–211. doi: 10.1016/j.fcr.2006.11.005.
- Bingham, I. J. *et al.* (2007b) 'Is barley yield in the UK sink limited? II. Factors affecting potential grain size', Field Crops Research, 101(2), pp. 212–220. doi: 10.1016/j.fcr.2006.11.004.
- Bingham, I. J. *et al.* (2009) 'Crop traits and the tolerance of wheat and barley to foliar disease', Annals of Applied Biology, 154(2), pp. 159–173. doi: 10.1111/j.1744-7348.2008.00291.x.
- Bingham, I. J. *et al.* (2019) 'In sink-limited spring barley crops, light interception by green canopy does not need protection against foliar disease for the entire duration of grain filling', Field Crops Research. doi: 10.1016/j.fcr.2019.04.020.

- Bingham, I. J. *et al.* (2021) 'Mechanisms by which fungicides increase grain sink capacity and yield of spring barley when visible disease severity is low or absent', *Field Crops Research*. Elsevier B.V., 261(November 2020), p. 108011. doi: 10.1016/j.fcr.2020.108011.
- Boote, K. *et al.* (1983) 'Coupling Pests to Crop Growth Simulators to Predict Yield Reductions.', *Phytopathology*, 73(11), pp. 1581–1587.
- Von Bothmer, R. and Komatsuda, T. (2011) 'Barley Origin and Related Species', in *Barley: Production, Improvement, and Uses*, pp. 14–62. doi: 10.1002/9780470958636.ch2.
- Bottalico, A. and Perrone, G. (2002) 'Toxigenic *Fusarium* species and mycotoxins associated with head blight in small-grain cereals in Europe', *European Journal of Plant Pathology*, 108(7), pp. 611–624. doi: 10.1023/A:1020635214971.
- Cavara, F. (1893) 'Über einige parasitische Pilze auf dem Getreide', *Zeitschrift für Pflanzenkrankheiten*, 3, pp. 16–26.
- Chou, H. M. *et al.* (2000) 'Infection of *Arabidopsis thaliana* leaves with *Albugo candida* (white blister rust) causes a reprogramming of host metabolism.', *Molecular plant pathology*, 1(2), pp. 99–113. doi: 10.1046/j.1364-3703.2000.00013.x.
- Cromey, M. G. *et al.* (2004) 'Effects of the fungicides azoxystrobin and tebuconazole on *Didymella exitialis*, leaf senescence and grain yield in wheat', *Crop Protection*, 23(11), pp. 1019–1030. doi: 10.1016/j.cropro.2004.03.002.
- Crous, P. *et al.* (2000) 'The genus *Mycosphaerella* and its anamorphs', *Studies in Mycology*. Centraalbureau Schimmelcultuur, Uppsalalaan 8, 3584 Ct Utrecht, Netherlands, (45), pp. 107–121.
- Crous, P. W. *et al.* (2009) 'Unravelling *Mycosphaerella*: do you believe in genera?', *Persoonia*. Rijksherbarium, Po Box 9514, 2300 Ra Leiden, Netherlands, 23, pp. 99–118. doi: 10.3767/003158509X479487.
- Crous, P. W., Kang, J.-C. and Braun, U. (2001) A Phylogenetic Redefinition of Anamorph Genera in *Mycosphaerella* Based on ITS rDNA Sequence and Morphology, *Mycologia*.
- Daub, M. E. and Ehrenshaft, M. (2000) 'The Photoactivated *Cercospora* Toxin Cercosporin : Contributions to Plant Disease and Fundamental Biology', *Annual review of phytopathology*, 38, pp. 461–490.
- Dinkins, R. D. *et al.* (2017) 'Transcriptome response of *Lolium arundinaceum* to its fungal endophyte *Epichloë coenophiala*', *New Phytologist*, 213(1), pp. 324–337. doi: 10.1111/nph.14103.
- Divon, H. H. and Fluhr, R. (2007) 'Nutrition acquisition strategies during fungal infection of plants', *FEMS Microbiology Letters*, 266(1), pp. 65–74. doi: 10.1111/j.1574-6968.2006.00504.x.
- Dussart, F. *et al.* (2018) 'Genome-based discovery of polyketide-derived secondary metabolism pathways in the barley pathogen *Ramularia collo-cygni*', *Molecular Plant Microbe Interactions*, p. doi:10.1094/MPMI-12-17-0299-R. doi: 10.1094/MPMI-12-17-0299-R.
- Dussart, F., Hoebe, P. N. and Spoel, S. H. (2018) 'Determining the role of the phytotoxic secondary metabolite rubellin D in the pathology of *Ramularia collo-cygni*, the fungus responsible

for *Ramularia* leaf spot disease of barley', in Proceedings Crop Production in Northern Britain, pp. 97–102.

Ehness, R. *et al.* (1997) 'Glucose and stress independently regulate source and sink metabolism and defense mechanisms via signal transduction pathways involving protein phosphorylation', *Plant Cell*, 9(10), pp. 1825–1841. doi: 10.1105/tpc.9.10.1825.

FAOSTAT (2020) Food and Agricultural Organization of the United Nations. Available at: <http://faostat3.fao.org/home/E> (Accessed: 30 August 2020).

Formayer, H., Huss, H. and Kromp-Kolb, H. (2004) 'Influence of Climatic Factors on the Formation of Symptoms of *Ramularia collo-cygni*', in Yahyaoui, A. *et al.* (eds) Proceedings of the Second International Workshop on Barley Leaf Blights. Aleppo, Syria., pp. 329–330.

Fotopoulos, V. *et al.* (2003) 'The Monosaccharide Transporter Gene, AtSTP4, and the Cell-Wall Invertase, at β fruct1, Are Induced in Arabidopsis during Infection with the Fungal Biotroph *Erysiphe cichoracearum*', 132(2), pp. 821–829. doi: 10.1104/pp.103.021428.ferred.

Frei, P. *et al.* (2007) 'Direct-PCR detection and epidemiology of *Ramularia collo-cygni* associated with barley necrotic leaf spots', *Journal of Phytopathology*, 155(5), pp. 281–288. doi: 10.1111/j.1439-0434.2007.01228.x.

Frei, P. and Gindro, K. (2015) '*Ramularia collo-cygni* - un nouveau champignon pathogene de l'orge', *Recherche Agronomique Suisse*, 6, pp. 210–217.

Gan, S. and Amasino, R. M. (1996) 'Cytokinins in plant senescence: from spray and pray to clone and play', *BioEssays*, 18(7), pp. 557–565.

Gaunt, R. E. (1995) 'The relationship between plant disease severity and yield.', *Annual review of phytopathology*, 33, pp. 119–144. doi: 10.1146/annurev.py.33.090195.001003.

Grossmann, K., Kwiatkowski, J. and Caspar, Gü. (1999) 'Regulation of phytohormone levels, leaf senescence and transpiration by the strobilurin kresoxim-methyl in wheat (*Triticum aestivum*)', *Journal of Plant Physiology*, 154(5–6), pp. 805–808. doi: 10.1016/S0176-1617(99)80262-4.

Grossmann, K. and Retzlaff, G. (1997) 'Bioregulatory effects of the fungicidal strobilurin kresoxim-methyl in wheat (*Triticum aestivum*)', *Pesticide Science*, 50(1), pp. 11–20. doi: 10.1002/(SICI)1096-9063(199705)50:1<11::AID-PS556>3.0.CO;2-8.

Hahn, M. *et al.* (1997) 'A putative amino acid transporter is specifically expressed in haustoria of the rust fungus *Uromyces fabae*', *Molecular Plant-Microbe Interactions*, 10(4), pp. 438–445. doi: 10.1094/MPMI.1997.10.4.438.

Havis, N. D. *et al.* (2006) 'Rapid nested PCR-based detection of *Ramularia collo-cygni* direct from barley', *FEMS Microbiology Letters*, 256(2), pp. 217–223. doi: 10.1111/j.1574-6968.2006.00121.x.

Havis, N. D. *et al.* (2015) '*Ramularia collo-cygni* - an emerging pathogen of barley crops', *Phytopathology*, 105(7), pp. 895–904. doi: 10.1094/PHYTO-11-14-0337-FI.

Havis, N. D., Nyman, M. and Oxley, S. J. P. (2014) 'Evidence for seed transmission and symptomless growth of *Ramularia collo-cygni* in barley (*Hordeum vulgare*)', *Plant Pathology*, 63(4), pp. 929–936. doi: 10.1111/ppa.12162.

- Havis, N., Evans, N. and Hughes, G. (2018) Development of UK wide risk forecast for *Ramularia* leaf spot in barley. AHDB Report PR600.
- Hecker, K. D. *et al.* (1998) 'Barley β -glucan is effective as a hypocholesterolaemic ingredient in foods', *Journal of the Science of Food and Agriculture*, 77(2), pp. 179–183. doi: 10.1002/(sici)1097-0010(199806)77:2<179::aid-jsfa23>3.0.co;2-0.
- Heiser, I. *et al.* (2004) 'Fatty acid peroxidation by rubellin B, C and D, phytotoxins produced by *Ramularia collo-cygni* (Sutton et Waller)', *Physiological and Molecular Plant Pathology*, 64(3), pp. 135–143. doi: 10.1016/j.pmpp.2004.08.002.
- Heiser, I., Sachs, E. and Liebermann, B. (2003) 'Photodynamic oxygen activation by rubellin D, a phytotoxin produced by *Ramularia collo-cygni* (Sutton et Waller)', *Physiological and Molecular Plant Pathology*, 62(1), pp. 29–36. doi: 10.1016/S0885-5765(03)00007-9.
- Heisterüber, D., Schulte, P. and Moerschbacher, B. . (1994) 'Soluble carbohydrates and invertase activity in stem rust-infected, resistant and susceptible near-isogenic wheat leaves', *Physiological and molecular plant pathology*. London: Elsevier India Pvt Ltd, 45(2), pp. 111–123. doi: 10.1016/S0885-5765(05)80070-0.
- Hideg, É., Kós, P. B. and Schreiber, U. (2008) 'Imaging of NPQ and ROS formation in tobacco leaves: Heat inactivation of the water-water cycle prevents down-regulation of PSII', *Plant and Cell Physiology*, 49(12), pp. 1879–1886. doi: 10.1093/pcp/pcn170.
- Hofer, K. *et al.* (2014) 'Mildew Locus O mutation does not affect resistance to grain infections with *Fusarium* spp. and *Ramularia collo-cygni*', *Igarss 2014*, (1), pp. 1–5. doi: 10.1007/s13398-014-0173-7.2.
- Hoheneder, F. *et al.* (2021) 'Ramularia leaf spot disease of barley is highly host genotype-dependent and suppressed by continuous drought stress in the field', *Journal of Plant Diseases and Protection*. Springer Berlin Heidelberg, (0123456789). doi: 10.1007/s41348-020-00420-z.
- Huss, H. (2004) 'The biology of *Ramularia collo-cygni*. Meeting the challenges of barley blights', in Yahyaoui, A. *et al.* (eds) *Proceedings of the second international workshop on barley leaf blights*. Aleppo, Syria., pp. 321–328.
- Jebbouj, R. and El Yousfi, B. (2009) 'Barley yield losses due to defoliation of upper three leaves either healthy or infected at boot stage by *Pyrenophora teres f. teres*', *European Journal of Plant Pathology*, 125(2), pp. 303–315. doi: 10.1007/s10658-009-9483-6.
- Johnson, K. (1987) 'Defoliation, Disease, and Growth: A Reply', *Phytopathology*, 77(11), pp. 7–9.
- Jordan, V. W. L., Best, G. R. and Allen, E. C. (1985) 'Effects of *Pyrenophora teres* on dry matter production and yield components of winter barley', *Plant Pathology*, 34(2), pp. 200–206. doi: <https://doi.org/10.1111/j.1365-3059.1985.tb01350.x>.
- Jukanti, A. K. and Fischer, A. M. (2008) 'A high-grain protein content locus on barley (*Hordeum vulgare*) chromosome 6 is associated with increased flag leaf proteolysis and nitrogen remobilization', *Physiologia Plantarum*, 132(4), pp. 426–439.

- Kennedy, S. P. *et al.* (2018) 'Grain number and grain filling of two-row malting barley in response to variation in post-anthesis radiation: Analysis by grain position on the ear and its implications for yield improvement and quality', *Field Crops Research*. Elsevier, 225(June), pp. 74–82. doi: 10.1016/j.fcr.2018.06.004.
- Kichey, T. *et al.* (2007) 'In winter wheat (*Triticum aestivum* L.), post-anthesis nitrogen uptake and remobilisation to the grain correlates with agronomic traits and nitrogen physiological markers', *Field Crops Research*, 102(1), pp. 22–32. doi: 10.1016/j.fcr.2007.01.002.
- Koch, K. E. (1996) 'Carbohydrate-modulated gene expression in plants', *Annual Review of Plant Physiology and Plant Molecular Biology*, 47(1), pp. 509–540. doi: 10.1146/annurev.arplant.47.1.509.
- Livne, A. and Daly, J. (1966) 'Translocation in healthy and rust-affected beans', *Phytopathology*, 56, pp. 170–175.
- Luo, Y. *et al.* (2018) 'Interactions between cytokinin and nitrogen contribute to grain mass in wheat cultivars by regulating the flag leaf senescence process', *Crop Journal*, 6. doi: 10.1016/j.cj.2018.05.008.
- Ma, X. *et al.* (2018) 'Comparative transcriptomics reveals how wheat responds to infection by *Zymoseptoria tritici*', *Molecular Plant-Microbe Interactions*, 31(4), pp. 420–431. doi: 10.1094/MPMI-10-17-0245-R.
- Mäe, A., Põllumaa, L. and Sooväli, P. (2018) '*Ramularia collo-cygni*: A new pathogen spreading in barley fields in Estonia', *Agricultural and Food Science*, 27(2), pp. 138–145. doi: 10.23986/afsci.69116.
- Makepeace, J. C. (2006) The effect of the mlo mildew resistance gene on spotting diseases of barley.
- Makepeace, J. C. *et al.* (2008) 'A method of inoculating barley seedlings with *Ramularia collo-cygni*', *Plant Pathology*, 57(6), pp. 991–999. doi: 10.1111/j.1365-3059.2008.01892.x.
- McGrann, G. *et al.* (2015) 'Contribution of the drought tolerance-related Stress-responsive NAC 1 transcription factor to resistance of barley to *Ramularia* leaf spot.', *Molecular plant pathology*, 16(201–209). doi: 10.1111/mpp.12173.
- McGrann, G. R. D. *et al.* (2014) 'A trade off between mlo resistance to powdery mildew and increased susceptibility of barley to a newly important disease, *Ramularia* leaf spot.', *Journal of experimental botany*, 65(4), pp. 1025–37. doi: 10.1093/jxb/ert452.
- McGrann, G. R. D. *et al.* (2016) 'The genome of the emerging barley pathogen *Ramularia collo-cygni*', *BMC Genomics*. *BMC Genomics*, 17(1), p. 584. doi: 10.1186/s12864-016-2928-3.
- McGrann, G. R. D. and Brown, J. K. M. (2018) 'The role of reactive oxygen in the development of *Ramularia* leaf spot disease in barley seedlings', *Annals of Botany*, 121, pp. 415–430. doi: 10.1093/aob/mcx170.
- McGrann, G. R. D. and Havis, N. D. (2017) 'Ramularia Leaf Spot: A Newly Important Threat to Barley Production', *Outlooks on Pest Management*. doi: 10.1564/v28_apr_05.

- McGrann, G. R. D., Miller, S. and Havis, N. D. (2020) 'The ENHANCED MAGNAPORTHE RESISTANCE 1 locus affects *Ramularia* leaf spot development in barley', *European Journal of Plant Pathology*. *European Journal of Plant Pathology*, 156(1), pp. 123–132. doi: 10.1007/s10658-019-01869-x.
- Meyer, S. *et al.* (2001) 'Inhibition of photosynthesis by *Colletotrichum lindemuthianum* in bean leaves determined by chlorophyll fluorescence imaging', *Plant, Cell and Environment*, 24(9), pp. 947–955. doi: 10.1046/j.0016-8025.2001.00737.x.
- Miethbauer, S. *et al.* (2006) 'Biosynthesis of photodynamically active rubellins and structure elucidation of new anthraquinone derivatives produced by *Ramularia collo-cygni*', *Phytochemistry*, 67(12), pp. 1206–1213. doi: 10.1016/j.phytochem.2006.05.003.
- Miethbauer, S., Heiser, I. and Liebermann, B. (2003) 'The phytopathogenic fungus *Ramularia collo-cygni* produces biologically active rubellins on infected barley leaves', *Journal of Phytopathology*, 151, pp. 665–668. doi: 10.1046/j.1439-0434.2003.00783.x.
- Newton, A. C. *et al.* (2011) 'Crops that feed the world 4. Barley: a resilient crop? Strengths and weaknesses in the context of food security', *Food Security*, 3(2), pp. 141–178. doi: 10.1007/s12571-011-0126-3.
- Owera, S., Farrar, J. and Whitbred, R. (1983) 'Translocation from Leaves of Barley Infected with Brown Rust', *New Phytologist*, 94(1), pp. 111–123.
- Oxley, S. *et al.* (2008) Impact and interactions of *Ramularia collo-cygni* and oxidative stress in barley. HGCA Project Report No. 431.
- Palma-Guerrero, J. *et al.* (2016) 'Comparative transcriptomic analyses of *Zymoseptoria tritici* strains show complex lifestyle transitions and intraspecific variability in transcription profiles', *Molecular plant pathology*, 17(6), pp. 845–859. doi: 10.1111/mpp.12333.
- Peraldi, a. *et al.* (2014) '*Brachypodium distachyon* exhibits compatible interactions with *Oculimacula* spp. and *Ramularia collo-cygni*, providing the first pathosystem model to study eyespot and ramularia leaf spot diseases', *Plant Pathology*, 63(3), pp. 554–562. doi: 10.1111/ppa.12114.
- Pinnschmidt, H. O., Sindberg, S. A. and Willas, J. (2006) 'Resistant barley varieties may facilitate control of *Ramularia* leaf spot', *Danish Research Centre for Organic Farming*, (November 2006), pp. 2006–2008.
- Pinnschmidt, H. and Sindberg, S. A. (2009) 'Assessing *Ramularia* leaf spot resistance of spring barley cultivars in the presence of other diseases', *Aspects of Applied Biology*, 92, pp. 71–80.
- Piotrowska, M. J. *et al.* (2016) 'Development and use of microsatellite markers to study diversity, reproduction and population genetic structure of the cereal pathogen *Ramularia collo-cygni*.', *Fungal genetics and biology : FG & B*. doi: 10.1016/j.fgb.2016.01.007.
- Piotrowska, M. J. *et al.* (2017) 'Characterisation of *Ramularia collo-cygni* laboratory mutants resistant to succinate dehydrogenase inhibitors', *Pest Management Science*, 73(6), pp. 1187–1196. doi: 10.1002/ps.4442.

- Robert, C. *et al.* (2004) 'Analysis and modelling of effects of leaf rust and *Septoria tritici* blotch on wheat growth.', *Journal of experimental botany*, 55(399), pp. 1079–1094. doi: 10.1093/jxb/erh108.
- Robert, C. *et al.* (2005) 'Wheat leaf photosynthesis loss due to leaf rust, with respect to lesion development and leaf nitrogen status', *New Phytologist*, 165(1), pp. 227–241. doi: 10.1111/j.1469-8137.2004.01237.x.
- Robert, C. *et al.* (2006) 'Quantification of the effects of *Septoria tritici* blotch on wheat leaf gas exchange with respect to lesion age, leaf number, and leaf nitrogen status', *Journal of Experimental Botany*, 57(1), pp. 225–234. doi: 10.1093/jxb/eri153.
- Roitsch, T. *et al.* (2003) 'Extracellular invertase: Key metabolic enzyme and PR protein', *Journal of Experimental Botany*, 54(382), pp. 513–524. doi: 10.1093/jxb/erg050.
- Salamati, S. and Reitan, L. (2006) *Ramularia collo-cygni* on spring barley, an overview of its biology and epidemiology, *Ramularia collo-cygni*: a new disease and challenge in Barley production; Proceedings of the First European Ramularia Workshop, Georg-August University, Göttingen, Germany. Edited by A. von Tiedemann, A. Schützendübel, and B. Koopman.
- Scholes, J. D. *et al.* (1994) 'Invertase: understanding changes in the photosynthetic and carbohydrate metabolism of barley leaves infected with powdery mildew', *New Phytologist*, 126(2), pp. 213–222. doi: 10.1111/j.1469-8137.1994.tb03939.x.
- Scholes, J. D. and Farrar, J. F. (1986) 'Increased Rates of Photosynthesis in Localized Regions of a Barley Leaf Infected With Brown Rust', *New Phytologist*, 104, pp. 601–612.
- Scholes, J. D. and Rolfe, S. A. (1996) 'Photosynthesis in localised regions of oat leaves infected with crown rust (*Puccinia coronata*): quantitative imaging of chlorophyll fluorescence', *Planta*, 199(4), pp. 573–582. doi: 10.1007/BF00195189.
- Scholes, J. D. and Rolfe, S. A. (2009) 'Chlorophyll fluorescence imaging as tool for understanding the impact of fungal diseases on plant performance: A phenomics perspective', *Functional Plant Biology*, 36(11), pp. 880–892. doi: 10.1071/FP09145.
- Scott, S. W. and Griffiths, E. (1980) 'Effects of controlled epidemics of powdery mildew on grain yield of spring barley', *Annals of Applied Biology*, 94(1), pp. 19–31. doi: 10.1111/j.1744-7348.1980.tb03892.x.
- Sjokvist, E. *et al.* (2018) 'Dissection of Ramularia Leaf Spot Disease by Integrated Analysis of Barley and *Ramularia collo-cygni* Transcriptome Responses', *Molecular Plant-Microbe Interactions*, 32(2), pp. 176–193. doi: 10.1094/mpmi-05-18-0113-r.
- Smedegaard-Petersen, V. and Stolen, O. (1981) 'Effect of Energy-Requiring Defense Reactions on Yield and Grain Quality in a Powdery Mildew-Resistant Barley Cultivar', *Phytopathology*, 71(4), pp. 396–399. doi: 10.1094/phyto-71-396.
- Stabentheiner, E., Minihofer, T. and Huss, H. (2009) 'Infection of barley by *Ramularia collo-cygni*: scanning electron microscopic investigations.', *Mycopathologia*, 168(3), pp. 135–43. doi: 10.1007/s11046-009-9206-8.

- Stam, R. *et al.* (2019) 'The Current Epidemic of the Barley Pathogen *Ramularia collo-cygni* Derives from a Population Expansion and Shows Global Admixture', *Phytopathology*. American Phytopathological Society, 109(12), pp. 2161–2168. doi: 10.1094/PHYTO-04-19-0117-R.
- Struck, C., Ernst, M. and Hahn, M. (2002) 'Characterization of a developmentally regulated amino acid transporter (AAT1p) of the rust fungus *Uromyces fabae*', *Molecular Plant Pathology*, 3(1), pp. 23–30. doi: 10.1046/j.1464-6722.2001.00091.x.
- Sutton, B. C. and Waller, J. M. (1988) 'Taxonomy of *Ophiocladium hordei*, causing lead lesion on triticale and other Gramineae', *Transactions of the British Mycological Society*, pp. 55–61. doi: 10.1016/S0007-1536(88)80180-3.
- Taylor, J. M. G., Paterson, L. J. and Havis, N. D. (2010) 'A quantitative real-time PCR assay for the detection of *Ramularia collo-cygni* from barley (*Hordeum vulgare*).', *Letters in applied microbiology*, 50(5), pp. 493–9. doi: 10.1111/j.1472-765X.2010.02826.x.
- The Scottish Government (2020) 'Cereal and Oilseed Rape Harvest 2020'.
- Thirugnanasambandam, a. *et al.* (2011) 'Agrobacterium-mediated transformation of the barley pathogen *Ramularia collo-cygni* with fluorescent marker tags and live tissue imaging of infection development', *Plant Pathology*, 60(5), pp. 929–937. doi: 10.1111/j.1365-3059.2011.02440.x.
- Tottman, D. R., Makepeace, R. J. and Broad, H. (1979) 'An explanation of the decimal code for the growth stages of cereals, with illustrations', *Annals of Applied Biology*, 93(2), pp. 221–234. doi: 10.1111/j.1744-7348.1979.tb06534.x.
- Voegelé, R. T. *et al.* (2001) 'The role of haustoria in sugar supply during infection of broad bean by the rust fungus *Uromyces fabae*', *Proceedings of the National Academy of Sciences of the United States of America*, 98(14), pp. 8133–8138. doi: 10.1073/pnas.131186798.
- Walters, D. R., Havis, N. D. and Oxley, S. J. P. (2008) '*Ramularia collo-cygni*: The biology of an emerging pathogen of barley', *FEMS Microbiology Letters*, 279(1), pp. 1–7. doi: 10.1111/j.1574-6968.2007.00986.x.
- Wu, Y. X. and Von Tiedemann, A. (2001) 'Physiological effects of azoxystrobin and epoxiconazole on senescence and the oxidative status of wheat', *Pesticide Biochemistry and Physiology*, 71(1), pp. 1–10. doi: 10.1006/pest.2001.2561.
- Wu, Y. X. and Von Tiedemann, A. (2002) 'Evidence for oxidative stress involved in physiological leaf spot formation in winter and spring barley', *Phytopathology*, 92(2), pp. 145–155. doi: 10.1094/PHYTO.2002.92.2.145.
- Zhao, D. *et al.* (2015) 'Overexpression of a NAC transcription factor delays leaf senescence and increases grain nitrogen concentration in wheat', *Plant Biology*, 17(4), pp. 904–913. doi: 10.1111/plb.12296.